

**TECHNO-ECONOMIC ANALYSIS OF AN OFF-GRID MICRO-
HYDROKINETIC RIVER SYSTEM AS A REMOTE RURAL
ELECTRIFICATION OPTION**

By

SANDILE PHILLIP KOKO

Submitted in fulfilment of the requirements for the degree:

**MAGISTER TECHNOLOGIAE:
ENGINEERING: ELECTRICAL**

In the

Faculty of Engineering and Information Technology:
School of Electrical, Electronic and Computer Engineering

At the

Central University of Technology, Free State

Supervisor: **Mr. K Kusakana** (M.Tech: Electrical Engineering)

Co-supervisor: **Prof. HJ Vermaak** (PhD: Electrical Engineering)

Bloemfontein

2014

Declaration

I, Sandile Phillip Koko hereby declare that this research project which has been submitted to the Central University of Technology, Free State for the degree of MAGISTER TECHNOLOGIAE: ENGINEERING ELECTRICAL, is my own independent work; complies with the Code of Academic Integrity, as well as other relevant policies, procedures, rules and regulations of the Central University of Technology, Free State, and has not been submitted before by any person in fulfilment (or partial fulfilment) of the requirements for the attainment of any qualification.



Student Signature:

Date: 2014-11-01

Acknowledgements

First and foremost, I would like to thank Almighty God for making everything possible for me by giving me strength in this study. Glory to our Almighty father, His Son Jesus Christ and the Holy Spirit!

I would like to express my sincere appreciation to my supervisors, Mr. Kanzumba Kusakana and Prof. Herman Jacobus Vermaak who were very supportive. Their continuous guidance, support and knowledge were indeed invaluable. They provided me with motivation and on-going encouragement throughout the study.

I would like to take this opportunity to thank my guardians (Vuyisile and Mateboho Koko), younger brother, Mlungisi Koko and younger sister, Qhathiwe Koko for their love, care and patient support in my studies. I also want to thank my three special lecturers, Mr. Lebohang Moji, Mr. Patrick Manditereza, and Dr. Nicolaas Luwes for their ever inspiration and moral support in furthering my studies.

Finally, I would like to thank the CUT and RGEMS for granting me the opportunity and financial assistance to undertake the study.

Abstract

Remote rural electrification via grid-extension is a challenging solution due to high connection costs and low electricity consumption rate. As a result, it is difficult to recover the initial investment costs. Therefore, electrification is made possible by means of the commonly used off-grid approaches such as solar, wind, diesel generator and conventional micro-hydro. However, owing to non-continuous availability of sunlight and wind, high cost of diesel fuel, and requirements for construction of diversion weirs, these off-grid approaches might not offer a cost-effective and reliable solution to low income rural residents.

There are many rural communities throughout the world without access to grid electricity and with access to flowing water. An off-grid micro-hydrokinetic river (MHR) system is one of the promising technologies to be used in remote rural areas with flowing water. It can bring sustainable improvement to their quality of life due to its high energy density and minimal environmental impact. This technology is still in the development stage and there is a lack of application, especially in rural areas. Hence, this study investigates the current status of MHR technology in rural applications.

To demonstrate the economic feasibility of an off-grid MHR system, a rural site with multiple energy sources within South Africa has been used. The economic benefit offered by this proposed system at the selected site is compared to the economic benefits offered by other commonly used standalone systems such as solar, wind and diesel generator (DG). This economic comparison has been performed by making use of a Hybrid Optimization Model for Electric Renewable (HOMER) simulation tool. Grid extension has also been used as a comparison method for obtaining an economical distance between grid lines and the remote rural site. The results highlighted the acceptable economic performance of the MHR system.

Finally, most of the available modelling and simulation tools for mechanical and electrical systems are not equipped with hydrokinetic modules. Hence, an MHR system model has been developed in MATLAB/Simulink in order to study its dynamic performance as submitted to variable water resource. Its performance has then been compared to the performance of a wind system counterpart for generating the same amount of electrical power. This proved/verified that the proposed system can generate electricity markedly cheaper than a wind system even in areas with adequate wind resource within South Africa.

Table of Contents

Declaration	ii
Acknowledgements	iii
Abstract	iv
Table of Contents	vi
List of Figures	ix
List of Tables	xi
Nomenclature	xii
Abbreviations	xv
CHAPTER 1: INTRODUCTION	1
1.1 Background.....	1
1.2 Problem Statement.....	4
1.3 Objectives of the Study.....	5
1.4 Research Methodology	5
1.5 Hypothesis.....	6
1.6 Limitation of the Study	7
1.7 Contribution to Knowledge.....	7
1.8 Research Output.....	8
1.9 Outline of the Dissertation	8
CHAPTER 2: LITERATURE REVIEW	10
2.1 Introduction.....	10
2.2 Status of Hydropower Generation and Potential in South Africa.....	10
2.3 Hydrokinetic Technology	12
2.4 Hydrokinetic Turbine Technologies and Studies.....	14
2.4.1 Horizontal axis turbines	15
2.4.2 Vertical axis turbines.....	15
2.4.3 Recent studies on micro-hydrokinetic river turbine developments.....	18
2.5 Hydrokinetic Generators	20
2.5.1 Induction generators	20
2.5.2 Synchronous generators	21
2.6 Hydrokinetic Resource Assessment Studies.....	24

2.7	Micro-Hydrokinetic Optimization Studies	25
2.7.1	Cost optimization	25
2.7.2	Performance evaluation.....	26
2.8	Micro-Hydrokinetic Manufacturers and Associated Technologies	28
2.9	Conclusion	30
	CHAPTER 3: ECONOMIC AND ENVIRONMENTAL ANALYSIS	31
3.1	Introduction.....	31
3.2	Economic Methods	31
3.2.1	Net present value and net present cost	32
3.3	Rural Load Forecast.....	33
3.4	Renewable Energy Resources Assessment.....	36
3.4.1	Solar resource	37
3.4.2	Wind resource	38
3.4.3	Hydrokinetic resource	38
3.5	System Sizing and Costs.....	38
3.5.1	Diesel generator.....	39
3.5.2	Battery storage system	40
3.5.3	PV panels.....	41
3.5.4	Wind turbine.....	42
3.5.5	Hydrokinetic turbine	43
3.5.6	Power electronic converter.....	44
3.5.7	Grid extension	45
3.6	HOMER Results and Discussion	45
3.6.1	Hydrokinetic system simulation results	46
3.6.2	Overall results summary and discussion	50
3.6.3	Supplementary results	52
3.7	Conclusion	54
	CHAPTER 4: MODELLING OF MICRO-HYDROKINETIC SYSTEM.....	56
4.1	Introduction.....	56
4.2	Hydrokinetic Characteristics.....	57
4.2.1	Modelling of hydrokinetic turbines.....	57
4.2.2	Modelling of mechanical power within hydrokinetic turbine.....	58
4.2.3	Drive train modelling	62

4.2.4	Modelling of a permanent magnet synchronous generator	65
4.2.5	Overall model of an off-grid micro-hydrokinetic system	74
4.3	Conclusion	75
CHAPTER 5: SIMULATION RESULTS AND DISCUSSION		76
5.1	Introduction.....	76
5.2	High Water Density Turbine Model	76
5.3	Performance Evaluation of the Developed Hydrokinetic Model.....	77
5.3.1	Limiting the turbine speed to protect the generator	80
5.3.2	Comparison of the hydrokinetic performance with wind system performance	82
5.4	Relationship between the Number of Poles and Gearbox Ratio.....	84
5.4.1	Case 1: PMSG with a large number of pole pairs	85
5.4.2	Case 2: PMSG with fewer pole pairs	87
5.5	Conclusion	89
CHAPTER 6: CONCLUSION AND FUTURE STUDIES		91
6.1	Conclusion	91
6.2	Suggestions for Further Studies	92
REFERENCES.....		94
APPENDICES		110
Appendix A: Hydrokinetic system report for optimal economic results		110
Appendix B: Solar system report for optimal economic results		111
Appendix C: Wind system report for optimal economic results.....		112
Appendix D: Diesel generator system report for optimal economic results		113

List of Figures

Figure 1.1: Coal usage in South Africa (excluding exports)	2
Figure 2.1: Areas with conventional micro-hydropower potential in South Africa	12
Figure 2.2: Horizontal axis turbines.....	16
Figure 2.3: Vertical axis turbines.....	16
Figure 3.1: Rural load profile for 5 typical rural households	35
Figure 3.2: Seasonal electrical load profile (with 7% daily and hourly variation factors)	36
Figure 3.3: Power curve of a 7.5kW XLR turbine.....	43
Figure 3.4: Power curve of a 1.5kW DHT turbine	44
Figure 3.5: HOMER schematic diagram for the hydrokinetic system model.....	46
Figure 3.6: Hydrokinetic system's optimization results	47
Figure 3.7: Average hydrokinetic electric production of the optimal system configuration ...	48
Figure 3.8: Hydrokinetic turbine output power of the optimal system configuration	48
Figure 3.9: Battery state of charge in optimal hydrokinetic system configuration.....	49
Figure 3.10: Battery state of charge frequency histogram.....	49
Figure 3.11: Breakeven grid extension distance (4.17km)	49
Figure 3.12: Load profile for a typical rural school.....	52
Figure 4.1: Block diagram of a hydrokinetic turbine scheme.....	56
Figure 4.2: Simulink block diagram of a turbine power coefficient model.....	60
Figure 4.3: Overall Simulink block diagram of the modelled high density hydrokinetic turbine	62
Figure 4.4: Simulink block diagram of a one-mass drive train.....	64
Figure 4.5: PMSG phasor diagram showing Park transformation.....	66
Figure 4.6: Simulink block diagram of Vabc_to_Vdq.....	68

Figure 4.7: Simulink block diagram of Idq_to_Iabc.....	69
Figure 4.8: d and q equivalent circuit of a PMSG	70
Figure 4.9: Simulink block diagram of the stator direct-axis current	71
Figure 4.10: Simulink block diagram of the stator quadrature-axis current	72
Figure 4.11: Simulink block diagram of the electromagnetic torque	73
Figure 4.12: Simulink block diagram of a PMSG	73
Figure 4.13: Overall MHR system Simulink model	74
Figure 5.1: Power coefficient versus tip speed ratio of the turbine (with $\beta=0^\circ$)	77
Figure 5.2: Dynamic response of MHR system for a step change of water speed	78
Figure 5.3: Simulation results showing protection of PMSG against over-voltage	81
Figure 5.4: Simulation results showing wind system performance in comparison with MHR system	83
Figure 5.5: Simulation results of a 20 pole pairs PMSG	85
Figure 5.6: Simulation results of a 2 pole pairs PMSG	88

List of Tables

Table 1.1: Small-scale hydropower classification by power generation	3
Table 2.1: Total capacity and potential for macro and small hydropower in SA	11
Table 2.2: Swept area for different rotor blade configurations.....	14
Table 2.3: Technical advantages and disadvantages of horizontal and vertical turbines	17
Table 2.4: Advantages and disadvantages of synchronous and induction generators	23
Table 2.5: Coefficient of power improvement of different modified Savonius rotor configuration stages	26
Table 2.6: Summary of the deflector optimum position tests results	27
Table 2.7: Effect of separator and scoop on maximum efficiency	28
Table 2.8: List of companies and associated technologies	29
Table 3.1: 24 hour daily load summary for one typical rural household.....	34
Table 3.2: Annual resource data at the selected site	37
Table 3.3: Technical parameter of Trojan T-105 battery.....	41
Table 3.4: Summary of optimum simulation results for different off-grid systems	51
Table 3.5: Annual resource data at the supplementary site	53
Table 3.6: Summary of optimum simulation results at the supplementary site.....	54
Table 4.1: Specifications of the selected horizontal turbine	60

Nomenclature

A	Swept area of a turbine [m^2]
A_{PV}	Total area of a PV panel [m^2]
B_m	Damping coefficient [N.m/s]
β	Blade pitch angle [degrees]
C_0	Initial investment cost [US\$]
C_{1-6}	Empirical power coefficient parameter of a turbine
C_{BAT}	Battery capacity [Ah]
CO_2	Carbon dioxide [kg/year]
C_p	Power coefficient of a turbine
$C_{p,max}$	Maximum power coefficient
C_T	Total annualised costs of a system [US\$]
d	Number of autonomous days
$\frac{d}{dt}$	A change with respect to change in time
D	Turbine diameter [m]
E	Induced voltage in a stator [Volts]
E_{DG}	Energy generated by a diesel generator [Wh]
E_{HK}	Energy generated by a hydrokinetic system [Wh]
E_L	Required daily load [Wh]
E_{PV}	Output energy of a solar PV [Wh]
E_W	Energy generated by a wind system [Wh]
f	Electrical frequency [Hz]
G	Gear ratio

H	Turbine height [m]
i	Discount rate
i_d, i_q, i_0	d, q and zero axis reference frame stator currents [Amperes]
I_h	Hourly irradiance [kWh/m ²]
J_{eq}	Equivalent rotational inertia of a generator and a turbine [kg.m ²]
J_g	Rotational inertial of a generator [kg.m ²]
J_{wt}	Rotational inertial of a turbine [kg.m ²]
L_d, L_q	d, q axis reference frame inductances [H]
m	Water mass [kg]
N	Lifespan of the system [years]
θ_g	Rotor angular position of a generator [degrees]
ρ	Water density [1000 kg/m ³]
p	Number of pole pairs
P_{DG}	Rated power of a diesel generator [W]
P_m	Mechanical power of a turbine [W]
P_w	Power of the moving water [W]
p_f	Packing factor
ρ_w	Air density [1.225 kg/m ³]
R	Turbine radius [m]
R_s	Stator resistance of a generator [Ω]
t	Time
T_e	Electromagnetic torque of a generator [N.m]
T_m	Mechanical torque of a turbine rotor shaft [N.m]
$T_{w:g}$	Mechanical torque from a water turbine to a generator [N.m]
US\$	US Dollar

v	Wind/Water speed [m/s]
v_d, v_q, v_0	d, q and zero axis reference frame stator terminal voltages [Volts]
V_s	DC system voltage
ω_e	Electrical angular velocity of a generator [rad/sec]
ω_g	Angular velocity of a generator [rad/sec]
ω_m	Mechanical angular velocity of a turbine [rad/sec]
λ	Tip-speed ratio
λ_{opt}	Optimum tip-speed ratio
η_{BAT}	Battery efficiency
η_{CONV}	Converter efficiency
η_{DG}	Diesel generator efficiency
η_g	Generator efficiency
η_{PC}	Power conditioning efficiency
η_{PV}	PV module efficiency
η_t	Turbine efficiency
ψ_d, ψ_q	d, q axis reference frame stator flux linkage components [Wb]
Ψ_{PM}	Magnetic flux of the rotor magnets [Wb]

Abbreviations

AC	Alternating Current
CF	Cash Flow
COE	Cost of Energy
CRF	Capital Recovery Factor
DC	Direct Current
DCF	Discounted Cash Flow
DG	Diesel Generator
DHT	Darrieus Hydrokinetic Turbine
DHV	Davidson-Hill Venturi
DME	Department of Minerals and Energy
DOD	Depth of Discharge
DoE	Department of Energy
ESKOM	Electricity Supply Commission
GHGs	Concentration of Greenhouse Gases
HOMER	Hybrid Optimization Model for Electric Renewable
IRP	Integrated Resource Plan
IRR	Internal Rate of Return
MHR	Micro-Hydrokinetic River
MPPT	Maximum Power Point Tracking
NASA	National Aeronautics and Space Administration
NPC	Net Present Cost
NPV	Net Present Value
NREL	National Renewable Energy Laboratory

O&M	Operation and Maintenance
PMSG	Permanent Magnet Synchronous Generator
PV	Photovoltaic
RCT	River Current Turbines
TV	Television
US	United State
VDC	Direct Current Voltage
WRSG	Wound Rotor Synchronous Generator

CHAPTER 1: INTRODUCTION

1.1 Background

Electrification can play an important role to support the economic and social development of isolated rural societies. Demand for electrical energy is increasing while availability of fossil fuels (coal, diesel and petrol) is decreasing [1]. Concentration of greenhouse gases (GHGs) in the atmosphere causes changes in the global climate. In this light, the Kyoto Protocol (1997) was established as an agreement which enforces countries to reduce their combined greenhouse gas emissions by at least 5% during the period 2008 to 2012 [2]. The South African government signed an agreement regarding the Kyoto protocol in March 2002. A new Kyoto protocol period came into force from the beginning of 2013 and will conclude at the end of 2017.

According to the environmental statistics, South Africa is among the top 20 countries in the world with a high emission level of carbon dioxide [3]. It is the largest emitter of GHGs in Africa due to its fossil-fuel powered economy. Figure 1.1 also shows that coal is mainly used to generate electricity since it is largely used by the South African electrical utility company (ESKOM) [4]. In 2010, the South African national department of energy (DoE) released an integrated resource plan (IRP) to increase its electricity production target from renewable energy sources to 17.8 GW (mainly from wind, solar, biomass and small scale hydro) by 2030 [5].

When considering rural electrification, one of the basic questions to be addressed is affordability. Most rural residents are low-income earners, with low living standards, limited education and little access to information. To improve the living conditions of poor rural households, it is important to provide the affordable and reliable electricity. Small remote

rural communities often require electricity for small loads such as lighting, refrigeration, entertainment, etc. [6,7]. A solution to remote rural electrification is made possible by means of approaches/techniques such as grid-extension, diesel generator (DG) or a small-scale off-grid renewable energy system. However, grid-extension for small isolated remote areas can be expensive [8,9]. The low consumption rate per unit disables the recovery of the initial grid-extension costs. Furthermore, electrical tariff increases makes grid-extension unsustainable for low-income remote rural communities.

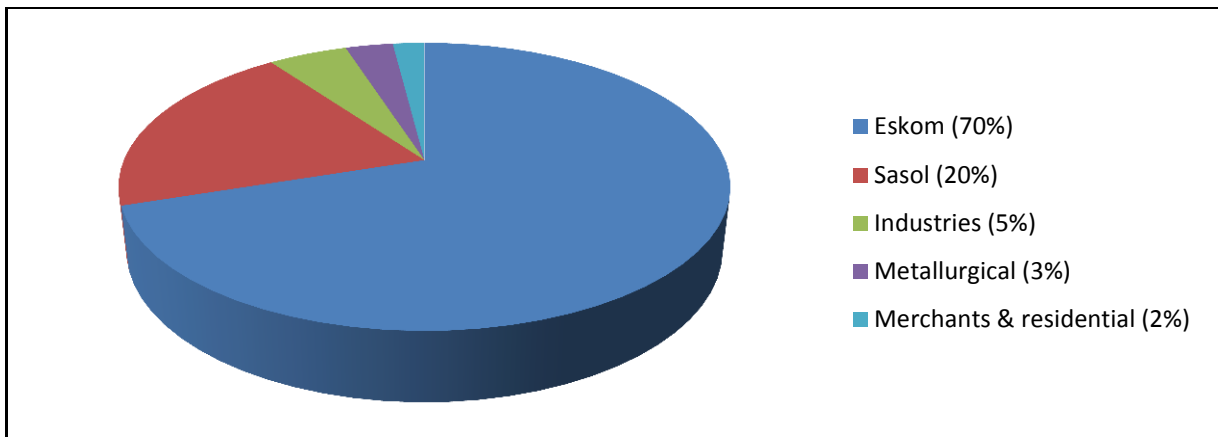


Figure 1.1: Coal usage in South Africa (excluding exports) [10]

DG is the most popular and affordable option for remote rural areas to compensate for grid extension [11]. It requires very low initial capital cost and can be used whenever needed. Nevertheless, a DG approach continues to be more unsustainable for remote rural residents due to factors such as the increase of diesel price, emission of GHGs and difficulties in transporting fuel to other remote areas. Consequently, this enables the use of renewable energy sources to be more economical.

Renewable technologies (biomass, wind, solar, hydro and geothermal) are offering clean sources of energy. They can provide a cost-effective source of electricity to small rural areas situated far from utility grid lines. Among different renewable energy technologies,

hydropower generation holds prime position in terms of its contribution to the world's electricity generation [12-15]. However, large scale hydropower has drawbacks such as the expensive construction of dams and disturbance of aquatic ecosystem. Hence, small-scale conventional hydropower is a better option to supply electricity to isolated rural areas in close proximity to adequate water resources [12]. There is no internationally agreed definition of small, mini and micro hydro plants, hence this study is considering the United States definition shown in Table 1.1 below [16].

Table 1.1: Small-scale hydropower classification by power generation

Classification	Size in KW
Small hydro	1,000-30,000
Mini hydro	100 – 1,000
Micro hydro	<100

Small-scale conventional hydropower is usually referred as a run-of-river system. It is a much more concentrated energy resource compared to wind and solar generation. It generates electricity throughout the day and night; hence, can offset the non-continuous availability of solar and wind energy. However, it has some economic limitations compared to other small-scale renewable energy sources. Minor civil engineering works such as diversion weirs, channels and pipelines need to be done and it can only operate in rivers with adequate elevation [12, 16 and 17]. Therefore, it cannot be used in run-of-rivers/waterways with little or no elevation at all. This results in neglect of a flowing water resource.

It has been proved that one-third of the world's population does not have access to electricity, but does have access to flowing water [18]. Apart from conventional hydropower generation, hydrokinetic is a new category of hydropower generation that can be used in waterways with

little or no elevation at all. Harnessing hydrokinetic energy is similar to converting wind energy into electrical energy. It generates electricity by making use of underwater wind turbines to extract the kinetic energy of flowing water instead of the potential energy of falling water. Hence, no construction of dams or diversions is necessary; it therefore creates a minimal environmental footprint [19-22]. It means that, theoretically, there are a huge number of potential sites available for micro-hydrokinetic power generation as opposed to conventional hydropower generation. Hydrokinetic is a promising new technology and few researches have been conducted. There is still a lack of its application, most especially in rural areas with flowing water resources within Africa. Additionally, its commercial viability still needs to be proved and analysed.

1.2 Problem Statement

- Some rural areas are not served by the grid and might be in close proximity to permanent water flow with little or no elevation. In such areas it is impossible to install a traditional micro-hydro system. An off-grid MHR system is a promising technology to install. People are unaware of this technology since it is still in the development stage.
- To improve the living conditions of rural residents, there is a need to discover a reliable and cost-effective electrification method. A techno-economic analysis of the proposed off-grid MHR system needs to be evaluated against the analyses of the other possible off-grid energy sources at the study site.
- Most of the available software packages/tools for modelling renewable energy systems do not have hydrokinetic components. Hence, it is difficult to study/analyse the performance of the off-grid MHR system.

1.3 Objectives of the Study

The aim of this study is to demonstrate the technical and economic viability of the proposed off-grid MHR system for rural residents not served by the grid and in close proximity to flowing water.

The objectives of this study are as follows:

- To review current status, various developments and technologies of the off-grid MHR technology locally and globally within a rural electrification context.
- To perform an economic benefits study of the proposed system in comparison with other possible electrification options (solar, wind and DG) within the study site.
- To develop a mathematical model for an off-grid MHR system.
- To simulate the proposed system in MATLAB/Simulink software as submitted to varying water flow and compared to a wind generation counterpart.

1.4 Research Methodology

To achieve the above-mentioned objectives, the methodology is as follows:

Literature Review: A thorough survey of small-scale hydrokinetic systems has been carried out in order to create an awareness regarding research gaps and usage. The survey includes technologies, developments, suggestions, evaluations, applications in rural electrification and hydrokinetic potential within South Africa.

Selection of rural community: A typical rural area in Kwazulu-Natal has been selected as a study site. The site is situated at 30.6° Latitude South and 29.4° Longitude East. Electricity requirement of the selected rural site has been established through load forecasting. The

proposed system is projected to supply basic needs such as lighting, communication and domestic motor applications. Annual renewable energy resources data of the selected site were collected [23-25]. National Aeronautics and Space Administration (NASA) and RETScreen have been used as climate database tools.

Economic and Environmental Analysis: Economic and environmental analysis of the proposed MHR system has been performed through the use of the Hybrid Optimization Model for Electric Renewable (HOMER) software. This software was developed by the National Renewable Energy Laboratory (NREL) of the United State of America (USA) [26]. It has been used to determine the best cost effective off-grid option (among hydrokinetic, Solar, DG and wind) to fulfil the basic electrical load requirement at the study site.

System Modelling and Simulation: A mathematical model has been developed to describe the performance of the proposed system. MATLAB/Simulink software was used to apply the developed model and simulate the behaviour of the proposed system under varying water speed and compared to a wind generation system.

1.5 Hypothesis

1. An off-grid micro-hydrokinetic river system generates electrical energy more cost-effectively than wind, solar or diesel generator supplying the same rural load at the study site.
2. In areas with both flowing water and an adequate wind resource within South Africa, an off-grid micro-hydrokinetic river system generates electricity markedly better and cheaper than a micro-wind system for the same amount of power generation.

1.6 Limitation of the Study

The study has been conducted with the following limitations:

- This study focuses only on literatures related to micro-scale hydrokinetic river systems (<100kW) since it is suitable for off-grid rural electrification. Large-scale hydrokinetic systems such as ocean, marine, etc., are not considered in the review.
- Mathematical modelling of batteries, power electronic and mechanical control circuits is beyond the scope of this study.
- No new turbine design was considered in this study since hydrokinetic turbines are already available in different forms.

1.7 Contribution to Knowledge

- The author presents a global review of relevant micro-hydrokinetic literatures based on recent development studies, suggestions, relevant technologies, turbine manufacturers, and applications for rural electrification. This will enable the researchers to identify more research gaps and the correct equipment for a specific application.
- The financial feasibility study of an off-grid MHR system as compared to solar, wind and DG systems at the specified study site has been conducted. This enables the correct selection of an affordable and reliable electrification option from among the existing ones.
- The development of a MATLAB/Simulink model to assist with performance evaluation of an off-grid MHR system during the planning stage is presented.

1.8 Research Output

Journal Publications:

- H.J. Vermaak, K. Kusakana, **S.P. Koko**, “*Status of Micro-Hydrokinetic River Technology in Rural Applications – a review of literature*”, *Renewable and Sustainable Energy Review*, Volume 29, pp. 625-633, January 2014.
- **S.P. Koko**, K. Kusakana, H.J. Vermaak, “*Micro-hydrokinetic for Remote Rural Electrification*”, *International Journal of Electrical, Computer, Electronics and Communications Engineering*, Volume 8 (11), pp. 1384-1388, November 2014.

Conference Papers:

- **S.P. Koko**, K. Kusakana, H.J. Vermaak, “*Modelling and Performance Analysis of a Micro-hydrokinetic River System as compared to Wind System*”, *South African Universities Power Engineering Conference (SAUPEC)*, 28-30 January 2015.

1.9 Outline of the Dissertation

Chapter 1 is an introduction to the dissertation which presents background, problem statement, objectives, methodology, hypothesis, delimitation of the study, as well as the research outputs.

Chapter 2 provides a comprehensive overview of current hydropower usage and the potential within South Africa. The primary focus is based on the global review of MHR applications for rural electrification. A review of current MHR technologies, developments, suggestions, evaluations, improvements as well as the turbine manufacturers is also included.

Chapter 3 provides economic and environmental analysis of the proposed off-grid MHR system when used to supply a rural load demand at the study site. This economic benefit is compared to the one offered by other possible off-grid electrification techniques such as solar photovoltaic (PV), wind generation or DG if used to supply the same rural load demand. This comparison has been performed by means of HOMER software.

Chapter 4 covers the development of the mathematical model for an off-grid MHR system. MATLAB/Simulink library has been used to develop the model.

Chapter 5 discusses the simulation results of the developed model. Performance of the proposed system is compared to that of a wind generation system in order to reveal the technical advantage/benefit of using this proposed technology even in areas of South Africa with both adequate wind and flowing water resources.

Chapter 6 presents the conclusions and suggests future areas of research to be carried out in order to promote the application of MHR technology.

CHAPTER 2: LITERATURE REVIEW

2.1 Introduction

This chapter presents a brief review of the current status and potential of hydropower generation in South Africa. It reviews the global status of a MHR system in remote rural applications. It also presents various hydrokinetic technologies, manufacturers and recent development studies focusing on efficiency improvement.

2.2 Status of Hydropower Generation and Potential in South Africa

South Africa has a considerable hydropower potential for small-scale to large-scale hydropower generation, as revealed by the department of minerals and energy (DME) of South Africa [27]. However, no major development has been made within the local hydropower industry for almost 30 years. Cheap and reliable grid electricity inhibits interest in hydropower technology [28]. Little attention has been paid to utilizing off-grid micro-hydropower for rural electrification.

Currently, around 700 MW installed hydropower capacity exists in South Africa, as shown in Table 2.1. The estimated firm potential for hydropower within South Africa stands at 5160 MW. This excludes pumped storage and imported hydropower. It shows that the firm hydropower potential of South Africa is almost 7 times greater than the presently installed hydropower capacity.

Figure 2.1 shows all areas with hydropower potential in South Africa. The Eastern Cape and Kwazulu-Natal provinces hold significant capacity for the development of small hydropower

plants. The commercial exploitation of South Africa's small-scale hydropower technology is also limited. Approximately 49% of the small-scale hydropower potential is in operation.

Table 2.1: Total capacity and potential for macro and small-scale hydropower in SA
(Excluding pump storage & imported) [27]

Hydropower Category and Size (MW, Kw)	Hydropower Type	Installed Capacity (MW)	Potential for Development	
			Firmly Established (MW)	Additional Long-Term (MW)
Pico (up to 20 kW)	Conventional	0,02	0,1	0,2
	Unconventional	-	-	60,0
Micro (20 kW to 100 kW)	Conventional	0,1	0,4	0,5
	Unconventional	-	-	3,3
Mini (100 kW to 1 MW)	Conventional	8,1	5,5	3
	Unconventional	-	-	2
Small (1 MW to 10 MW)	Conventional	25,7	27	20
	Transfers	-	25	5
	Refurbishment	-	11	-
Subtotal for small/mini/micro and pico hydropower in South Africa		33,92	69	94
Conventional macro hydropower (> 10 MW)	Diversion fed	-	3 700	1 500
	Storage regulated head	653	1 271	250
	Run-of-river	-	120	150
Subtotal for renewable hydropower in SA		687	5 160	1 994

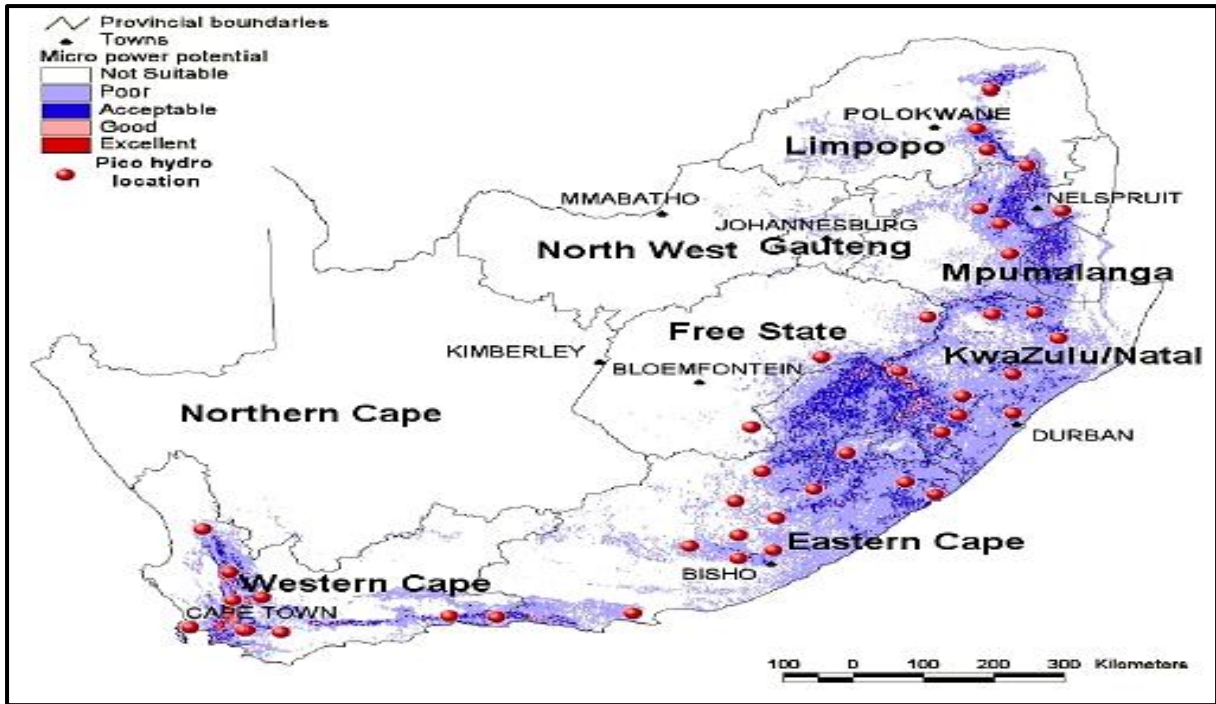


Figure 2.1: Areas with conventional micro-hydropower potential in South Africa [27, 28]

It is clear that Table 2.1 did not include the potential power production from unconventional hydrokinetic technology. Hence, there is a vast amount of untapped clean energy that can be found in low elevation water-flow and waterways. This is where hydrokinetic energy comes into play. Hence, theoretically South Africa has a large amount of hydropower potential compared to the estimated potential. Small-scale hydrokinetic technology can make a significant contribution to the energy needs in remote rural areas of South Africa. It is cheaper than the conventional small-scale hydropower technology since it does not require civil engineering works [12, 16 and 17].

2.3 Hydrokinetic Technology

Hydrokinetic technology is obtained from waves, tides, ocean currents, natural flow of water in rivers, or marine thermal gradients [29,30]. However, the scope of this project is limited to

applications in free-flowing rivers only, since it is suitable for small-scale electrification. Hydrokinetic technology shares lot of similarities with wind turbine systems in terms of the physical principles of operation and electrical hardware, as shown by equation (2.1) [31]. Since water is 800 times denser than air, hydrokinetic turbines extract enough power even at low speed [18, 32-35]. This simply implies that the amount of energy generated by a hydrokinetic turbine is much greater than that produced by a wind turbine of equal diameter and performance under equal wind and water speed.

$$P_{HK} = 0.5 \times \rho \times A \times v^3 \times C_p \quad (2.1)$$

Where, ρ = water density (1000 Kg/m³);

A = hydrokinetic turbine swept area (m²);

v = water speed (m/s);

C_p = power coefficient of a hydrokinetic turbine.

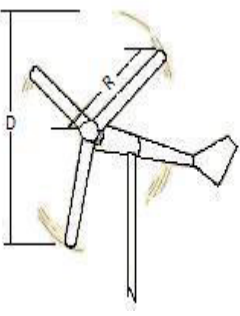
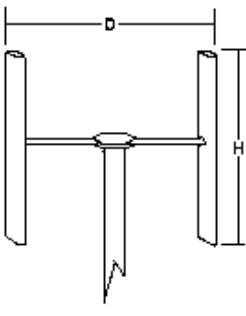
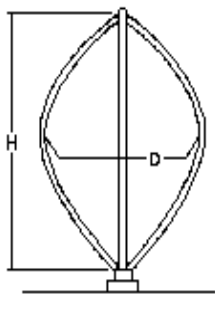
Hence, compared to wind generation, hydrokinetic has high energy density and good predictability since the direction of the flowing water does not change [36-38]. The swept area is calculated based on the turbine configuration as shown in Table 2.2 below.

Where, D = turbine diameter (m);

H = turbine height (m);

R = turbine radius (m).

Table 2.2: Swept area for different rotor blade configurations [39]

Rotor blade arrangement	 <p style="text-align: center;">Conventional rotor</p>	 <p style="text-align: center;">H-Darrieus rotor</p>	 <p style="text-align: center;">Darrieus rotor</p>
Swept Area	$A = \pi \cdot R^2$	$A = DH$	$A = 0.65DH$

2.4 Hydrokinetic Turbine Technologies and Studies

Numerous conversion concepts have been developed to extract kinetic energy from flowing water. Among these concepts, hydrokinetic turbines are the most commonly used ones. Hydrokinetic turbines are rotary machines that use kinetic energy of moving water to generate mechanical energy by making use of blades. When used in rivers or artificial waterways, it is generally referred to as river current turbines (RCT) [40, 41]. RCT are generally within the range of 1 kW to 10 kW [42]. They are typically configured either as horizontal or vertical axis turbines similar to those developed for wind generation. The selection of turbine type depends on the flow type, velocity and desired electrical output of the system [43]. Technical advantages and disadvantages associated with horizontal and vertical turbines are presented in Table 2.3 below.

2.4.1 Horizontal axis turbines

Horizontal axis turbines have axes parallel to the fluid flow and employ propeller type rotors. Various arrangements are shown in Figure 2.2. Inclined axis turbines (i) have mostly been studied for small river energy converters. Other axial-flow turbines (ii, iii & iv) are similar to wind turbines in terms of design and structural point of view [40, 43-45].

2.4.2 Vertical axis turbines

The vertical axis turbines (Figure 2.3) have rotor axes orthogonal to the water flow but parallel to the water surface. They can be divided into vertical axis (axis vertical to water plane) and in-plane axis (axis on the horizontal plane of the water surface). The in-plane axis turbine (i) is generally a drag based device and is said to be less efficient than its lift-based counterparts. Among the vertical axis turbines (ii, iii, iv, v & vi), the most commonly used ones are the Darrieus type turbines. The straight bladed Darrieus type, namely H and Squirrel cage are considered as feasible options for hydro applications [42, 44]. In cases in which the water flow rate is relatively limited, H-Darrieus can be useful [29].

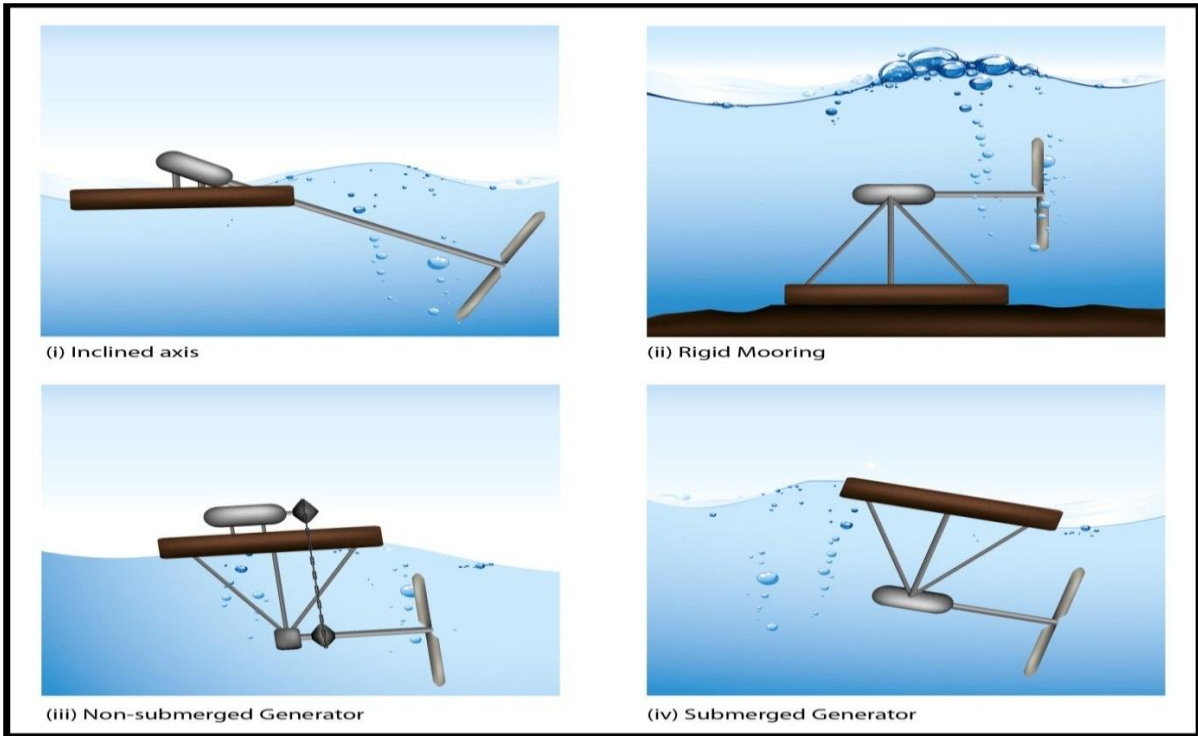


Figure 2.2: Horizontal axis turbines [40, 44]

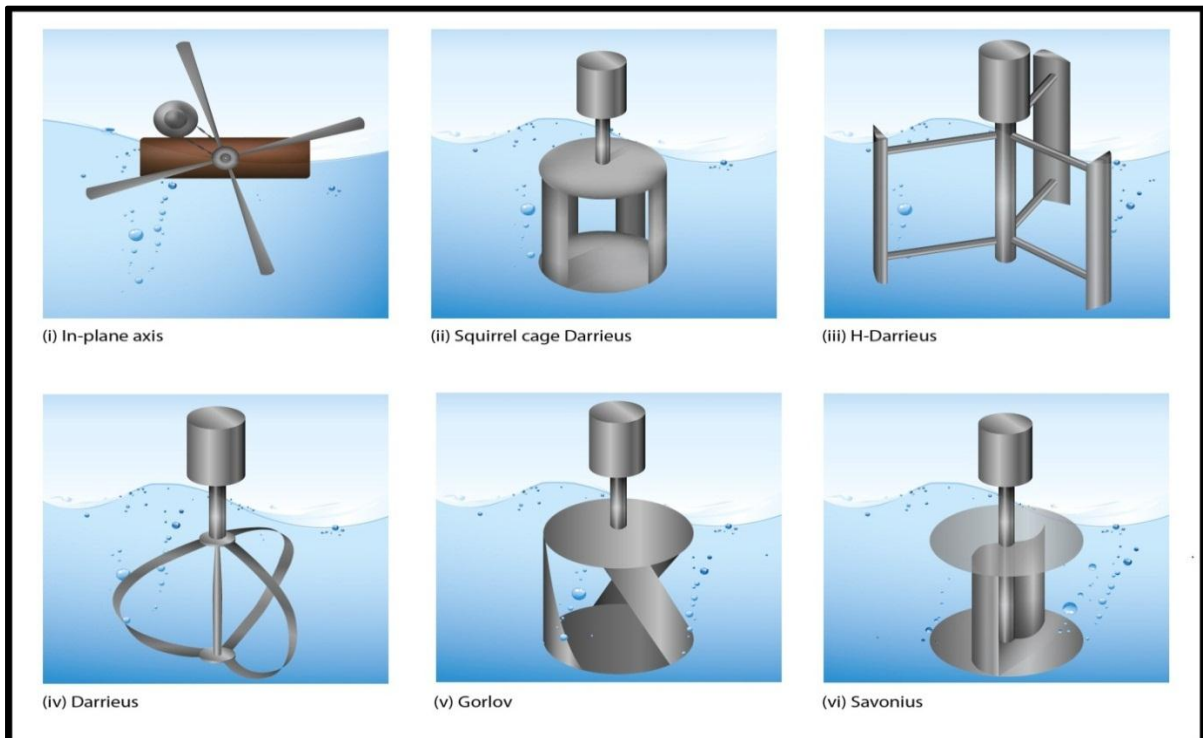


Figure 2.3: Vertical axis turbines [40, 44]

Table 2.3: Technical advantages and disadvantages of horizontal and vertical turbines

Turbine Configurations	Advantages	Disadvantages
Horizontal Axis Turbines	Self-starting capability [40, 44].	High generator coupling cost due to underwater placement [40, 44].
	Gearbox elimination possible through the use of a duct [31].	Ducts cannot be easily used for floating purpose [40].
	Optimum performance is achieved at higher rotor speed (marine/tidal conversion), this facilitates the reduction of reduced gear coupling [40].	
	Active control by blade pitching allows greater flexibility in over speed protection and efficient operation [40].	
Vertical Axis Turbines	Low generator coupling costs due to placement above water [29, 31, and 40].	Due to low starting torque, may require starting mechanism [40, 42, and 44].
	Emits less noise due to reduced blade tip losses [40].	Generates torque ripple in the output [40, 42, and 44].
	Can rotate unidirectional even with bi-directional fluid flow [40, 43-45].	Lower efficiency [40, 42, 44 and 45].
	Cylindrical shape of the Darrieus turbine allows	Due to the difficulty of connecting the generator to the

	convenient mounting of various ducts [40].	turbine a bevelling gear is needed to convert the horizontal rotational movement into vertical movement [31].
	More suitable for operation under shallow channel with varying water velocity and shallow stream with limited water flow rate [29, 40].	

2.4.3 Recent studies on micro-hydrokinetic river turbine developments

Some recent studies on development and performance evaluation of hydrokinetic river turbines were carried out as discussed below.

Anyi and Kirke [46] reviewed works involving small axial flow hydrokinetic turbines specifically for generating electrical power for off-grid remote communities, and suggested improvements to overcome a major problem. Turbines mounted on pontoons or suspended using pivot arms from river banks or from jetties are reported able to produce about 1 kW to 2 kW of electrical power suitable for remote homes. A deflection device and system that uses a rotor with swept-back blades was suggested to overcome debris problems. By making the system resistant to debris, efficient axial flow turbines could be used practically in tropical rivers.

Kirke [47] reviewed the recent developments in open flow current turbine design and explored some potential advantages of ducted or “diffuser-augmented” current turbines.

These include improved safety, protection from weed growth, increased power output and reduced turbine and gearbox size for a given power output.

Van Arkel et al. [20] introduced a new type of hydrokinetic power generator, ideally suited to relatively small shallow rivers and channels. The design utilizes rectangular hydroplanes ('sails') moving around the device. The device extracts energy from a flow of water using an elongated vertical axis turbine, where a series of sails are mounted between two belts at the top and bottom of the device, rotating in the horizontal plane. The concept would be ideally suited to relatively shallow rivers and channels, because it can be designed to fill more of the channel's cross-sectional area than the circular rotor of a standard marine turbine or array of turbines.

Birjandi et al. [48] investigated the macro-turbulent flow structures' interaction with vertical hydrokinetic river turbine. The results aim to characterize flows in rivers to improve our understanding of the impact of turbulent inflow structures on hydrokinetic power generation, and to contribute to the optimization of vertical and horizontal axis hydrokinetic turbines. Furthermore, power spectrum measurements provided data to improve the fatigue lifetime estimation of vertical turbines, as the scale and intensity of turbulent structures can play an important role.

Kirke [49] carried out some tests on several helical and straight blade Darrieus type cross flow hydrokinetic turbines with and without variable pitch, with and without slatted diffusers. Variable pitch has been suggested to increase starting torque and efficiency, ducts to increase power output and helical blades to produce smooth torque. These tests were performed at velocities ranging from less than 1m/s up to 5m/s in the Nerang River in Australia and Campbell River in Canada. The helical blades made little difference to efficiency and starting torque but the turbine ran smoothly, unlike that with fixed pitch straight blades. The diffuser increased power output by a factor of up to 3 compared to the same turbine without a

diffuser, but this augmentation factor was not achieved in all tests, and the cost-effectiveness of the diffuser is doubtful. These findings suggest that variable pitch cross flow hydrokinetic turbines should be further investigated.

2.5 Hydrokinetic Generators

Electric generators are devices that convert mechanical energy into electrical energy. Generators can generally give direct current (DC) or alternating current (AC). Choosing a generator for specific application is governed by a number of factors such as the prime mover speed, required output power, range of operation and use. Hydrokinetic plants use the same generators as used by conventional hydro and wind power generation. Generally, the two commonly used generators in wind and hydrokinetic turbine systems are synchronous and induction generators [31]. Hermann [38] demonstrated that using a DC generator to charge batteries via small micro hydropower plants is not a viable solution for rural electrification. DC generator usage is restricted due to low transmission efficiency and high maintenance of brushes and commutator segments. Hence, only synchronous and induction generators are reviewed in this section. Table 2.3 highlights the advantages and disadvantages of PMSG and Induction generators only.

2.5.1 Induction generators

Induction generators are the most common types of electrical generators used in stand-alone power generation systems. These types of generators are also favoured for small-scale electricity production due to their simplicity, robustness, small protection capacity and small size per generated kW [50]. Induction generators such as doubly-fed and squirrel cage, are

available in the market [31, 51]. Most commonly used are the squirrel cage rotor types since they are brushless. When using induction generators in isolated operation i.e. for off-grid operation, the excitation is conducted through a parallel connection of a capacitor bank [52]. Advantages and disadvantages are shown in Table 2.4 below.

2.5.2 Synchronous generators

These types of generator are equipped with a DC electric or fixed magnet excitation system. The one equipped with a DC electric excitation is called a wound rotor synchronous generator (WRSG) and the one equipped with fixed magnet excitation is called PMSG. The main advantage of a WRSG compared to a PMSG is that it can produce reactive power and also regulate the voltage. This allows an opportunity to control the power factor based on the electrical load conditions. Nonetheless, PMSG has gained more popularity among turbine manufacturers. Instead of demanding the external DC excitation source, it uses a fixed magnet excitation system. It has cornered the market in small-scale hydro and hydrokinetic energy conversion systems as well. It is simple and has high reliability, low noise and high power density [31]. It can run isolated from the grid and produce power since excitation is not grid-dependent. Rotor copper losses and frequent maintenance are eliminated due to the absence of brushes, slip rings and rotor windings. The disadvantage of a PMSG is that the frequency of the induced voltage changes with the mechanical speed of the rotor. Hence, a frequency converter is needed to match the induced voltage frequency with the grid frequency. A grid side converter is also needed to regulate output voltage and power factor since the field provided by magnets cannot be regulated [53]. PMSGs are classified based on the rotor configuration. They have a wound stator with either non-salient pole (cylindrical) rotor or salient pole rotor.

- *Non-salient pole rotor*

Non-salient pole rotors consist of the cylindrical rotor made up of solid forged steel. The magnets are hidden inside the rotor. The rotors have higher axial length and produce low noise level. They are generally used in high speed application.

- *Salient pole rotor*

Salient pole (surface mounted) rotors consist of the magnets mounted on the surface of the rotor instead of inside. This on-surface mounting leads to simplicity in rotor design. The rotors have higher axial length and have low noise levels. They are generally used in low and medium speed application since they consist of a large number of poles compared to non-salient pole rotors. Due to low speed operation of multi-pole, the rotor shaft can be directly attached to the turbine. The absence of a gearbox reduces system cost and prevents regular maintenance and mechanical losses.

Table 2.4: Advantages and disadvantages of synchronous and induction generators

Generator Type	Advantages	Disadvantages
Synchronous Generators (Permanent Magnet type)	No extra field excitation needed compared to a wound rotor synchronous generator [54].	Frequency inverter and rectifier needed during variable speed.
	Have higher efficiency and low inertia due to direct drive permanent magnet [54, 55].	To get a suitable frequency at low speed, it requires large number of poles and an increase in turbine radius.
	Can operate at slower speeds, hence allowing the direct-drive train without gearbox [54].	The field provided by magnets is not controllable.
	Lower maintenance costs due to absence of brushes.	
	High torque density minimizes the size [31].	
	They are simple to use and provide reliable power generation at high power factor [54].	
	Longer lifespan due to high quality magnets [56].	
Induction Generators	Can supply constant voltage and constant frequency at variable speeds [31].	Lower efficiency compared to synchronous generator.
	High reliability [29].	Needs speed faster than the synchronous speed. At low river flow speeds, a need exists for a speed increaser.
	Cheap and simple to design [29].	Consumes reactive power leading to poor power factor.

2.6 Hydrokinetic Resource Assessment Studies

A convincing aspect of power generation from hydrokinetic technology is the predictability of the resource. Immediately the water flow speeds at a site have been well characterized it is possible to make accurate predictions of the electricity that would be generated by an array of turbines. The direction of the water currents facilitates the decision of ensuring optimal device orientation at the site or selecting the type of device suitable for a site [57]. When the energy is extracted in any river, the extractor is operating at different speeds and within different levels [58]. The data needed for the development of a hydrokinetic energy generation location become highly site specific. To date, such assessments of hydrokinetic resources are limited, but nevertheless increasing. In addition, the global river databases are not readily usable for river energy analysis.

Lalander [59] showed that the models that have so far been used to estimate the resource in Norway Dal River are uncertain, since they do not account for the fact that the velocities and the water levels are altered when energy is extracted. A channel in the Dal river, the Söderfors channel, is situated downstream of a hydropower plant and was simulated with the numerical model MIKE. To demonstrate these variations, water level alteration via turbines was simulated. It was shown to be a lot less than the water level alteration caused by the level change in the downstream lake. Velocity profiles measured at several different locations were used to estimate how the power coefficient was changed. Four turbine configurations were studied and it was shown that changes in the power coefficient were prominent only for a vertical shear profile with a strong gradient.

Briand and Ng [60] presented the approach developed by RSW (consulting engineers) firm to design a hydrokinetic site in a riverine environment. This approach was studied from resource assessment to detailed engineering design. It focuses on the development of hydrokinetic

sites from the first stages of identifying river reaches with potential (resource assessment, ranking sites from most interesting to least interesting) to justify hydrologic, hydraulic, environmental, and economic studies (pre-feasibility and feasibility studies) and finally to do a detailed engineering design of a prototype and of an eventual turbine farm.

Duvoy and Toniolo [61] developed a new tool called HYDROKAL for hydrokinetic resource assessment in rivers. This tool includes a user-defined efficiency factor to account for turbine efficiency, which is fundamental for estimating the energy that could be harvested from the river. For each river cross-section along the computational domain, maximum velocity and specific discharge are identified to assist in estimating the stability of the river reach and, thus, the feasibility of installing an in-stream turbine. A Python script was also developed to export the results from HYDROKAL to CCHE2D. HYDROKAL is applied to a reach of the Tanana River at Nenana, Alaska, USA.

2.7 Micro-Hydrokinetic Optimization Studies

With energy demands and costs increasing, improving the energy efficiency of a generation system is critical since it can have an impact on the reduction of greenhouse gases emission. Several MHR technology optimization techniques/methods based on cost and performance were studied.

2.7.1 Cost optimization

Anyi and Kirke [62] demonstrated that the construction of an optimum hydrokinetic turbine blade can be accomplished by using common tools, common materials and simple jigs. The simplified method of blade construction allows it to be made in a remote village near to

where it will be used and maintained. This will reduce the total cost of a turbine system significantly, because by producing turbine components locally, the costly currency exchange and importation cost can be avoided. Furthermore, local construction creates job opportunities which could help remote people financially.

2.7.2 Performance evaluation

Golecha et al. [63] carried out an experimental investigation on the performance improvement of a modified Savonius rotor by providing a deflector plate on the returning blade side. The experiment was conducted to find the adequate configuration of the deflector plates on the returning blade side and advancing blade side. Results conclude that the deflector plate at its optimal position increases the power coefficient (C_p) by 50% for a single-stage modified rotor. The performance deteriorates by increasing the number of stages. This suggests that the use of a single stage modified Savonius rotor is better compared to two and three stages. A summary of the performance tests results of different Savonius rotor configuration stages is shown in Table 2.5 below.

Table 2.5: Coefficient of power improvement of different modified Savonius rotor configuration stages

No. of stages of modified Savonius rotor	% C_p improvement
Single stage	50%
Two stage (phase shift of 0°)	42%
Two stage (phase shift of 90°)	31%
Three stage	15%

Golecha et al. [64, 65] studied the performance of a modified Savonius water turbine with two deflector plates. The objective of this study was to identify the optimal position of the deflector plate placed upstream to the flow, which would increase the power generated by the rotor. The results suggested that the two deflector plates placed at their optimal positions upstream to the flow increased the maximum power coefficient ($C_{p,max}$) to 0.35, as opposed to 0.21 with a single deflector plate on the returning blade side and 0.14 without a deflector plate. This shows the promise of using deflector plates on both the advancing blade side and returning blade side to increase the performance of the modified Savonius rotor. A summary of the deflector optimum position tests results is shown in Table 2.6.

Table 2.6: Summary of the deflector optimum position tests results

No. of stages of modified Savonius rotor	$C_{p,max}$	Tip speed ratio
Zero deflector plate	0.14	0.7
Single deflector plate <i>(on the returning blade side)</i>	0.21	0.82
Two deflector plates <i>(additional deflector blade on advancing blade side)</i>	0.35	1.08

Batten et al. did the design of a floating free stream energy converter in [66]. In [67] they analysed the potential of using the floating body structure to increase the efficiency of this free stream energy converter. It was proved that the use of the separators and scoops can be a cost effective method of increasing the power output. From the results, it was shown that the addition of a 90° separator caused the generated power to increase by almost 100%. For the 45° separator the increase in generated power was not so large. The inclusion of a scoop to the 45° separator increased the generated power to almost that of the 90° separator. The

detailed efficiency test results on the effect of the separator and scoop are shown in Table 2.7 below. Floating water wheels may be a viable option for small-scale electricity generation in remote locations due to their simplicity and low costs.

Table 2.7: Effect of separator and scoop on maximum efficiency

Condition	Efficiency (based on blade area)
No Separator	41%
90° Separator	87%
45° Separator	70%
45° Separator & Scoop	81%

2.8 Micro-Hydrokinetic Manufacturers and Associated Technologies

Technology selection involves finding different manufacturers of technologies. Some companies have already developed hydrokinetic river technologies. Table 2.8 below shows the list of companies and relevant technologies. Specifications such as minimum/maximum operating speed and maximum output power based on the types of the manufactured turbines are also shown.

Table 2.8: List of companies and associated technologies

Manufacturers	Device Name	Turbine Type	Min/Max Speed	Power Output
Lucid Energy Pty. Ltd (USA) [68]	Gorlov Helical Turbine	Helical Darrieus Cross-axis	0.6 m/s /no limit	Up to 20kW, depends on size
Thropton Energy Services (UK) [69, 70]	Water Current Turbine	Axis flow propeller	0.6/ m/s depends on diameter	Up to 2kW at 240V
Tidal Energy Pty. Ltd (Australia) [71]	Davidson-Hill Venturi (DHV) Turbine	Cross flow Turbine	Min 2 m/s	From 4.6kW
Seabell Int. Co., Ltd. (Japan) [72]	Stream	Dual, Cross- axis	0.6 m/s /no limit	0.5 -10kW models
New Energy Corporation Inc. (Canada) [73]	EnCurrent Hydro Turbine	Cross-axis	Max 3 m/s for maximum power	5kW (and 10kW)
Eclectic Energy Ltd. (UK) [74]	DuoGen-3	Axial flow propeller	Min 0.93 m/s /4.63 m/s max	8 amps at 3.09 m/s
Alternative Hydro Solutions Ltd (Canada) [70]	Free-stream Darrieus Water Turbine	Cross-axis	0.5m/s depends on diameter	Up to 2-3kW
Energy Alliance Ltd (Russia) [69]	Sub-merged Hydro Unit	Cross-axis	Min 3 m/s	1-5kW (and >10kW)

2.9 Conclusion

A global review of relevant hydrokinetic literatures for rural electrification and the technologies involved was presented in this chapter. Many development studies based on efficiency improvement of MHR turbines have already been done. There is a lack of applications and studies demonstrating the technical, economic and environmental benefits offered by the off-grid MHR system. Moreover, there are no studies demonstrating the optimal sizing technique of this proposed system. This hinders the deployment of MHR technology.

South Africa has a considerable hydropower potential for small- to large-scale hydropower. Moreover, there are many flowing water resources with low or no elevation at all. These water resources are neglected since people are unaware of the potential electrification benefit. Hence, resource assessment study of different rivers in close proximity to isolated rural dwellings within South Africa needs to be undertaken. This will facilitate the use of untapped flowing water resources.

This chapter also revealed different small-scale hydrokinetic turbine manufacturers available worldwide, as well as technologies involved. There are different types of turbines and generators to be used for hydrokinetic generation. It is important to make the right selection for a specific application. Thus, their benefits and drawbacks of different hydrokinetic technologies were presented in this chapter.

CHAPTER 3: ECONOMIC AND ENVIRONMENTAL ANALYSIS

3.1 Introduction

In this study, a typical area with adequate availability of flowing water, solar and wind resources has been selected, as mentioned in chapter 1. The selection of the best off-grid energy source among the existing ones requires a comparative economic analysis. Therefore, the primary objective of this chapter is to demonstrate the economic benefits offered by each individual off-grid energy source. For a better comparative purpose, one off-grid energy source at a time has been simulated to supply electricity to the rural load at no electricity shortage. DG as a non-renewable energy source is also included among the above mentioned off-grid renewable energy sources. Grid extension has also been considered as a comparison tool for determining an economical distance between grid transmission lines and the study site. These techno-economic analyses have been performed by means of HOMER software. Finally, a second rural site with multiple renewable energy sources has also been selected for supplementary analysis.

3.2 Economic Methods

To perform a comparative cost analysis, financial indicators such as payback period, net present value (NPV) and internal rate of return (IRR) are generally used [75]. This allows for a suitable project selection decision. HOMER software usually shows the net present cost (NPC) to analyse the life-cycle cost of the system in order to determine the cost effectiveness

of the system [76]. The user must enter both technical and financial information of system components so that it can calculate the cost of installing and operating the system over its lifetime. It will then list the optimization results by starting with configurations offering least NPC.

3.2.1 Net present value and net present cost

NPV (US\$) is the most common financial decision-making technique used in selecting a project. It involves costs and benefits offered by a project over its entire lifespan. It employs streams of cash flows ($C_0, CF_1, CF_2, \dots, CF_N$) to estimate the current value of money. The best project to be selected is the one that offers the largest positive NPV since it reveals more capital. HOMER determines the NPV of an investment/project by making use of equation (3.1) below [75, 77].

$$NPV = \frac{CF_1}{(1+r)} + \frac{CF_2}{(1+r)^2} + \dots + \frac{CF_N}{(1+r)^N} - C_0 = \sum_{t=1}^N \frac{CF_t}{(1+i)^t} - C_0 \quad (3.1)$$

Where, C_0 = initial investment cost (US\$);

CF_t = net cash flow of the investment in year t (US\$);

i = discount rate;

N = lifespan of the system (years).

If an NPV is negative, it usually suggests that an investment will result into a loss instead of a net profit. HOMER shows a negative NPV by making use of a positive NPC (US\$). NPC is important because it includes not only investment, but also costs such as total cost of installing, operating and maintaining the system over its lifetime. The project offering the

lowest NPC is the best cost-effective option. HOMER calculates the NPC by making use of equation (3.2) below [78].

$$NPC = \frac{C_T}{CRF} \quad (3.2)$$

where, C_T = total annualised costs of system (US\$);

CRF = capital recovery factor.

CRF is the ratio of the constant annual payments to the present value of receiving that constant annuity over a specified time. By using a specified interest rate, CRF can be determined as follows [78]:

$$CRF = \frac{i(1+i)^N}{(1+i)^N - 1} \quad (3.3)$$

3.3 Rural Load Forecast

To ensure a satisfactory quality of life in rural areas, electricity is used for lighting, communication and domestic motor applications [79]. In rural areas without access to a public grid, radio is the most widely used electronic communication mass medium. Nevertheless, Television (TV) has also been included in the load forecast. Motor applications such as refrigerator, fan and washing machine are also included. Table 3.1 shows the actual data of the available appliances within the market.

After 10 pm up until 5 am when people are asleep, all electrical appliances except the refrigerators might be off. From 5 am to 7 am, the lights and radio might be on since the

parents and children are preparing to go to work and school, respectively. From 09 am to 11 am, the washing machine might be used by a housekeeper or housewife. This is just a worst case scenario since a washing machine might not be used every day.

Table 3.1: 24 hour daily load summary for one typical rural household

Appliance	Quantity (per household)	Total Power Consumption (kW)	Usage Time (hour)	Common Usage Interval(s)
Lights (11W CFL)	3	0.033	6	05:00 - 07:00 & 18:00 - 22:00
Radio (10W)	1	0.01	12	05:00 - 17:00
TV (70W)	1	0.07	6	16:00 - 22:00
Refrigerator (500W)	1	0.5	24	00:00 - 00:00
Fan (6.5W)	1	0.065	6	12:00 - 18:00
Washing Machine (500W)	1	0.5	3	09:00 - 11:00 18:00 - 19:00

From 12 pm to 06 pm, the fan might be on due to the high ambient temperature. Starting from 04 pm up until 10 pm TV might be on. Lights are switched on again from 06 pm up until bedtime. From 06 pm to 07 pm, a washing machine might be used to wash laundry worn during the day.

In this study, the estimated load profile is based on supplying a small rural load consisting of 5 two-roomed houses. Hence, it is assumed that each house has three lamps; two for indoor lighting and one for outdoor lighting. In renewable energy systems, energy efficiency plays a crucial role in minimizing the investment costs. Hence, the estimated load profile shown in Figure 3.1 is based on appliances shown in Table 3.1 above. In this study, it is assumed that

the load demand is constant throughout the year since the proposed off-grid MHR system is not designed or planned to supply appliances such as heaters, air-conditioners, electrical kettles, stoves, etc. With the exception of the fan, all appliances are used during all seasons of the year. Hence, a summer season has been used as a worst case scenario.

Many poor rural residents of South Africa are employed by farmers to earn a stable income. In this study, it is assumed that the energy or power required by each rural household is equal since residents in a typical village tend to copy one another, especially when they have almost the same income. The peak power demand for each house when all appliances are used at the same time is calculated to be:

$$(0.011 \times 3 + 0.01 + 0.07 + 0.5 + 0.065 + 0.5) = 1.178 \text{ kW}$$

In a rare case, wherein all appliances within 5 houses are used at the same time, the peak power demand will be 5.86kW. Based on Table 3.1, the peak demand is estimated to be 5.51kW, as shown in Figure 3.1 below.

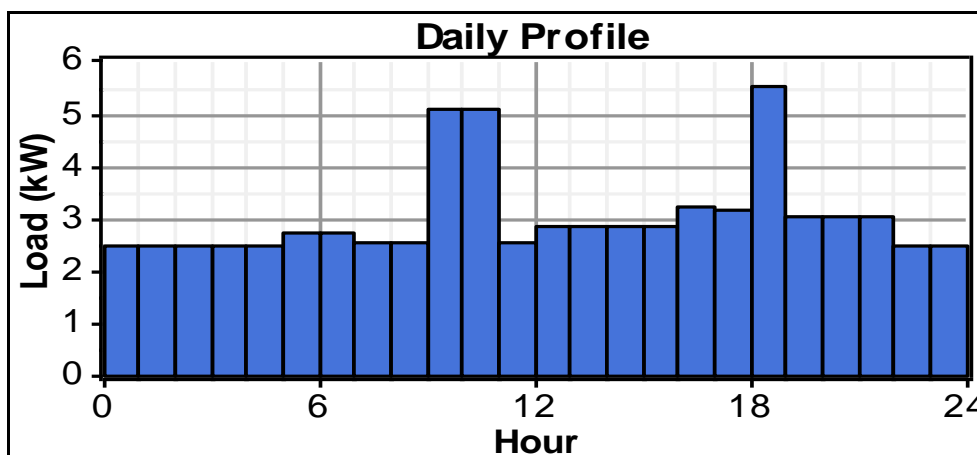


Figure 3.1: Rural load profile for 5 typical rural households

From a practical point of view, it is impossible for the load to follow the same pattern every day. Hence, HOMER uses random variability to estimate the realistic load demand from a given load profile. This caters for differences/fluctuations which may occur each day within a load profile. In this study, a daily variation of 7% and hourly variation of 7% were used to better simulate the realistic variability of the load profile. To satisfy these variations, HOMER generated a new annual load profile shown in Figure 3.2 below. It consists of the peak load demand of 7.02kW with the scaled annual average energy of 73.1kWh/day.

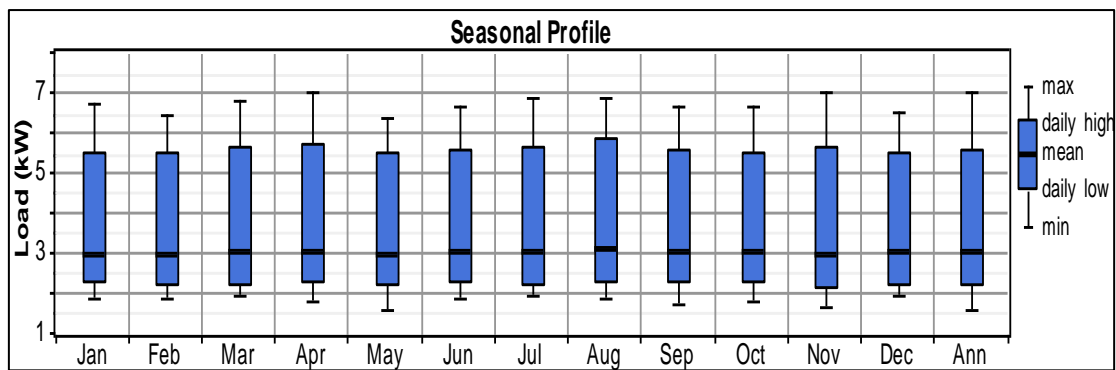


Figure 3.2: Seasonal electrical load profile (with 7% daily and hourly variation factors)

3.4 Renewable Energy Resources Assessment

The potential energy of solar, wind and hydrokinetic resources for the study site were considered. The annual summaries of these renewable energy sources were discovered as shown in Table 3.2 below [23-25]. NASA and RETScreen were used as climate database tools.

3.4.1 Solar resource

Solar radiation levels in South Africa are among the highest in the world. Average daily radiation level varies between 4.5 and 6.5kWh/m² [80]. The solar resource profile over one year period at the study site is shown in Table 3.2 below. The average solar radiation level of this study site is 4.964kWh/m²/day. High radiation levels take place during the months of January, November and December. The solar radiation is available throughout the year. Hence, it shows that there is large amount of PV power to be obtained within the study site.

Table 3.2: Annual resource data at the selected site

Months	Daily Radiation Level (kWh/m ² /day)	Wind Speed (m/s)	Water Speed (m/s)
January	6.230	4.100	5.310
February	5.830	3.900	7.250
March	5.210	3.800	6.090
April	4.460	3.900	1.810
May	3.810	4.100	2.670
June	3.330	4.500	2.180
July	3.620	4.500	1.840
August	4.290	4.600	1.540
September	5.080	4.800	1.410
October	5.410	4.600	1.690
November	6.000	4.300	2.830
December	6.350	4.000	5.270
Average	4.964	4.26	3.306

3.4.2 Wind resource

A wind power generation system converts the kinetic energy of the wind into useful electrical energy. The wind kinetic energy is proportional to the cube of the wind speed. The annual average wind speed at the study site is 4.26 m/s at an anemometer height of 10m. The peak wind speed occurs at 15h00 of each day. The daily wind speed variation (diurnal pattern strength) is 0.25 and the wind speed randomness (autocorrelation factor) is 0.85.

3.4.3 Hydrokinetic resource

Hydrokinetic turbines are commonly referred to as ‘underwater wind turbines’ since they share lot of similarities with wind turbines. The only difference is that water is denser than wind while a wind speed is faster than a water speed. Table 3.2 shows that the average monthly water velocity at the study site is 3.306m/s. The flowing water reaches high velocities during January, February, March and December each year.

3.5 System Sizing and Costs

All selected system components are selected based on meeting the peak demand of 7.02kW. System components costs consist of capital, replacement, and operation and maintenance (O&M) costs. The currency used in HOMER is US Dollars. One US\$ was equivalent to 10.84 South African Rand when the study was conducted. In an off-grid system, electrical energy needs to be stored when the demand is less than the generated capacity, and then used if required. For each individual standalone system, the battery storage method was included during simulations.

3.5.1 Diesel generator

DGs are generally used to provide electricity in isolated rural areas. They are made up of a combustion engine fuelled with diesel and coupled to a synchronous alternator. They are selected in accordance with the electrical load requirements. It is important to select a large enough DG that can best meet the peak load demand. For efficient operation, the user must ensure that the load demand is between 80-90% of the DG's rated capacity [81]. This condition will be used as a DG sizing criterion in this study.

The energy generated (E_{DG}) by a DG with a rated output (P_{DG}) is expressed as follows [82]:

$$E_{DG} = P_{DG} \times \eta_{DG} \times t \quad (3.4)$$

Where, P_{DG} = rated power of a DG (W);

η_{DG} = DG efficiency.

The cost of the DG is linked to its size. In this study, an 8kW, 50Hz, 120/240VAC, Isuzu DG demanding a capital cost of US\$6599 has been selected to fulfil the load requirement [83]. The O&M cost is assumed to be US\$0.5/hour with a fuel consumption rate of 0.55 litre/ kWh [84]. The economic lifespan of a diesel generator is generally 20,000 operating hours [85]. During the study (March 2014), the South Africa price of purchasing diesel fuel was around US\$1.35/litre [86]. Operating a DG is expensive in terms of both fuel and carbon dioxide emission. Hence, the fixed international emission penalty cost of US\$2.25/ton of carbon dioxide was also taken into account.

3.5.2 Battery storage system

A battery storage system has been incorporated in each system. It will allow storage of excess energy when the load demand is less than the generated capacity. This will significantly enhance the reliability of the off-grid system. Batteries are connected in series and parallel to yield the required voltage and capacity. To prolong the lifespan of the battery, most manufacturers advise limiting the depth of discharge to almost 20%. When sizing the battery bank used to supply AC load, the capacity of the battery (C_{BAT}) is calculated as follows [87]:

$$C_{BAT} (Ah) = \frac{E_L \times d}{V_s \times \eta_{BAT} \times \eta_{CONV} \times DOD} \quad (3.5)$$

Where, E_L = required daily load (Wh);

d = number of autonomous days;

V_s = system voltage on the DC side (V);

η_{BAT} = battery efficiency;

η_{CONV} = converter efficiency;

DOD = depth of discharge (%).

A Trojan T-105 deep cycle battery has been considered for each individual off-grid system. The technical parameters of this battery are available within the HOMER datasheet and are shown in Table 3.3 below. In the simulation, batteries have been arranged in strings of 4 batteries per string to yield 24Vdc to be connected as an input of the inverter. The South African market price of purchasing this battery is US\$189 and it has a lifespan of 5 years when assuming 80% depth of discharge [88]. The O&M cost is estimated to be 2% of the capital cost per year [89].

Table 3.3: Technical parameter of Trojan T-105 battery

Parameter	Value
Nominal voltage	6V
Nominal capacity	225 Ah
Maximum charge current	11 A
Round trip efficiency	85 %
Maximum state of charge	30 %
Life time throughput	845 kWh

3.5.3 PV panels

Several cells are connected together to form a PV panel. A PV panel converts solar irradiation directly into DC output voltage. The output current and panel efficiency are directly proportional to the solar radiation level [90]. The output energy (E_{PV}) of a solar PV system can be expressed as follows [91]:

$$E_{PV} = A_{PV} \times \eta_{PV} \times \eta_{PC} \times p_f \times I_h \quad (3.6)$$

Where, A_{PV} = total area of the PV panel (m^2);

η_{PV} = PV module efficiency;

η_{PC} = power conditioning efficiency;

p_f = packing factor;

I_h = hourly irradiance (kWh/m^2).

The South African purchase price of a 1kW polycrystalline PV panel is US\$1321/kW [88]. The O&M cost is considered to be US\$25/kW/year over a lifetime of 20 years [85]. During simulation, HOMER determined the optimum number of solar panels needed to meet the load demand at no electricity shortage.

3.5.4 Wind turbine

For a wind generation system, the output power is determined by the available wind speed. Hourly energy generated (E_w) by a wind system is expressed as follows [82]:

$$E_w = 0.5 \times \rho_w \times A \times v^3 \times C_p \times \eta_g \times \eta_t \times t \quad (3.7)$$

Where, ρ_w = air density (1.225Kg/m³);

A = wind turbine swept area (m²);

v = wind speed (m/s);

C_p = power coefficient of a wind turbine;

η_g = generator efficiency;

η_t = turbine efficiency.

Due to wind speed fluctuation, a wind turbine system's rating is usually higher than the average electrical demand. Hence, it is beneficial to combine wind power generation with an energy storage device. This will reduce the unreliability/uncertainty of wind generation [92]. The data from different manufacturers of wind turbines are already available in HOMER. In this study, a 7.5kW DC XLR wind turbine manufactured by Bergey Wind-power has considered. The capital cost of purchasing this turbine is US\$24,200 [93]. The lifespan is

estimated to be 25 years with O&M cost being 2% of the capital cost per year [89]. The turbine's power curve at a hub height of 25m is shown in Figure 3.3 below.

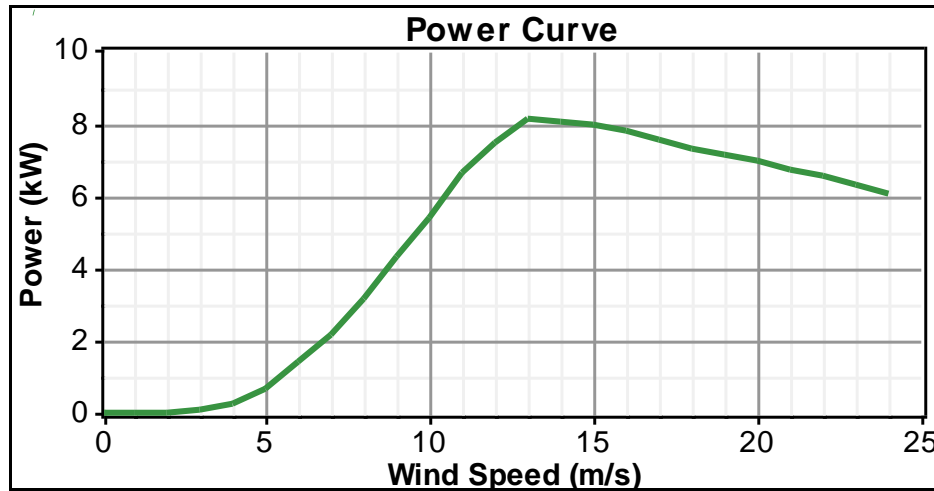


Figure 3.3: Power curve of a 7.5kW XLR turbine

3.5.5 Hydrokinetic turbine

For a hydrokinetic generation system, the output power is affected by the speed of the flowing water as a variable. Hence, hourly energy generated (E_{HK}) by a hydrokinetic system is expressed as follows:

$$E_{HK} = 0.5 \times \rho \times A \times v^3 \times C_p \times \eta_g \times \eta_t \times t \quad (3.8)$$

Where, η_g = efficiency of a generator;

η_t = efficiency of a turbine.

HOMER is not equipped with a hydrokinetic module in its component library. The wind power modules have been used instead since hydrokinetic turbines operate similarly to wind

turbines [94, 95]. The anemometer height and the turbine hub height are made equal so that HOMER does not scale the wind speed data [96]. A 1.5kW DC Darrieus hydrokinetic turbine (DHT) of 1.25m diameter and 1.25m height has been chosen for simulation. This turbine was developed by Alternative Hydro Solutions in Canada. The power-curve based on the manufacture's information is shown in Figure 3.4 below. Subsequently, there is no available information regarding the output power at speeds above 2m/s. Hence, it is assumed that at water velocities above 2m/s there is no rise in output power. This turbine system requires an investment cost of US\$15,000 [97]. Similar to a wind turbine system, the lifespan is estimated to be 25 years with O&M cost being 2% of the capital cost per year.

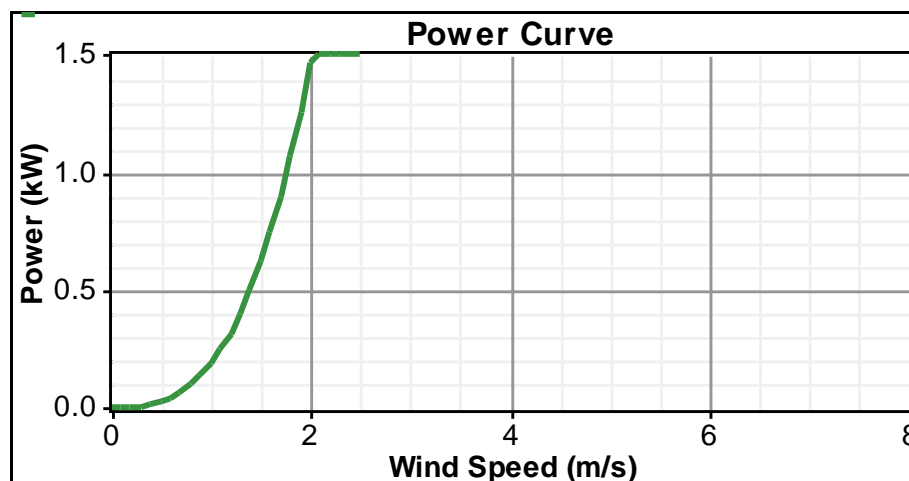


Figure 3.4: Power curve of a 1.5kW DHT turbine

3.5.6 Power electronic converter

A converter has been chosen to vary DC to AC and to charge the battery as well. The chosen converter consists of both the battery charger and a standalone true sine wave inverter suitable to supply sensitive electronic appliances as well. It is an 8kW, 50Hz, 230Vac Victron MultiPlus inverter/charger with efficiency of 96%. It can accept different DC voltage ranges

such as 9.5-17VDC, 19-33VDC or 38-66VDC. Since the peak load demand of this study is 7kW, this converter can supply up to a maximum of 7.68kW power when considering its efficiency. The South African purchase price of this converter is US\$5,509 [88]. Its O&M cost is assumed to be 1% of its capital cost per year with a lifespan of 10 years [89].

3.5.7 Grid extension

Electric grid extension is generally preferred where the adequate load demand exists. It is a reliable and efficient conventional method for supplying electricity since it allows a 24-hour provision. It minimizes the consumers' maintenance cost when compared to DG. The cost of grid extension in this study is only used to observe whether grid extension is more viable than standalone systems. It is used as a comparison tool to obtain an economical distance between the grid line and the remote rural load. The capital cost of grid extension per kilometre is considered to be US\$8000/km, with the O&M cost of US\$1500/km/year [98, 99]. During the period of the study, South African local grid electricity price was US\$0.11/kWh.

3.6 HOMER Results and Discussion

After entering all the inputs data, HOMER determined the most economical configuration for each individual system to adequately serve the rural load demanding 73kWh/day. The purchasing costs of different renewable energy technologies can decrease over time at different rates. This makes a selection decision difficult. For a simplified comparison, a worst case scenario has been considered for each system by assuming that the replacement costs are equal to the capital costs after the lifespan of each component. The O&M costs are also assumed to be evenly distributed over the entire project lifetime.

For a better comparison, each off-grid system has been simulated as a sole supply source offering a 24-hour electricity service to the same rural load for 8760 hours/year. All systems were simulated to have 0% annual capacity shortage at 6% annual interest rate for a 25 year period. Furthermore, other costs such as labour, installation, licensing as well as financial incentives offered by local government, are not included in the simulation. Cable costs are not included since they are reasonably low compared to the overall system cost [82].

3.6.1 Hydrokinetic system simulation results

Figure 3.5 shows the schematic diagram for the hydrokinetic energy generation system as used in the HOMER software model. It can be seen that the primary load to be supplied demands 73kWh per day and the peak load is found to be 7kW. The water resource data shown in Table 3.2 and the hydrokinetic system component costs discussed in section 3.5.5 have been entered into the model. The power curve parameters of a 1.5kW DC DHT were also entered in the wind power module. The anemometer height and the turbine hub height were made equal so that HOMER does not scale the wind speed data.

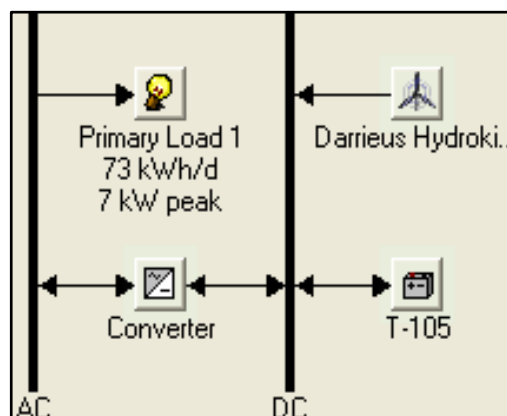


Figure 3.5: HOMER schematic diagram for the hydrokinetic system model

Figure 3.6 shows the first 10 optimal hydrokinetic configurations' results. The highlighted row represents the feasible configuration since they are sorted based on total NPC. The top one represents the most cost-effective configuration while the bottom ones represent the least cost-effective configurations. The optimal configuration consists of 6 DHT turbines, 72 Trojan T-105 batteries and an 8kW converter in order to meet the rural load demand at the lowest cost. The cost of energy is found to be US\$0.442/kWh at a 100% renewable energy fraction and at no capacity shortage. Hence, the probability of capacity shortage is 0%.

			DHT	T-105	Conv. (kW)	Initial Capital	Operating Cost (\$/yr)	Total NPC	COE (\$/kWh)	Ren. Frac.	Capacity Shortage
			6	72	8	\$ 109,117	3,254	\$ 150,718	0.442	1.00	0.00
			6	76	8	\$ 109,873	3,314	\$ 152,237	0.446	1.00	0.00
			6	80	8	\$ 110,629	3,374	\$ 153,756	0.451	1.00	0.00
			6	84	8	\$ 111,385	3,433	\$ 155,275	0.455	1.00	0.00
			6	88	8	\$ 112,141	3,493	\$ 156,794	0.460	1.00	0.00
			7	40	8	\$ 118,069	3,077	\$ 157,400	0.462	1.00	0.00
			6	92	8	\$ 112,897	3,553	\$ 158,313	0.464	1.00	0.00
			7	44	8	\$ 118,825	3,136	\$ 158,919	0.466	1.00	0.00
			6	96	8	\$ 113,653	3,612	\$ 159,832	0.469	1.00	0.00
			7	48	8	\$ 119,581	3,196	\$ 160,438	0.470	1.00	0.00

Figure 3.6: Hydrokinetic system's optimization results

The system's operational characteristics such as annual electricity production, battery state of charge and breakeven distance are shown in Figure 3.7- Figure 3.10 below. Figure 3.7 shows that the electric production is below 6kW during the months of April, July, August, September and October. The reason for this low electric production is the low average water speed during these months.

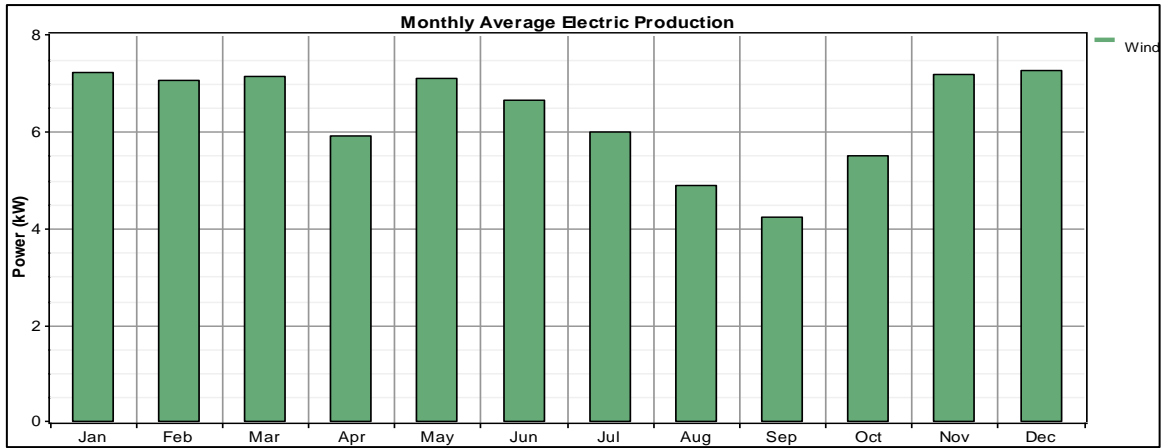


Figure 3.7: Average hydrokinetic electric production of the optimal system configuration

Figures 3.8-3.10 demonstrate the output power from the hydrokinetic turbine and battery condition for each month of the calendar year. From Figure 3.9, it can be seen that, during the month of September, the battery state of charge is very low compared to all other months, since the water speed is very low (1.41m/s). The optimum hydrokinetic system allows the battery to be in a fully charged state for approximately 84% of the year as shown in frequency histogram (Figure 3.10). Hence, the lifespan of the batteries is sustained. The system offers 62,331kWh of energy production per year. Its breakeven grid extension distance was found to be 4.17 km as shown in Figure 3.11.

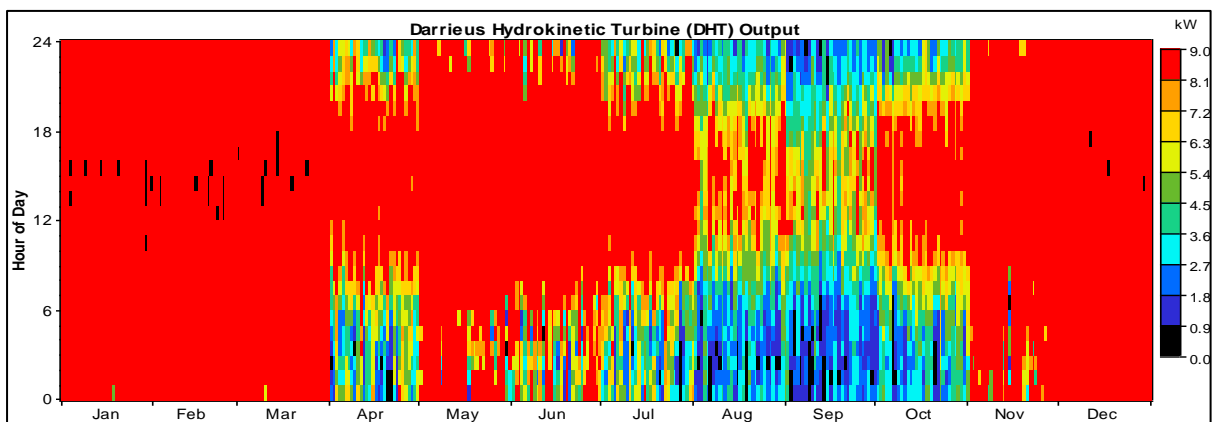


Figure 3.8: Hydrokinetic turbine output power of the optimal system configuration

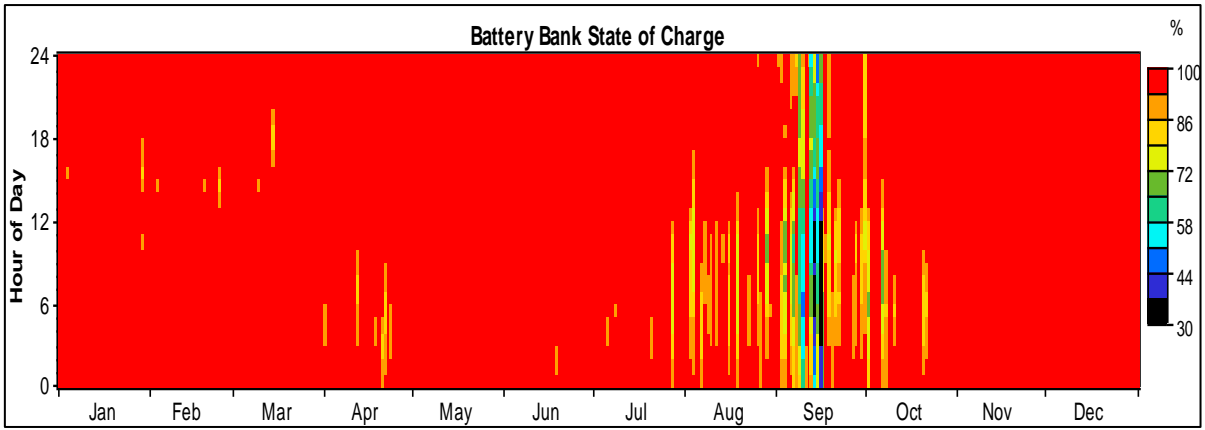


Figure 3.9: Battery state of charge in optimal hydrokinetic system configuration

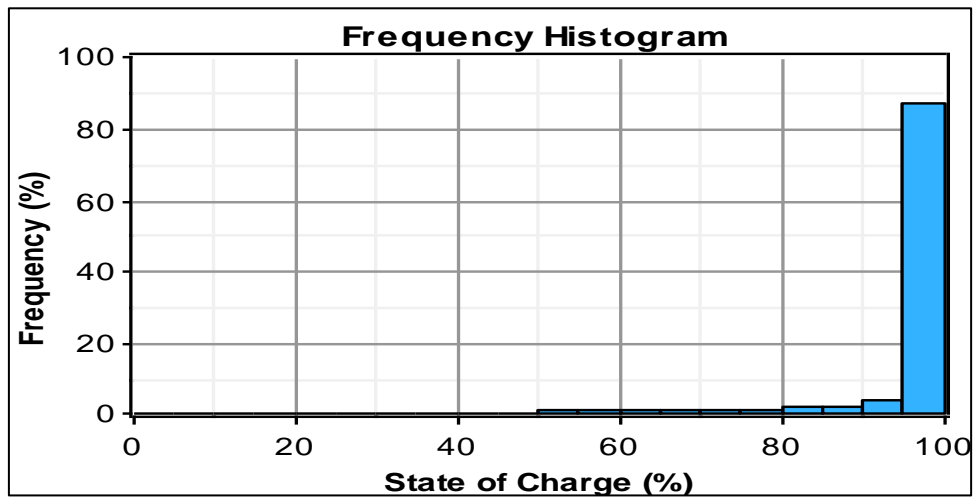


Figure 3.10: Battery state of charge frequency histogram

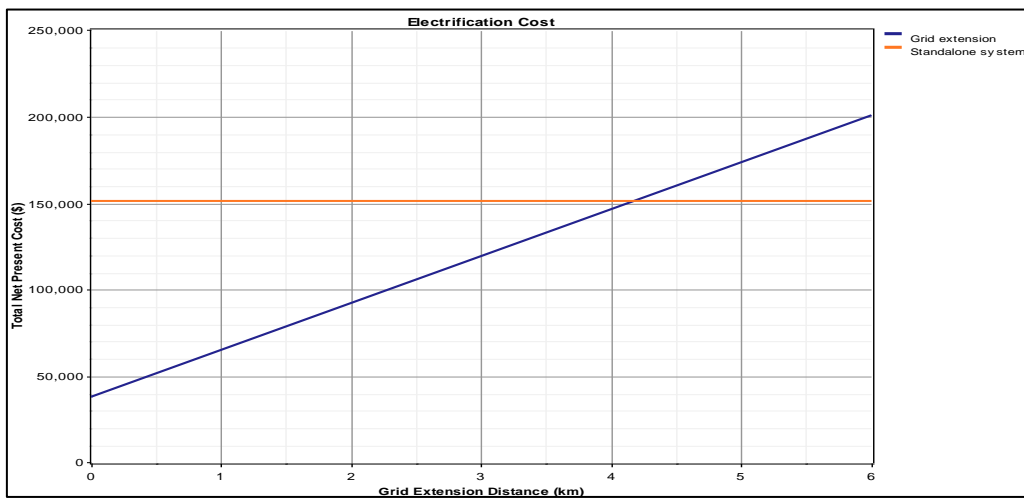


Figure 3.11: Breakeven grid extension distance (4.17km)

3.6.2 Overall results summary and discussion

After entering all required inputs for each system, HOMER determined the most optimized and cost effective configuration per system. Table 3.4 below summarises and highlights technical and economic dissimilarities of different off-grid supply options as obtained from optimal system configuration results. The detailed reports of the optimal economic results for each system are shown in Appendix A – D.

The simulation results show that all the off-grid systems are generating electricity at 0% capacity shortage to satisfy the load demand. It can be seen that the DG requires the lowest capital cost of US\$27,984 (R303,347) compared to other standalone systems. Nevertheless, according to investment selection criteria, DG is not the best option to consider. It does not provide the lowest COE and NPC as do the hydrokinetic and solar systems. Furthermore, it pollutes the environment by emitting 27,919 kg of carbon dioxide gas per year.

Among the three simulated renewable energy systems, a solar PV system requires the lowest capital cost of US\$99,547 (R1, 079,089). However, the economic comparison results clearly show that significant financial benefits are to be gained by selecting an off-grid micro-hydrokinetic system for the study site. Its 24 hours generation capability makes it more competitive than a solar PV system. It has the lowest NPC of US\$151,841 (R1, 645, 956) and offers the lowest COE of US\$0.442/kWh (R4.79c/kWh). It has the lowest operating cost of US\$3,254 (R35, 273), with the highest electricity production of 62,331kWh/year.

Grid extension distance reveals that the total cost of using an MHR project for 25 years is equivalent to the cost of installing a grid extension line of a 4.17 km length. If the local grid lines are situated more than 4.17 km away from the study site, it is then appropriate to consider an MHR system rather than grid extension. A solar PV system is the second best

option to consider. It provides the lowest COE at US\$0.482/kWh (R5.22c/kWh) compared to wind and DG systems.

Table 3.4: Summary of optimum simulation results for different off-grid systems

	Hydrokinetic	Solar	Wind	DG
Optimal system architecture	DHT (6 turbines) +72 batteries + 8kW converter	PV (42kW) + 204 batteries + 8kW converter	XLR (6 turbines) + 388 batteries + 8kW converter	DG (8kW) + 84 batteries + 8kW converter
Total Rated Capacity to meet the demand (kW)	9kW	42kW	45kW	8kW
Capital cost (US\$)	109,117	99,547	224,041	27,984
(Rand)	1,182,828	1,079,089	2,428,604	303,347
NPC (US\$)	150,718	164,346	340,039	291,734
(Rand)	1,633,783	1,781,511	3,686,023	3,162,397
O&M (US\$)	27,192	23,983	56,576	31,234
(Rand)	294,761	259,976	613,283	338,577
COE (US\$/kWh)	0.442	0.482	0.998	0.855
(Rand/kWh)	4.79	5.22	10.82	9.27
Operating cost (US\$/year)	3,254	5,069	9,074	20,632
(Rand/year)	35,273	54,948	98,362	223,651
Annual electricity production (kWh/year)	62,331	60,808	49,510	32,128
Breakeven grid extension distance (km)	4.17	4.67	30.5	9.35
Capacity shortage (%)	0	0	0	0
Carbon dioxide emission (kg/year)	0	0	0	27,919

3.6.3 Supplementary results

The second study site with flowing water, solar and wind resources has been used to perform supplementary feasibility analysis. This site is simulated to supply a typical remote rural school with a load profile shown in figure 3.12 below. The load demands 34.452kWh energy per day and the peak load is 7.172kW.

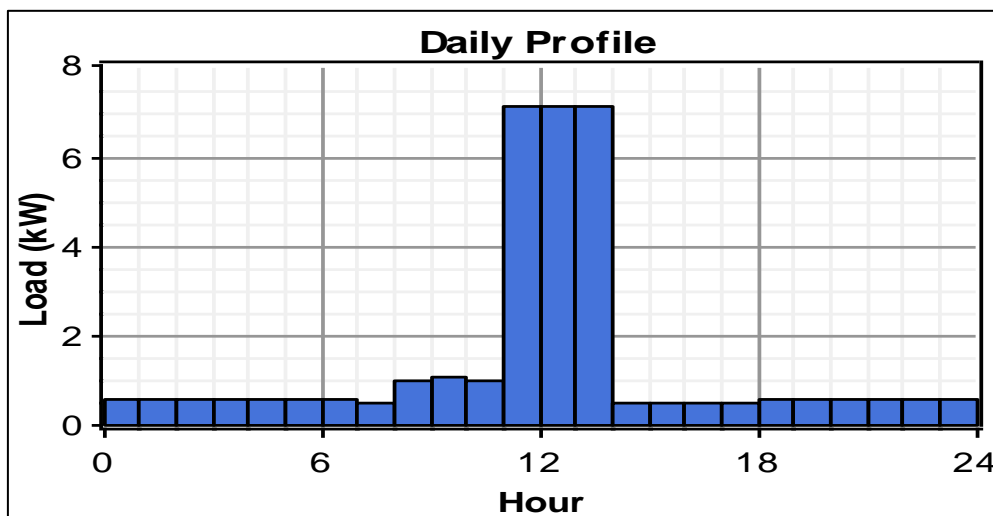


Figure 3.12: Load profile for a typical rural school

A summary of renewable energy resources within the supplementary site is given in Table 3.5 below [23-25]. Similar to the main study site, after entering all required inputs to HOMER software, each off-grid system was simulated to yield 0% energy shortage at 6% interest rate. From Table 3.6 below, it can be seen that an off-grid MHR system still offers the best investment opportunity when compared to solar, wind or DG system. Its optimal configuration consists of 3 DHT turbines, 44 Trojan T-105 batteries and an 8kW converter to meet the load demand.

Table 3.5: Annual resource data at the supplementary site

Months	Daily Solar Radiation Level (kWh/m²/day)	Wind Speed (m/s)	Water Speed (m/s)
January	8.44	6.60	6.410
February	7.50	5.90	5.270
March	6.22	5.80	3.830
April	4.66	5.10	3.120
May	3.43	4.90	2.470
June	3.01	5.30	2.160
July	3.21	5.10	1.580
August	4.10	5.30	1.220
September	5.33	5.60	1.710
October	6.82	6.20	2.430
November	7.96	6.20	4.190
December	8.51	6.00	6.600
Average	5.76	5.7	3.047

Table 3.6: Summary of optimum simulation results at the supplementary site

	Hydrokinetic	Solar	Wind	DG
Optimal system architecture	DHT (3 turbines) +44 batteries + 8kW converter	PV (21kW) + 96 batteries + 8kW converter	XLR (3 turbines) + 184 batteries + 8kW converter	DG (8kW) + 60 batteries + 8kW converter
Total Rated Capacity to meet the demand (kW)	4.5kW	21kW	22.5kW	8kW
Capital cost (US\$)	58,825	51,394	112,885	23,448
(Rand)	637,663	557,111	1,223,673	254,176
NPC (US\$)	81,456	85,077	171,405	145,147
(Rand)	882,983	922,235	1,858,030	1,573,393
O&M (US\$)	14,334	12,053	28,157	17,568
(Rand)	155,381	130,655	305,222	190,437
COE (US\$/kWh)	0.506	0.529	1.065	0.902
(Rand/kWh)	6.07	5.73	11.54	9.78
Operating cost (US\$/year)	1,770	2,635	4,578	9,520
(Rand/year)	19,187	28,563	49,626	103,197
Annual electricity production (kWh/year)	36,463	35,310	24,855	14,477
Breakeven grid extension distance (km)	2.35	2.48	15.5	4.69
Capacity shortage (%)	0	0	0	0
Carbon dioxide emission/year	0	0	0	13,113

3.7 Conclusion

This chapter used the HOMER to perform a feasibility analysis of an off-grid MHR system as opposed to solar, wind and diesel generator systems. The results indicated that financial and environmental benefits could be gained by selecting an MHR system to fulfil the remote rural

load requirement. Based on the simulation results, an MHR system is selected owing to its lowest NPC and COE, as well as the highest annual electricity production rate. This chapter also revealed the economic distance from the grid lines to the study site if any of the simulated off-grid systems is considered. This will make it easier for planners/designers should they propose to implement any of the above simulated off-grid systems.

CHAPTER 4: MODELLING OF MICRO-HYDROKINETIC SYSTEM

4.1 Introduction

In this chapter the dynamic mathematical model is developed to analyse the behaviour of the proposed off-grid MHR system. Most of the available modelling and simulation tools for mechanical and electrical systems are not equipped with hydrokinetic modules. This chapter develops a mathematical model for each component of the MHR system through the use of MATLAB/SIMULINK library. These components include a high density hydrokinetic turbine, mechanical drive-train, and a PMSG as shown in Figure 4.1 below. A horizontal turbine and a non-salient pole PMSG have been considered in the model. This study aims to investigate the performance characteristic of a hydrokinetic system under variable water speed. Hence, modelling of power electronic devices and control technology of variable water turbines is beyond the scope of this study.

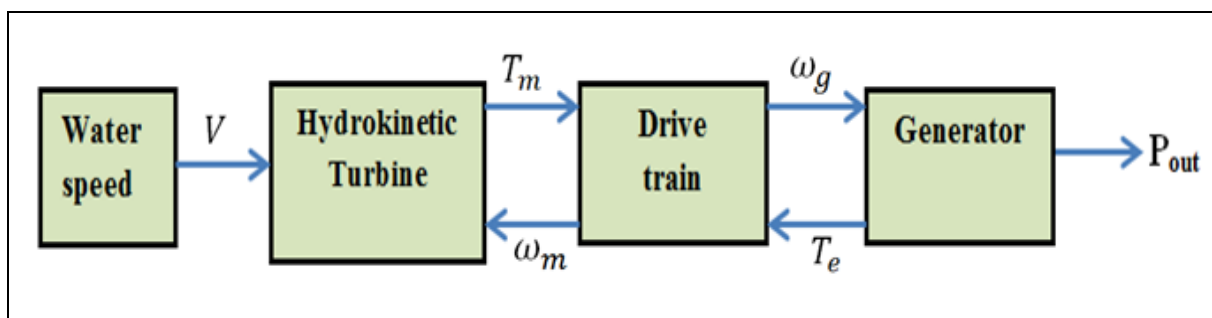


Figure 4.1: Block diagram of a hydrokinetic turbine scheme

4.2 Hydrokinetic Characteristics

There are many concepts for harnessing this energy, but a turbine is the most common and proven one. Small-scale hydrokinetic turbines are available from 0.5 to 5kW sizes and can be used in any flow with a velocity of 0.5m/s or more [44]. The amount of electricity that can be generated is dependent on the volume and velocity of the water resource. It operates similarly to wind generation system in terms of operation and rotor blade configurations. The modelling of the overall system is discussed below.

4.2.1 Modelling of hydrokinetic turbines

The kinetic energy from flowing water is extracted and transformed into mechanical rotational energy by means of zero head turbine blades. The relationship of the kinetic energy (E_k) of flowing water and the water speed is expressed as follows [100]:

$$E_k = \frac{1}{2}mv^2 \quad (4.1)$$

Where, m = water mass (kg);

v = water speed (m/s).

Hence, the power of the moving water (assuming constant velocity) is expressed as

$$P_w = \frac{dE_k}{dt} = \frac{1}{2}\rho Av^3 \quad (4.2)$$

Where ρ is the water density (1000 kg/m³) [101] and A is the swept area of turbine rotor blades (m²). Similar to a wind turbine, the swept area depends on the arrangement of the rotor blade.

4.2.2 Modelling of mechanical power within hydrokinetic turbine

The mechanical power (P_m) that a hydrokinetic turbine extracts using the swept area of the rotor disc is less than the available power of the moving water (P_w). Hydrokinetic turbines can only harness a fraction of the total kinetic power due to losses entailed. So, the rotor power coefficient of the turbine, C_p can be expressed as [100].

$$C_p = \frac{P_m}{P_w} \quad C_p < 1 \quad (4.3)$$

This coefficient is limited to $16/27=0.593$ by the well-known Betz law [102,103]. The upper limit is for highly efficient machines with low mechanical losses. Mechanical systems such as gearbox, bearings, shape of blades, etc., produce more losses. Hence, less water power is actually converted into usable electricity.

By substituting equation (4.3) into (4.2), the extracted output power of a hydrokinetic turbine from water flow is given by equation (4.4) below [37, 43]. Hence, the total available power (watts) captured by hydrokinetic turbine is dependent on water density, cubic velocity of the water, the cross sectional area and co-efficient of a turbine.

$$P_m = \frac{1}{2} \rho A v^3 C_p \quad (4.4)$$

C_p depends on the tip-speed ratio, λ and the blade pitch angle, β (degrees) and can be expressed by equation (4.5) [56,101,104]. Blade pitch angle is defined as the angle between the plane of rotation and the blade cross-section chord. For a hydrokinetic system, the tip speed ratio can be defined as a ratio between the turbine blade tip speed and the water speed. Usually the best efficiency is obtained when $\beta=0$ degrees.

$$C_p(\lambda, \beta) = c_1 \left(c_2 \frac{1}{\lambda_i} - c_3 \beta - c_4 \right) e^{\left(\frac{-c_5}{\lambda_i} \right)} + c_6 \lambda \quad (4.5)$$

Where, c_1 to c_6 are the empirical power coefficients parameters of the turbine;

The parameter $\frac{1}{\lambda_i}$ can be solved by making use of the following equation [101,104-107]:

$$\frac{1}{\lambda_i} = \frac{1}{\lambda + 0.08\beta} - \frac{0.035}{1 + \beta^3} \quad (4.6)$$

The tip speed ratio can be determined as follows [108]:

$$\lambda = \frac{\omega_m \cdot R}{v} \quad (4.7)$$

Where, ω_m = mechanical angular speed of the turbine rotor shaft (rad/sec);

R = turbine radius (m).

These empirical power coefficients depend on the turbine type and can be different for various turbines. Figure 4.2 below is the Simulink model for determining the power coefficient of the turbine at a blade pitch angle of zero degrees. The empirical coefficients of a typical horizontal turbine c_1 to c_6 , are 0.5176, 116, 0.4, 5, 21 and 0.0068 respectively [56,

109]. A horizontal turbine has been selected due to its self-starting capability, which is not available in the vertical turbine. The overall parameters of a modelled turbine are given in Table 4.1 below.

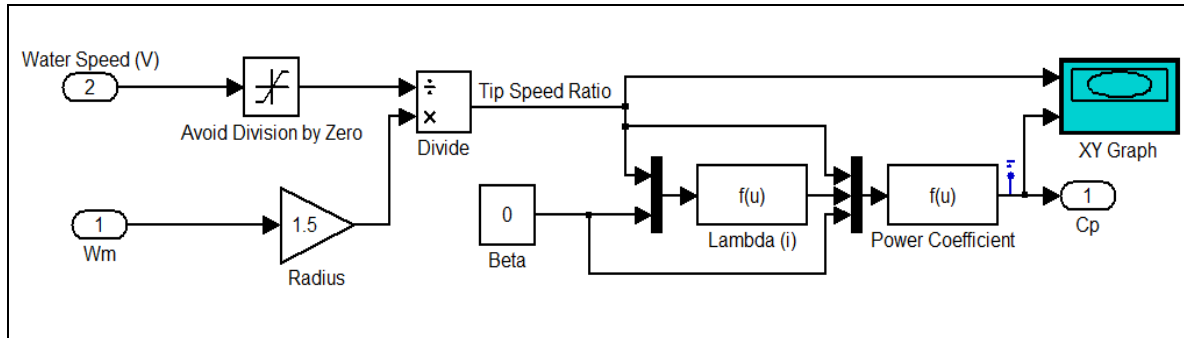


Figure 4.2: Simulink block diagram of a turbine power coefficient model

Table 4.1: Specifications of the selected horizontal turbine

Parameters	Value and SI units
Rotor radius (R)	1.5 m
Number of blades	3
Swept area by the rotor blade (A)	7 m ²
Maximum Power coefficient ($C_{p,max}$)	0.48
Optimal tip speed ratio (λ_{opt})	8.1
Coefficients (C1, C2, C3, C4, C5, C6)	0.5176, 116, 0.4, 5, 21, 0.0068
Blade pitch angle (β)	0

In order to achieve maximum power extraction from a variable speed turbine, a turbine must operate at a maximum power coefficient ($C_{p,max}$). $C_{p,max}$ is achieved when β is kept at zero degrees for an optimum tip speed ratio (λ_{opt}). Hence, when $\beta = 0$ degrees, the optimal tip speed ratio must then be maintained by controlling the rotor speed of the PMSG, as shown by

equation (4.7). Henceforth, higher energy conversion efficiency is maintained at variable speeds.

Maximum power point tracking (MPPT) control is commonly used to maintain this higher energy conversion efficiency. MPPT can be achieved by making use of mechanical sensors or power electronics converters with pulse signals to control the speed of a generator shaft [54]. Compared to power electronics converters, these mechanical sensors usually lead to inaccurate measurements. It was proved that the optimum power coefficient ($C_{p,max}$) can be maintained constant at variable speed by estimating the rotor speed based on direct axis current and voltage values [54].

Since the modelling of power electronic devices and control technology is beyond the scope of this study, a hydrokinetic turbine has been modelled as shown in Figure 4.4 below. The following assumptions were made to simplify turbine modelling:

- $C_{p,max}$ was assumed to be equal to 0.48 for different water speeds in order to ensure optimal power extraction from flowing water.
- the turbine swept area is assumed to be constant.
- the mechanical power P_m was assumed to be at constant maximum value, when the speed exceeds the rated speed of the Generator. This was made possible by making use of a saturation block from Simulink library. It was connected at the output of the P_m as shown in Figure 4.3 below.

Based on the above-mentioned assumptions, since the dimensions of the turbine are also fixed, it means that the turbine output power depends on the water flow velocity. The manual switch has been used to select between constant and variable water speed.

The mechanical torque of the turbine rotor shaft, T_m (N.m) can be expressed as shown in equation (4.8) below [110,111]. It was made negative to enable the permanent magnet synchronous machine to operate as a generator.

$$T_m = \frac{P_m}{\omega_m} \quad (4.8)$$

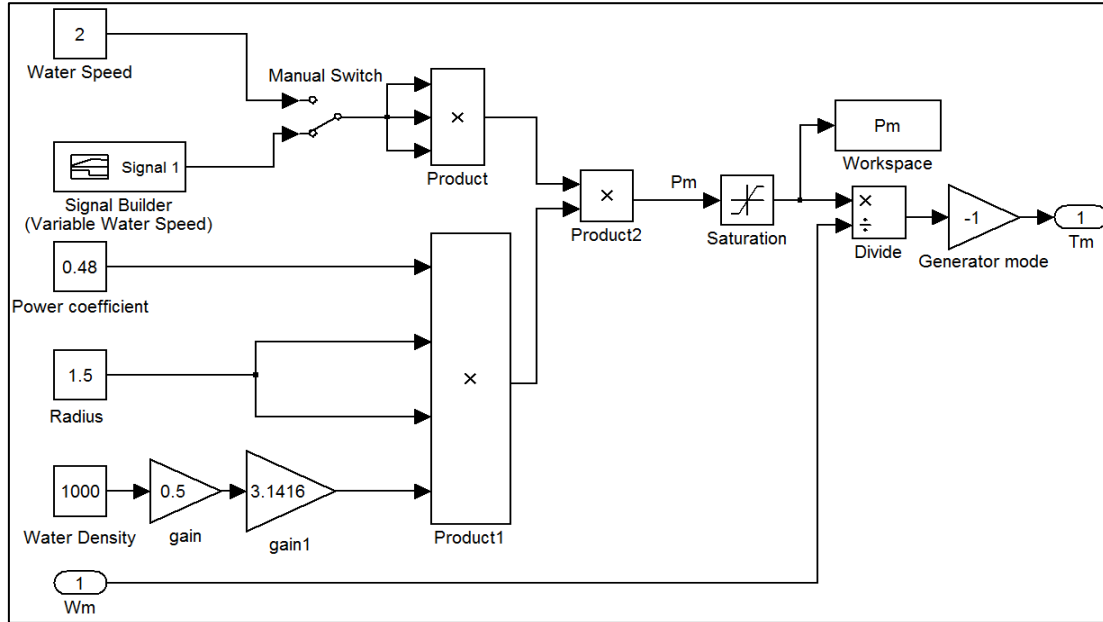


Figure 4.3: Overall Simulink block diagram of the modelled high density hydrokinetic turbine

4.2.3 Drive train modelling

The role of the drive train within a hydrokinetic system is to enable the conversion of kinetic energy of flowing water into useful mechanical energy. Typically, it consists of a rotor hub, rotor shaft, gearbox, and a shaft connected to a generator. The drive train can either be geared or directly driven. The gearbox within the drive train connects the low speed shaft (on the turbine side) with the high speed shaft (on the generator side). This enables the provision of high rotational speed required by the generator to provide electricity up to a certain level. Nevertheless, the use of a gearbox increases project costs, and reduce the reliability and efficiency of the system due to regular maintenance and energy losses [54]. Hence, connecting the low speed shaft directly to the generator without the use of a gearbox is a preferred efficient method.

A drive train can be modelled by means of different methods, such as a three-mass, two-mass or one-mass drive train model [56]. Since the aim of this study is to determine the interaction between water density and electrical output energy, the drive train was treated as one-mass drive train model. This means that all inertia components are modelled as a single rotating mass. By neglecting all inertia effects of the chain, the mechanical torque from water turbine to the generator ($T_{w:g}$ (N.m)) and the rotor angular speed of the generator (ω_g) via the shaft can be obtained by using equation (4.9) and (4.10), respectively [100,111].

$$T_{w:g} = \frac{T_m}{G} \quad (4.9)$$

$$\omega_g = \omega_m \cdot G \quad (4.10)$$

Where, G =gear ratio.

Based on equation (4.9) and (4.10) above, it can be seen that if a gearbox is used, both the rotational speed and torque differ from the turbine side (low speed & high torque side) to the generator side (high speed & low torque side). If $G=1$, it means that a turbine drives a generator directly without a gearbox. Hence, this implies that $T_m=T_{w:g}$ and $\omega_m=\omega_g$. The mechanical torque transferred from the water turbine to the generator through the drivetrain enables electromagnetic torque (T_e) of the generator to take place. The relationship between T_e and $T_{w:g}$ can be expressed as follows [100]:

$$T_e = J_{eq} \frac{d\omega_g}{dt} + B_m \omega_g + T_{w:g} \quad (4.11)$$

Where, B_m = damping coefficient (N.m/s);

J_{eq} = equivalent rotational inertia of a generator and turbine (kg.m²), which is determined by equation (4.12), below:

$$J_{eq} = J_g + \frac{J_{wt}}{G^2} \quad (4.12)$$

Where, J_g = rotational inertial of a generator (kg.m²);

J_{wt} = rotational inertia of a water turbine (kg.m²).

One of the advantages of PMSG is that they are low inertia machines. Usually J_{eq} is almost equal to J_{wt} since J_g is negligibly small [55]. Figure 4.4 below shows a one-mass drive train Simulink block diagram. The following assumptions were made during modelling:

- the turbine inertia (5 kg.m²) was used as an equivalent inertia of the system.
- rotational damping coefficient was assumed to be zero.

From equation (4.11), the angular acceleration of the generator shaft ($\frac{d\omega_g}{dt}$) can be expressed as shown in equation (4.13) below:

$$\frac{d\omega_g}{dt} = \frac{T_e - T_{w:g}}{J_{eq}} - \frac{B_m}{J_{eq}} \omega_g \quad (4.13)$$

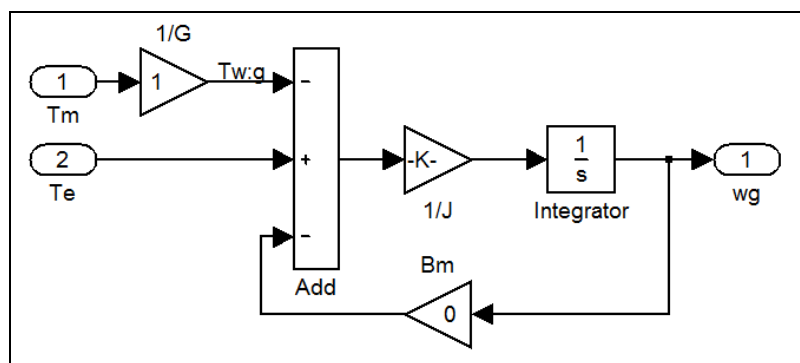


Figure 4.4: Simulink block diagram of a one-mass drive train

4.2.4 Modelling of a permanent magnet synchronous generator

Electrical machines with high torque density are normally considered in order to minimize the weight and size. It has been proved that PMSG's have higher torque density than the conventional generators since they use less material [110]. Furthermore, they are generally used for small- to medium-sized electric power generation since they can operate at low speed without requiring a gearbox [56]. As a result, a PMSG has been considered in this study to produce electrical energy from the mechanical energy of the flowing water.

To demonstrate the useful hydrokinetic power that can be generated by means of a PMSG, a key subject is to develop an adequate equivalent model. Synchronous machine models for power systems are usually based on assumptions such that the damping effect is negligible (of both the rotor and the magnets), the magnetic flux distribution in the rotor is sinusoidal, magnetic circuit is unsaturated, iron losses are negligible and absence of field current dynamics [107,111]. Hence, permanent magnets flux (ψ_{PM}) can be fully described by a vector and the internal voltage induced in the stator, and can be expressed as follows:

$$\psi_{PM} = \frac{\omega_e}{E} = \frac{2\pi \cdot f}{E} \quad (4.14)$$

Where, ω_e = electrical angular speed of the generator (rad/sec);

E = internal voltage induces in the stator (V);

f = electrical frequency (Hz).

In order to study a response of the PMSG, an appropriate transformation can be applied to the stator variables. The Park transformation is a commonly used method for three-phase machine models. It is used to transform the parameters and equation from the stationary form into direct-quadrature (dq) axis [110]. It converts the 3 phase alternating current quantities to direct current quantities, meaning ABC to dq transformation. For a salient pole permanent

magnet synchronous machine, d and q axis inductances are almost equal due to a large and constant air gap. The dynamic model of a permanent magnet synchronous machine is derived from a two-phase synchronous reference frame, in which the q-axis is 90° ahead of the d-axis with respect to the direction of rotation, as shown in Figure 4.5. θ_e is the electrical angle between the stator phase A axis and the d-axis.

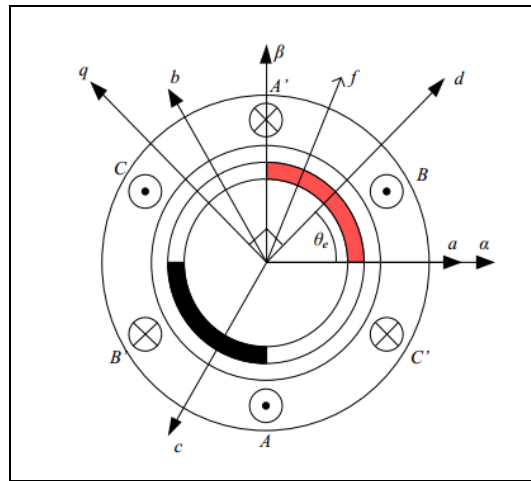


Figure 4.5: PMSG phasor diagram showing Park transformation [112]

The relationship between the electrical angular speed and rotor angular speed of the generator is expressed as follows [100]:

$$\omega_e = p \cdot \omega_g \quad (4.15)$$

Where, p = the number of pole pairs.

The relationship between ω_e and θ_e is expressed as follows:

$$\frac{d\theta_e}{dt} = \omega_e \quad (4.16)$$

When a rotor position is known, Park's transformation is applied. This transformation is used to compute the direct-axis, quadratic axis, and zero sequence quantities in a two-axis rotating reference frame for a three-phase sinusoidal signal. Equation (4.17) shows the conversion of three phase voltage variables (V_{abc}) to dc voltage variables (V_{dq0}) [113-115].

$$\begin{bmatrix} v_d \\ v_q \\ v_0 \end{bmatrix} = \frac{2}{3} \begin{bmatrix} \cos \theta_e & \cos(\theta_e - \frac{2\pi}{3}) & \cos(\theta_e + \frac{2\pi}{3}) \\ \sin \theta_e & \sin(\theta_e - \frac{2\pi}{3}) & \sin(\theta_e + \frac{2\pi}{3}) \\ \frac{1}{2} & \frac{1}{2} & \frac{1}{2} \end{bmatrix} \begin{bmatrix} V_a \\ V_b \\ V_c \end{bmatrix} \quad (4.17)$$

For simplicity, the zero phase sequence component is ignored and equation (4.17) becomes,

$$\begin{bmatrix} v_d \\ v_q \end{bmatrix} = \frac{2}{3} \begin{bmatrix} \cos \theta_e & \cos(\theta_e - \frac{2\pi}{3}) & \cos(\theta_e + \frac{2\pi}{3}) \\ \sin \theta_e & \sin(\theta_e - \frac{2\pi}{3}) & \sin(\theta_e + \frac{2\pi}{3}) \end{bmatrix} \begin{bmatrix} V_a \\ V_b \\ V_c \end{bmatrix} \quad (4.18)$$

Converting V_{dq0} back to V_{abc} is made possible by means of reverse Park's transformation as shown in equation (4.19) below [114,115].

$$\begin{bmatrix} V_a \\ V_b \\ V_c \end{bmatrix} = \begin{bmatrix} \cos \theta_e & \sin \theta_e & 1 \\ \cos(\theta_e - \frac{2\pi}{3}) & \sin(\theta_e - \frac{2\pi}{3}) & 1 \\ \cos(\theta_e + \frac{2\pi}{3}) & \sin(\theta_e + \frac{2\pi}{3}) & 1 \end{bmatrix} \begin{bmatrix} v_d \\ v_q \\ v_0 \end{bmatrix} \quad (4.19)$$

When zero phase sequence component is ignored, equation (4.19) becomes,

$$\begin{bmatrix} V_a \\ V_b \\ V_c \end{bmatrix} = \begin{bmatrix} \cos \theta_e & \sin \theta_e \\ \cos(\theta_e - \frac{2\pi}{3}) & \sin(\theta_e - \frac{2\pi}{3}) \\ \cos(\theta_e + \frac{2\pi}{3}) & \sin(\theta_e + \frac{2\pi}{3}) \end{bmatrix} \cdot \begin{bmatrix} v_d \\ v_q \end{bmatrix} \quad (4.20)$$

This type of transformation is the same for three phase current variables (Iabc) and dc current variables (Idq) conversions as well. Voltage variables are just replaced with current variables.

Figure 4.6 and 4.7 show the Simulink block diagram for transforming Vabc_to_Vdq and Idq_to_Iabc, respectively.

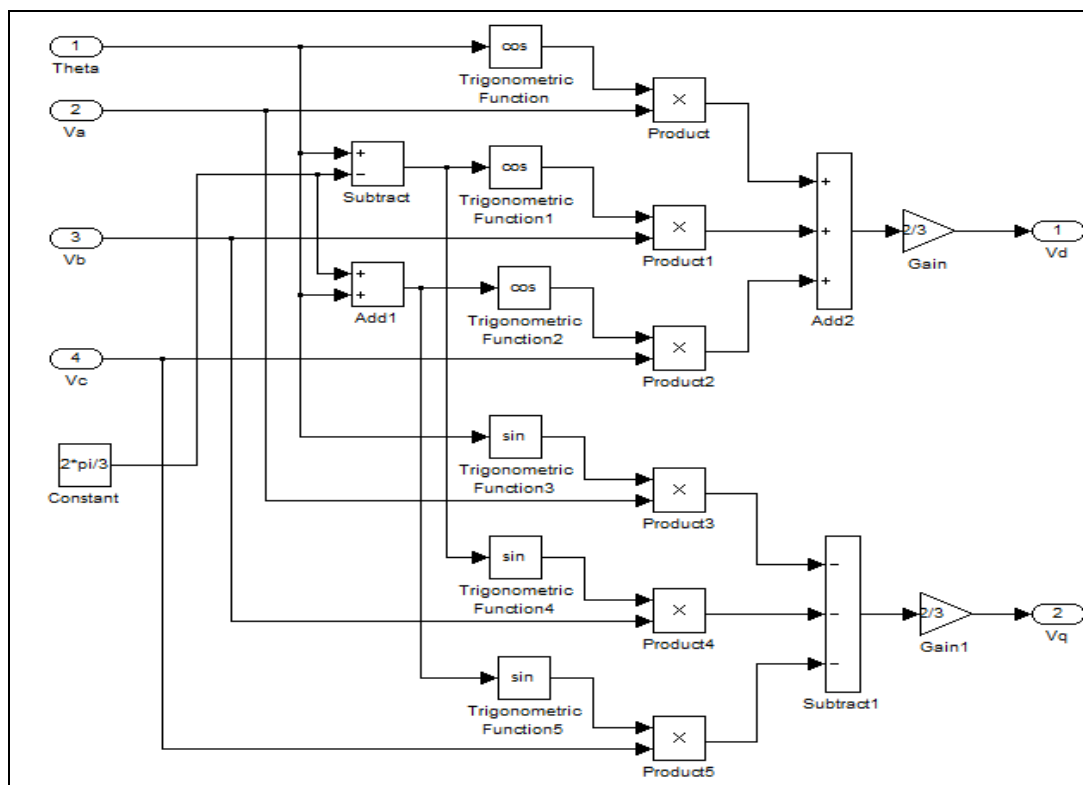


Figure 4.6: Simulink block diagram of Vabc_to_Vdq

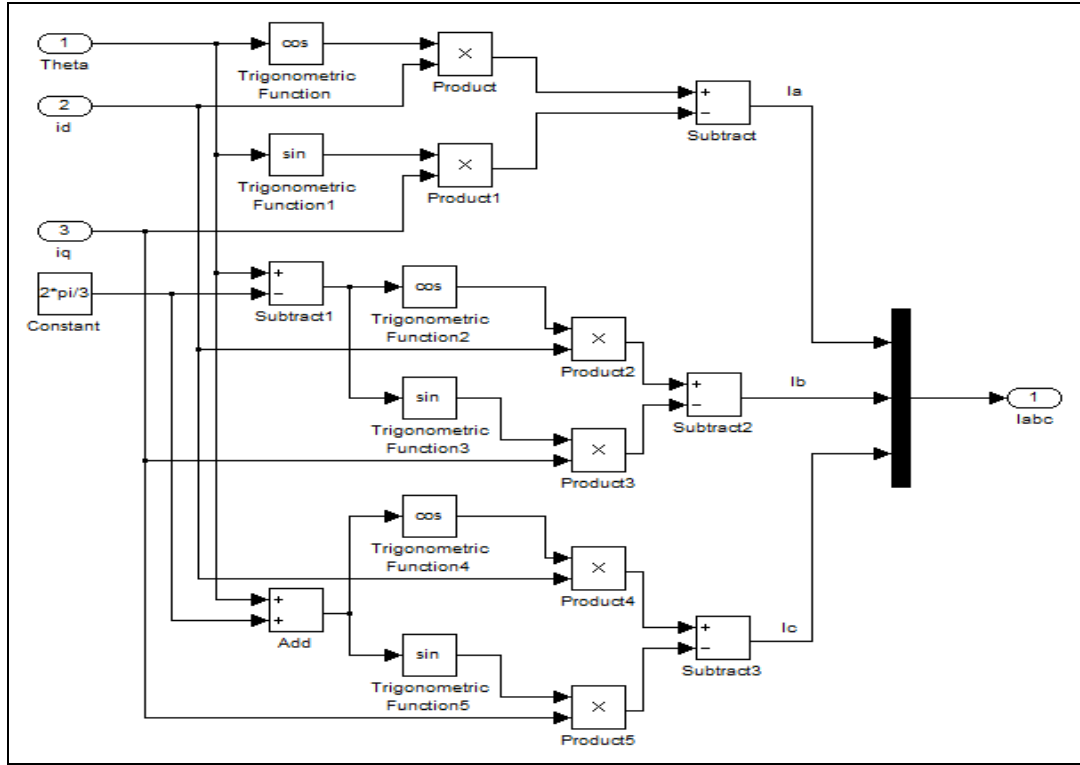


Figure 4.7: Simulink block diagram of Idq_to_Iabc

The stator flux linkage components in the dq frame can be expressed as follows [107,116,117]:

$$\psi_d = L_d \cdot i_d + \psi_{PM} \quad (4.21)$$

$$\psi_q = L_q \cdot i_q \quad (4.22)$$

Where, $L_d, L_q =$ d, q axis reference frame inductances;

$i_d, i_q =$ d, q axis reference frame stator currents;

By assuming that the flow direction of negative stator current is out of the generator positive polarity terminals, the stator voltages of PMSG in a dq reference frame are expressed as follows:

$$v_d = R_s \cdot i_d + \frac{d\psi_d}{dt} - \omega_e \cdot \psi_q \quad (4.23)$$

$$v_q = R_s \cdot i_q + \frac{d\psi_q}{dt} + \omega_e \cdot \psi_d \quad (4.24)$$

Where: v_d and v_q are the stator terminal voltages in the d, q axis reference frame (V);

R_s = stator resistance (Ω);

By looking at equations (4.23) and (4.24), the equivalent circuit of the PMSG in the dq axis reference frame can be drawn as shown in Figure 4.8 below.

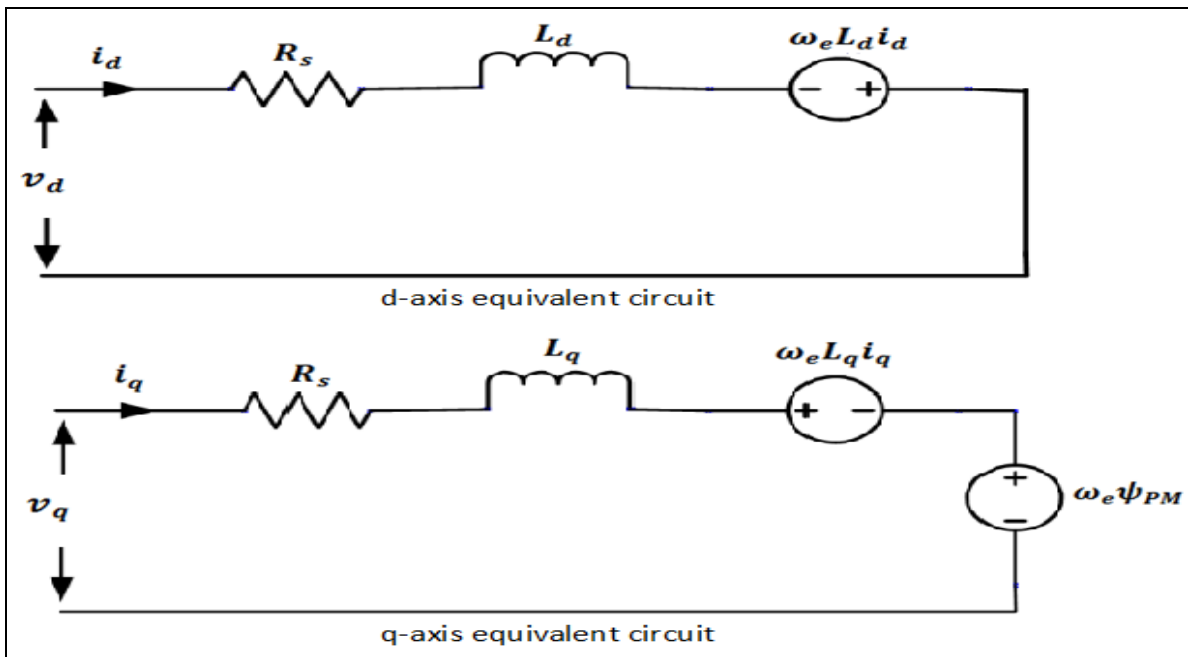


Figure 4.8: d and q equivalent circuit of a PMSG [118]

Hence, by substituting equations (4.21) and (4.22) in (4.23) and (4.24), the PMSG model in the dq reference frame in terms of voltages and currents is given as [56,119,120]:

$$v_d = R_s \cdot i_d + L_d \frac{di_d}{dt} - \omega_e L_q i_q \quad (4.25)$$

$$v_q = R_s \cdot i_q + L_q \frac{di_q}{dt} + \omega_e \psi_{PM} + \omega_e L_d i_d \quad (4.26)$$

In order to determine the output currents of the generator, equations (4.25) and (4.26) can be rearranged to obtain the following equations:

$$\frac{di_d}{dt} = \frac{v_d}{L_d} - \frac{R_s}{L_d} i_d + \frac{L_q}{L_d} \omega_e i_q \quad (4.27)$$

$$\frac{di_q}{dt} = \frac{v_q}{L_q} - \frac{R_s}{L_q} i_q - \frac{L_d}{L_q} \omega_e i_d - \frac{\psi_{PM}}{L_q} \omega_e \quad (4.28)$$

Hence, Simulink block diagrams for stator direct-axis and quadrature-axis current are shown in figures 4.9 and 4.10, respectively.

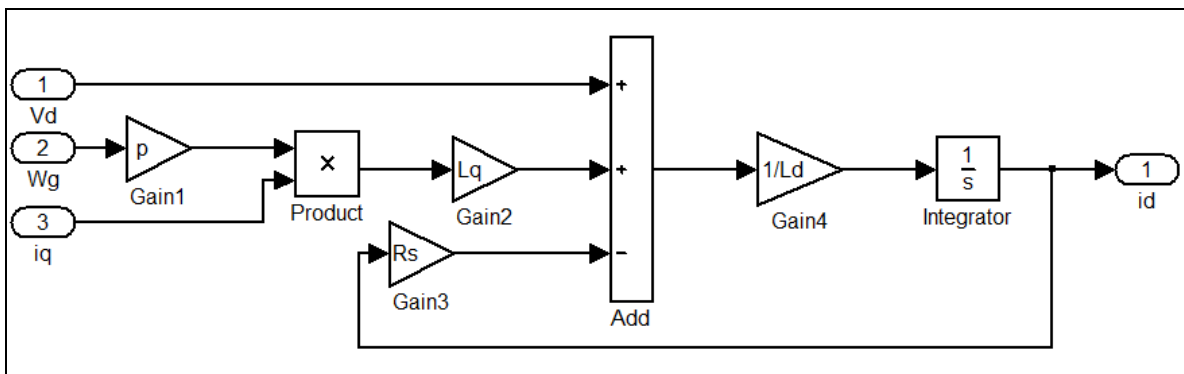


Figure 4.9: Simulink block diagram of the stator direct-axis current

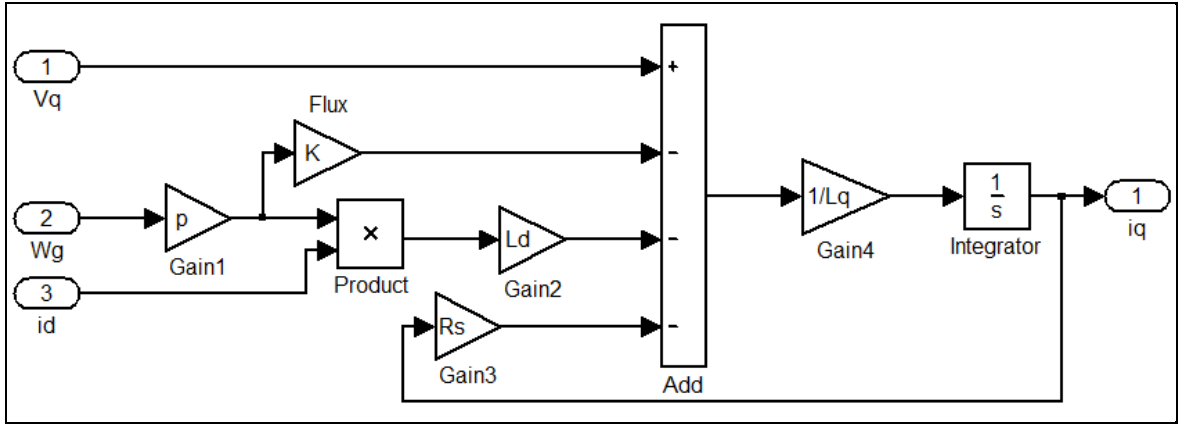


Figure 4.10: Simulink block diagram of the stator quadrature-axis current

In the rotor reference frame, the developed electromagnetic torque is given by the cross-product of the stator flux and stator current and expressed as [121]:

$$T_e = \frac{3}{2} p(\psi_d \cdot i_q - \psi_q \cdot i_d) \quad (4.29)$$

By substituting equations (4.21) and (4.22) into (4.29), the developed electromagnetic torque can then be expressed as

$$T_e = \frac{3}{2} p(\psi_{PM} \cdot i_q + (L_d - L_q) i_d \cdot i_q) \quad (4.30)$$

Hence, Figure 4.11 shows the Simulink block diagram for an electromagnetic torque. This block can be used to model either salient pole or non-salient pole electromagnetic torque.

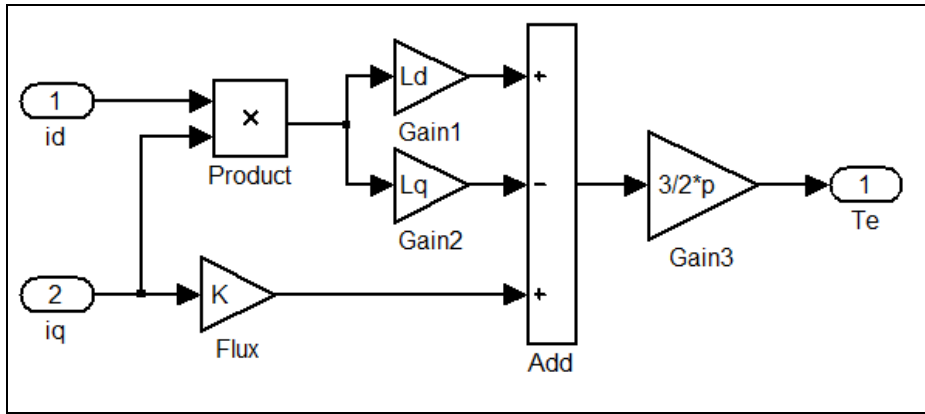


Figure 4.11: Simulink block diagram of the electromagnetic torque

Figure 4.12 below shows the overall model of a PMSG after combining Figures 4.9, 4.10 and 4.11. The parameters of any selected PMSG can be entered in figure 4.12 for simulation purposes.

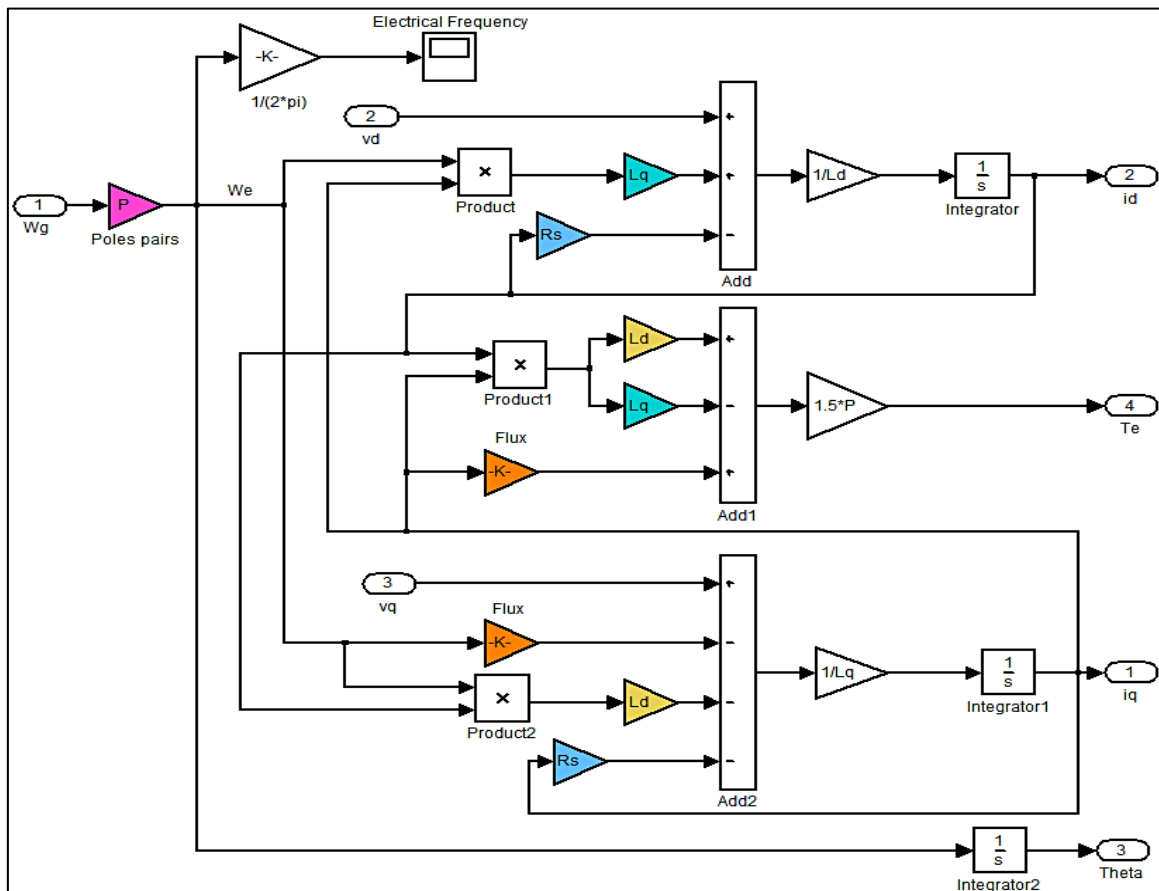


Figure 4.12: Simulink block diagram of a PMSG

4.2.5 Overall model of an off-grid micro-hydrokinetic system

An overall MHR system model was built by interconnecting the blocks of different system parts. High density hydrokinetic turbine, drive-train, and PMSG models were connected together after being configured as subsystems blocks to reduce the complexity of the diagram. The overall model is shown in Figure 4.13 below. A three phase balanced load is supplied by the ABC currents at the output of the PMSG model. The ABC stator voltages are transformed back to the dq-axis voltages within the synchronous reference frame. The dq-axis voltages are fed back as inputs to the generator model [122]. The input to the overall model is the water speed connected to the high water density turbine model. The outputs are the generated three phase voltages and currents.

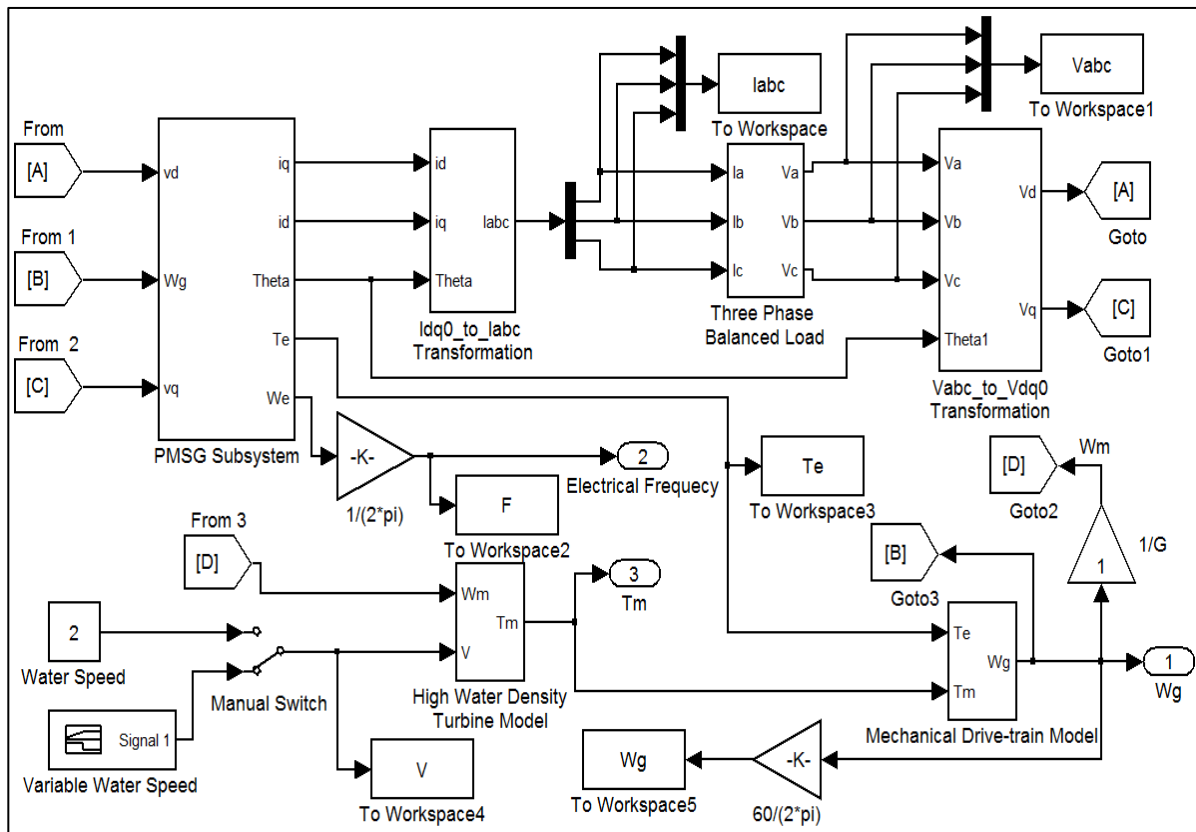


Figure 4.13: Overall MHR system Simulink model

4.3 Conclusion

In this chapter, the mathematical model for off-grid micro-hydrokinetic has been presented. This mathematic model has been used to develop the Simulink model for the overall system. The model was comprised of turbine, drive-train and a direct driven permanent magnet synchronous generator (PMSG) modelling. This model can be used by designers to model a micro- hydrokinetic river system during the planning stage by simply inserting the parameters of the selected turbine and PMSG to be used. The performance of an off-grid MHR system and effects of variable water speed on the systems' behaviour can be analysed. This model can be used to simulate a hydrokinetic system using a PMSG with either salient pole or non-salient pole rotor.

CHAPTER 5: SIMULATION RESULTS AND DISCUSSION

5.1 Introduction

This chapter demonstrates the simulation results based on the hydrokinetic model developed in chapter 4 using a MATLAB/Simulink software program. The aim is to test/reveal the correctness/effectiveness of the developed model. This is done by studying the dynamic behaviour of MHR system under variable water speed. Globally, most common domestic loads are 120V or 230V AC appliances. Hence, different PMSGs will be used when studying the performance of the hydrokinetic system based on variable water speed and different numbers of poles to yield 120V and 230V. The performance of the modelled hydrokinetic system will also be compared to the performance of a wind generation system counterpart. The results will reveal the system that is more efficient in delivering the same amount of electrical power. A Simulink signal builder has been used for variable step input in order to see how the system responds to a change in water speed. The step input signal and the selected time are only used for simulation purposes in order to show how the developed model is responding.

5.2 High Water Density Turbine Model

The coefficients c_1 to c_6 (0.5176, 116, 0.4, 5, 21 and 0.0068, respectively) [56,109] were entered into the Simulink block diagram of a turbine shown in Figure 4.2. The relationship between power coefficient and tip speed ratio of the modelled turbine has been determined

from the XY Graph. The maximum power coefficient, $C_{p(\max)}$ was found to be 0.48 when $\beta = 0$ degrees as shown in Figure 5.1 below.

After proving that the optimum power coefficient of the turbine is 0.48 at tip speed ratio of 8.1 (for $\beta = 0$ degrees), it was then assumed that it remains constant at variable water speeds. Hence, the value of $C_{p(\max)}$ was entered as a constant in the high density turbine model shown Figure 4.3.

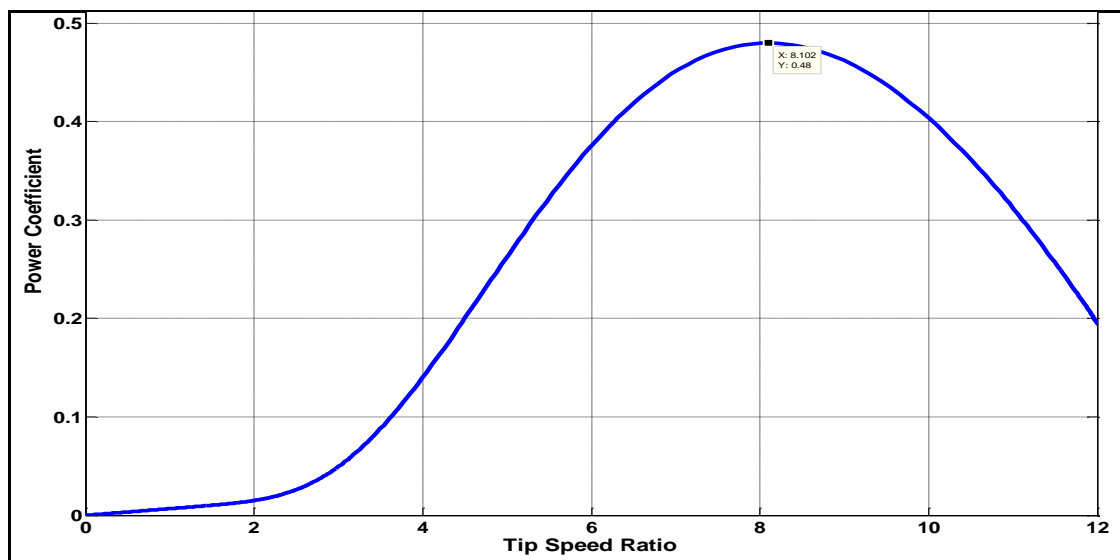
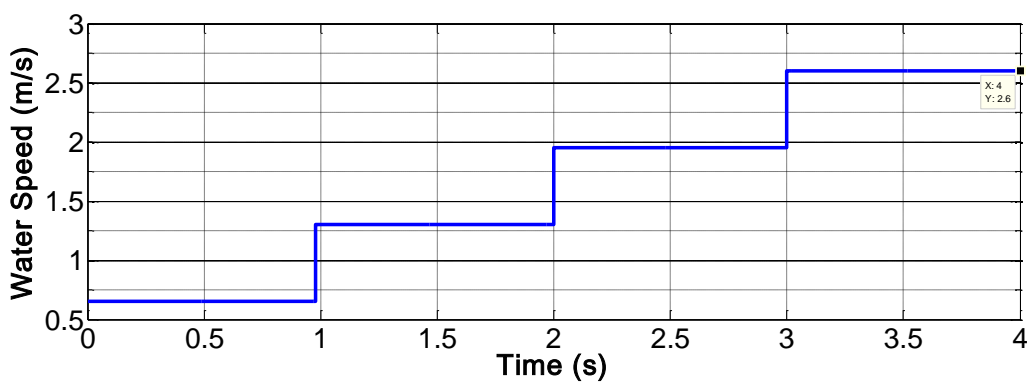


Figure 5.1: Power coefficient versus tip speed ratio of the turbine (with $\beta=0^\circ$)

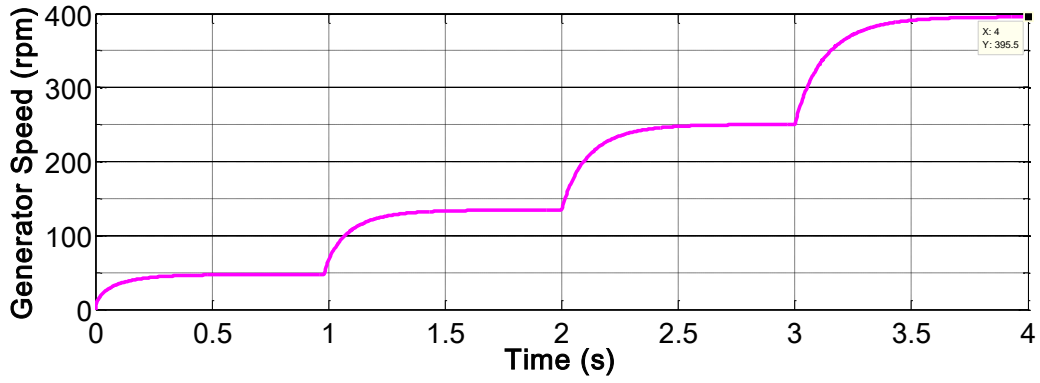
5.3 Performance Evaluation of the Developed Hydrokinetic Model

The developed model can be used to study the performance of the MHR system generating any commonly used voltage level such as 120V or 230V to supply domestic appliances. The designer will merely enter the parameters of the system components to be used. In this section, the parameters of a 2kW, 120V, 17A, 50Hz, 400rpm surface mounted PMSG were entered in the developed model. These parameters are as follows: it has 8 pole pairs, stator resistance of 2Ω , stator d-axis and q-axis reactance of 1mH each and permanent magnet flux

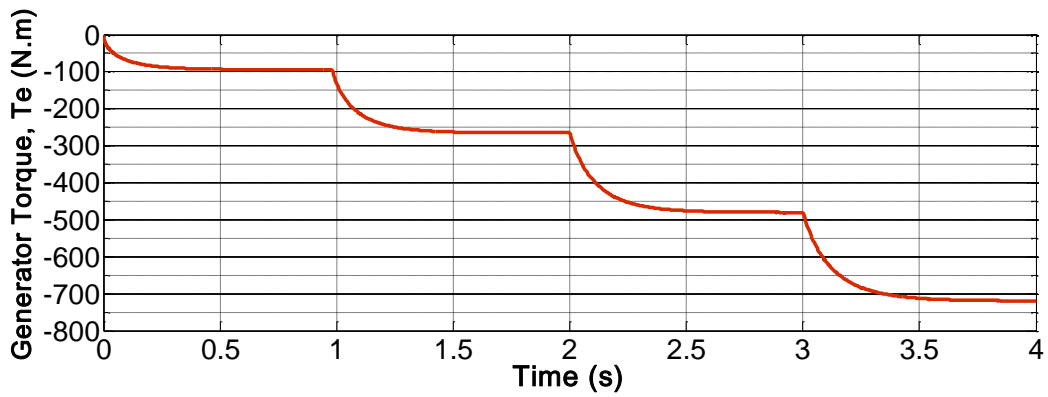
of 0.46Wb [118,123]. To study the dynamic response of the MHR system under different water speeds, the step input representing water velocity has been used for simulation purposes only. The performance results are shown in Figures 5.2 (a) through (f). The speed of the water has been increased in steps of 0.65 m/s for 4 seconds as shown in Figure 5.2 (a). Furthermore, a 2kW three phase balanced load is directly connected to the output of a generator to represent a full-load. From figure 5.2 (d), (e) and (f), it can be seen that as the water speed increases, the generated voltage, load current and frequency are gradually increasing as well. When the water speed is increased from 1.95m/s to 2.6m/s (from $t = 3s$ to $t = 4s$), the generator is rotating at a speed of 395.5rpm which is close to its rated full load speed. At that moment, the parameters such as the generated voltage, frequency and the load current are 126.6V, 51.23Hz and 17.58A respectively. This demonstrates the effectiveness of the developed model since these parameters are close to the rated ones. The electromagnetic torque of the generator shown in Figure 5.2(c) varies with the water speed. The negative value of the electromagnetic torque indicates that the permanent magnet synchronous machine operates as a generator.



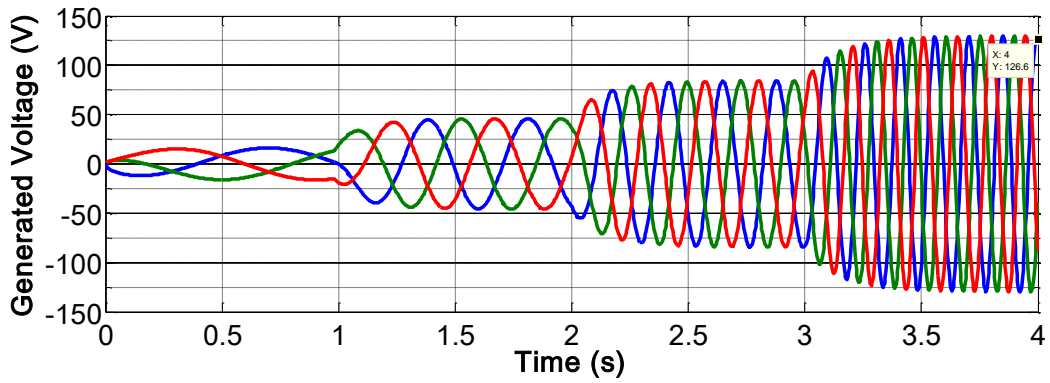
5.2 (a) Water speed



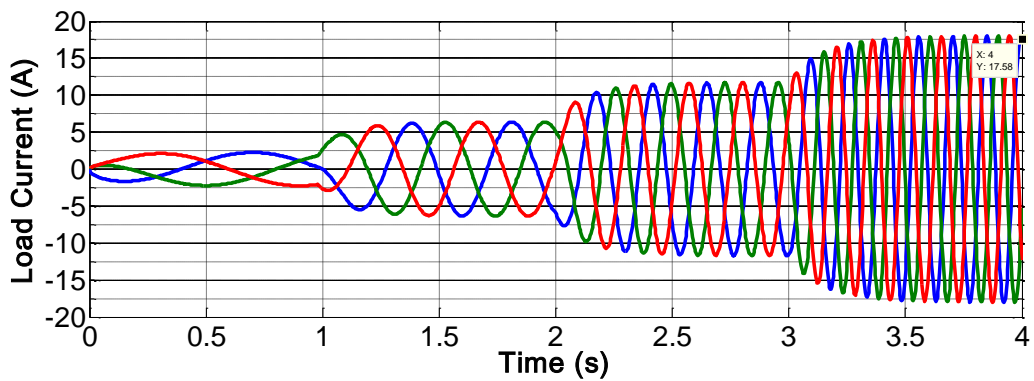
5.2 (b) Generator speed



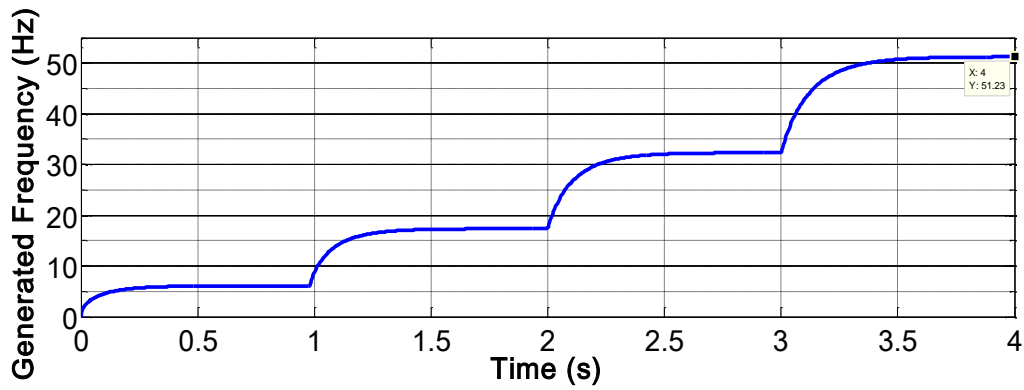
5.2 (c) Generator torque



5.2 (d) Generated voltage



5.2 (e) Load current



5.2 (f) Generated Frequency

5.3.1 Limiting the turbine speed to protect the generator

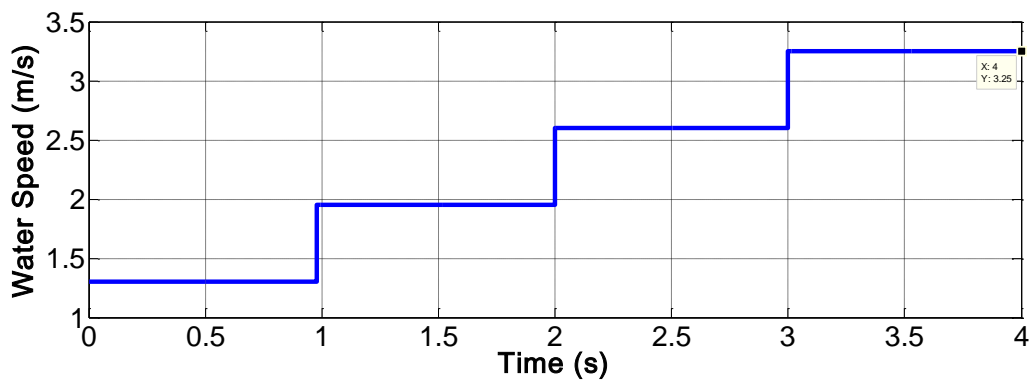
From Figure 5.2 above, it can be noticed that, as the water speed rises, the output voltage of the generator also rises due to an increase in the generator speed. When the water speed reaches 2.6m/s, the generator is almost rotating at its rated speed to generate the rated voltage and frequency.

However, a problem arises when the water speed is higher than 2.6m/s; an appropriate control strategy should be applied to protect the PMSG against over-voltage. This over-voltage will cause an overcurrent within the stator windings of the PMSG. Hence, the control of a turbine is of vital importance to keep the extracted power within its rated values [56]. Since the control of a turbine is beyond the scope of the study, a Simulink saturation block has been used in Figure 4.3 to impose the maximum voltage limit.

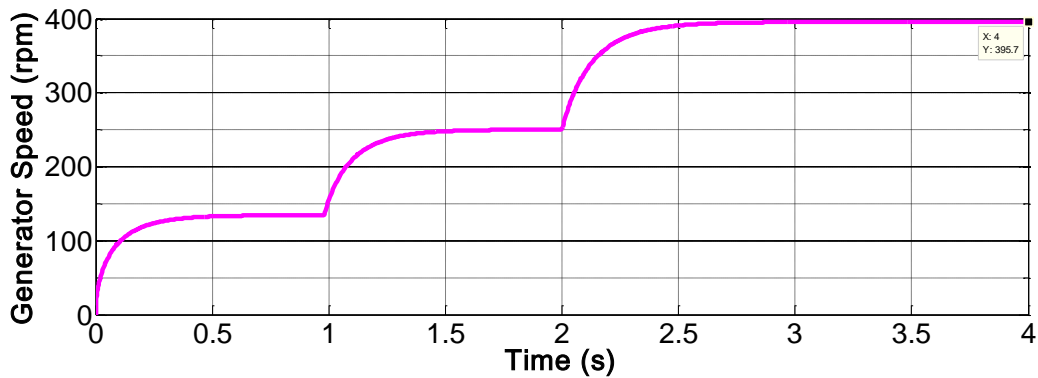
Figures 5.3 (a) through (d) show the simulation results when the water speed was increased from 1.3m/s to 3.25m/s in steps of 0.65m/s. All measured parameters (generated voltage, generated frequency, generator speed) are directly proportional to the water speed. When the speed of the water reaches 2.6m/s (from $t=2s$ to $t=3s$), the generator is approaching its rated speed. Moreover, it can be seen that when the speed of the water exceeded 2.6m/s (from $t=3s$

to $t=4s$), the generated voltage and frequency were maintained at the rated levels. This will protect the generator against over-voltage.

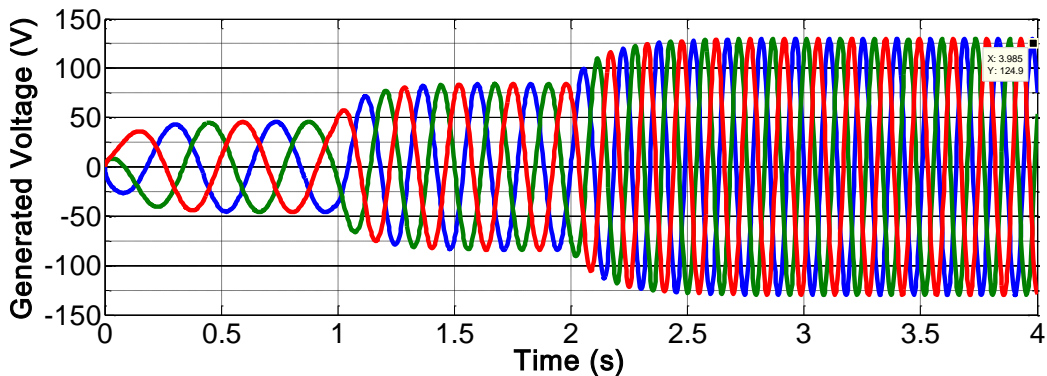
In wind power generation, a turbine also needs protection against high speeds (around 25 m/s) by means of a braking system [124]. Unlike wind turbines, MHR turbines operate at very low speeds since the speed of flowing water is less than wind speed. Hence, chances of damaging a turbine structure due to over-speeding are very slim.



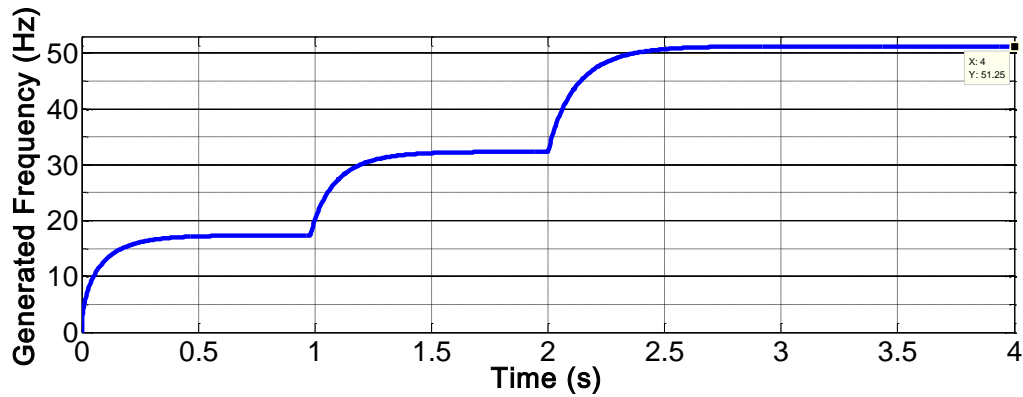
5.3 (a) Water speed



5.3 (b) Generator speed



5.3 (c) Generated voltage



5.3 (d) Generated frequency

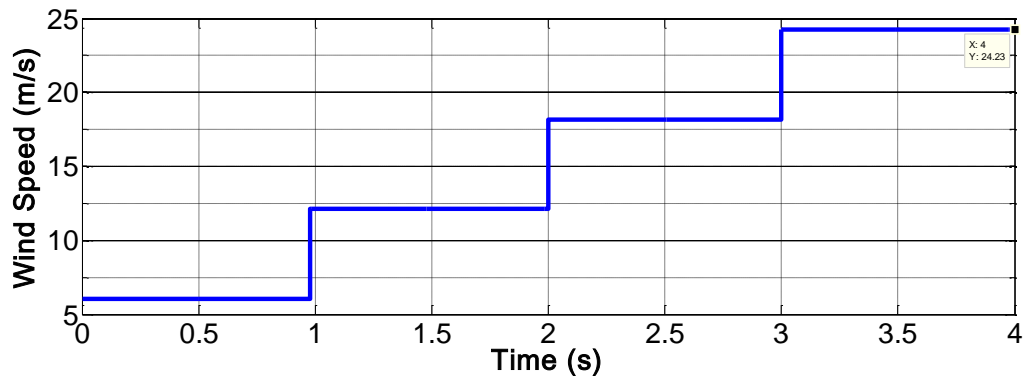
5.3.2 Comparison of the hydrokinetic performance with wind system performance

By assuming a constant wind speed, if a wind resource is used to drive the same turbine, the wind speed of 24.299 m/s is needed to enable the same PMSG to rotate at its rated speed, as shown in Figures 5.4 (a) through (e). Such speed is practically impossible within South Africa, since the average wind speed ranges between 4 to 7 m/s [125]. Hence, in order to generate the same voltage as generated by the hydrokinetic system, one of the following techniques can be applied:

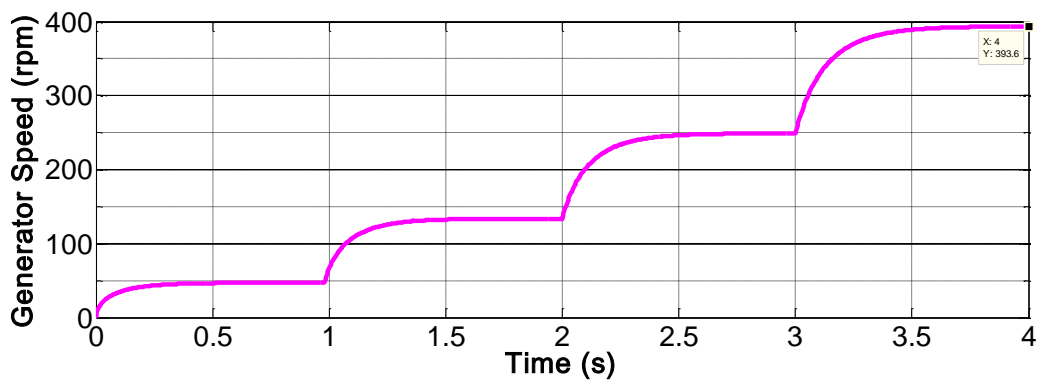
- If the same PMSG is to be used, the size of the turbine blades should be increased. This increase depends on the level of the average wind speed. The lesser the average wind speed, the larger the blade size.
- If the same turbine size is to be used, a PMSG with larger number of pole pairs should be considered.
- If the same turbine and the same PMSG are to be used, a gearbox should be added to the system.

However, any of the above-mentioned techniques will result into high/extra additional costs. Furthermore, a gearbox will also reduce the efficiency and reliability of the system due to

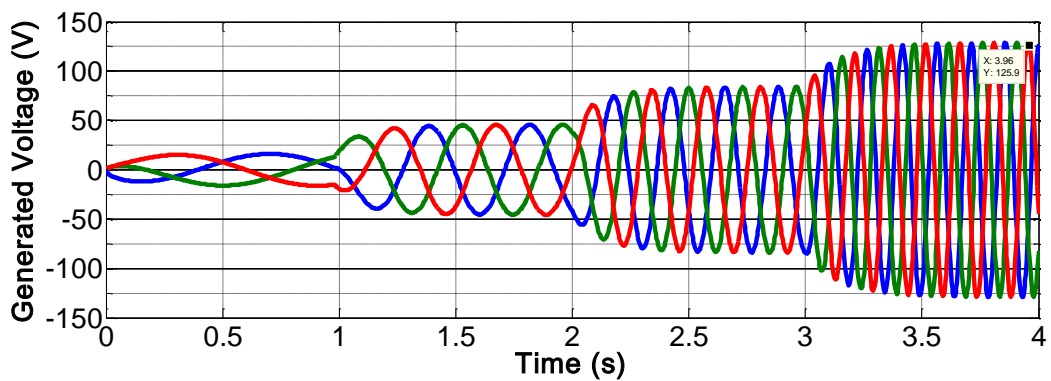
regular maintenance requirement. Therefore, a MHR system can be built markedly smaller and cheaper than a wind system of the same rated power.



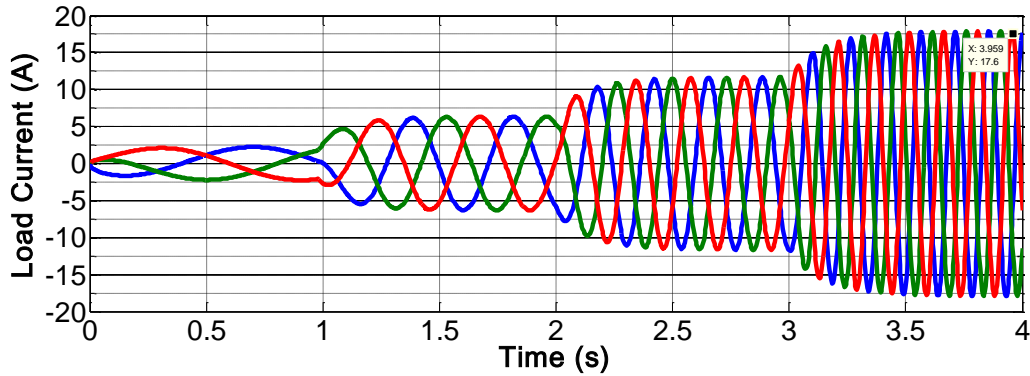
5.4 (a) Wind speed



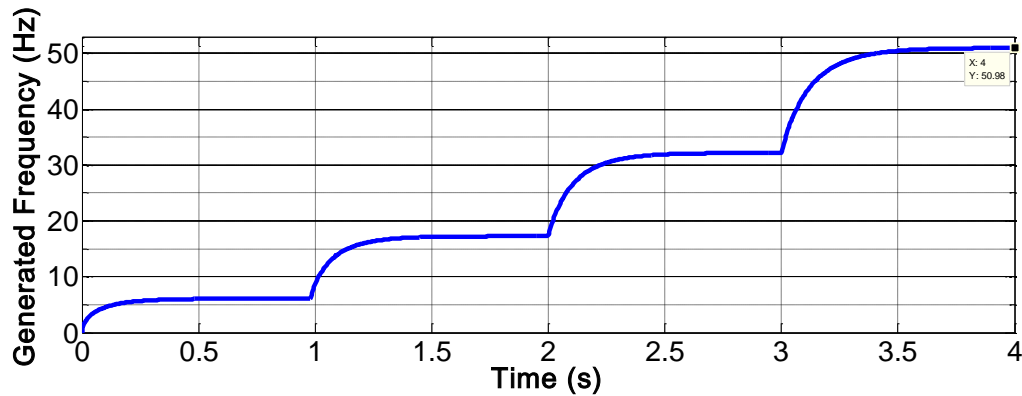
5.4 (b) Generator speed



5.4 (c) Generated voltage



5.4 (d) Load current



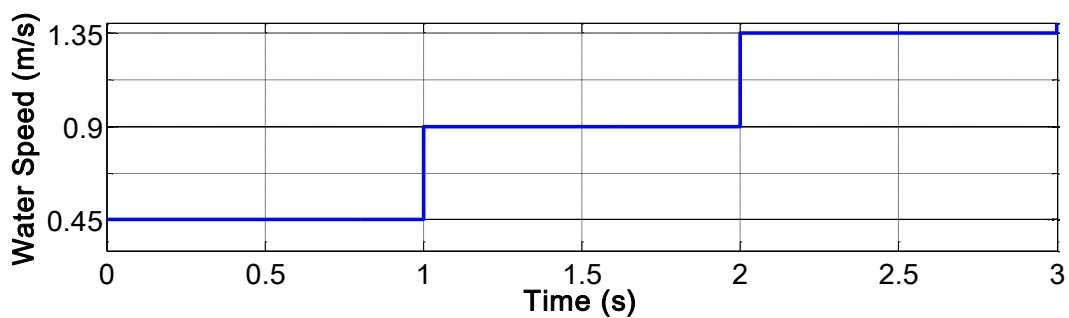
5.4 (e) Generated frequency

5.4 Relationship between the Number of Poles and Gearbox Ratio

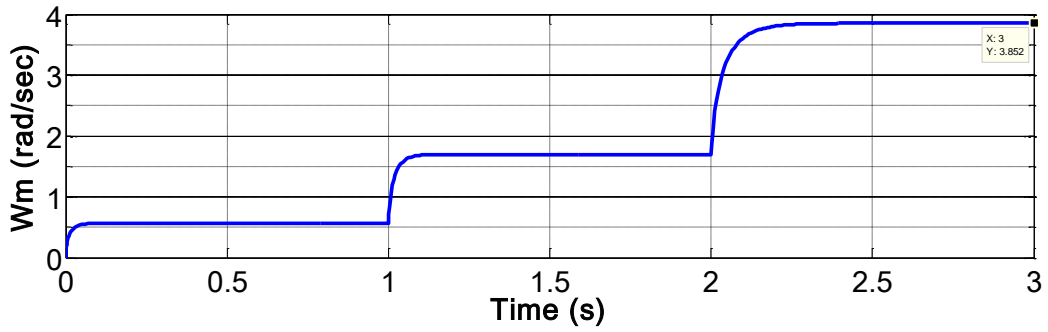
This section demonstrates the performance analysis of the developed MHR model based on the relationship between the number of poles and gearbox ratio. This analysis can be done on a 120V MHR system as well. In this section, it has been done on a system generating 230V. Two different PMSGs with different numbers of poles and capable of generating 230V at 50Hz, were selected. The first case simulation uses a PMSG with large number of pole pairs while the second case comprises a PMSG with fewer pole pairs. It has been assumed that the water flow velocity varies from 0.45m/s to 1.35m/s.

5.4.1 Case 1: PMSG with a large number of pole pairs

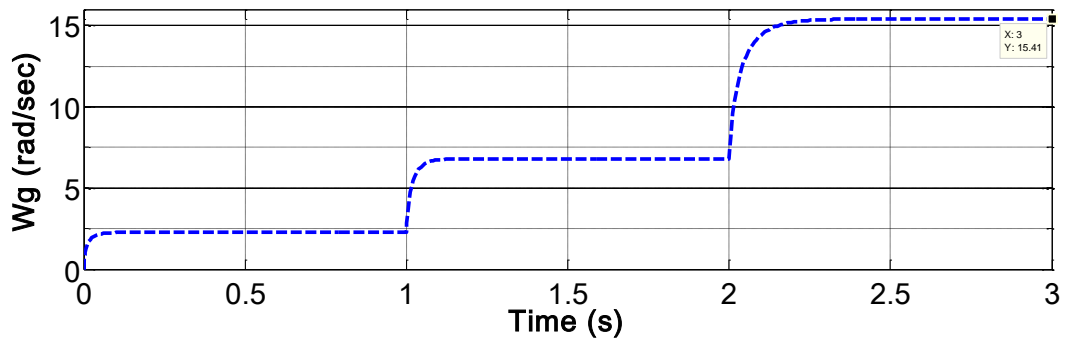
Case 1 has been simulated by making use of a surface mounted PMSG consisting of 20 pole pairs, stator resistance of 1.107Ω , stator d-axis and q-axis of 0.3mH each and permanent magnet flux of 0.148Wb . The simulation results are shown in Figures 5.5 (a) through (f) below. Based on the operation principle of synchronous generators, the angular speed of the generator together with the number of poles determines the frequency of the induced voltage. Hence, in order for this 20 pole generator to induce a voltage at a required frequency of 50Hz , it needs to be driven at a speed of 150rpm . Due to low water speed steps shown in Figure 5.5 (a) below, a gear ratio of $1:4$ has been used to allow the generator to rotate faster than the turbine speed. From Figures 5.5 (b) and (c), it can be noticed that, at any point in time, the angular speed of the generator is four times more than the angular speed of the turbine, due to the gear ratio. When the speed of the water increases to 1.35m/s (from $t=2\text{s}$ to 3s), the generator speed approaches almost 150rpm . Hence, the generated voltage was 322V -peak (228Vrms) at a frequency close to 50Hz .



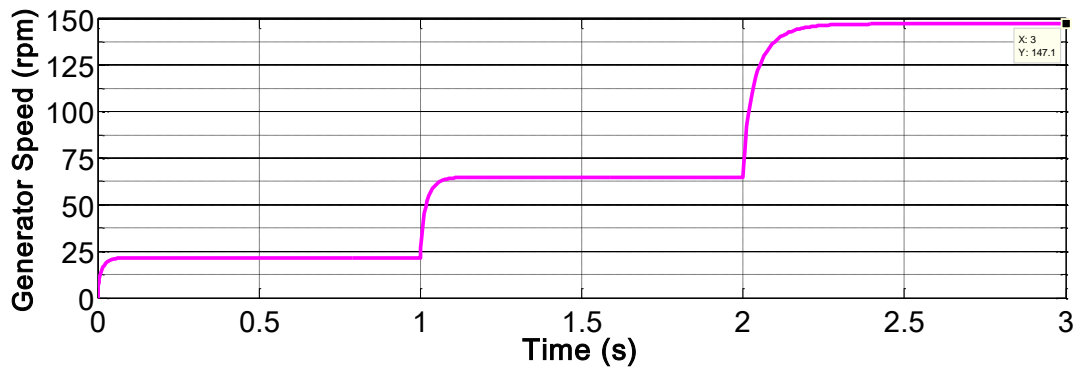
5.5 (a) Water speed



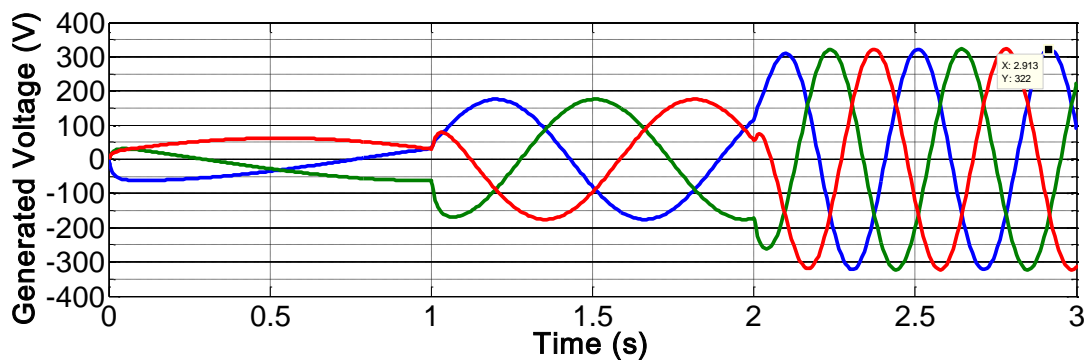
5.5 (b) Mechanical angular speed of the turbine



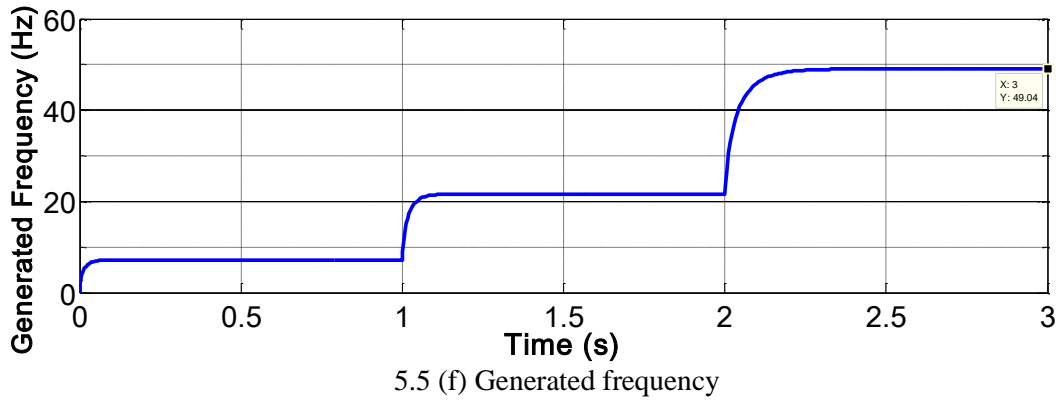
5.5 (c) Angular speed of the generator



5.5 (d) Generator speed

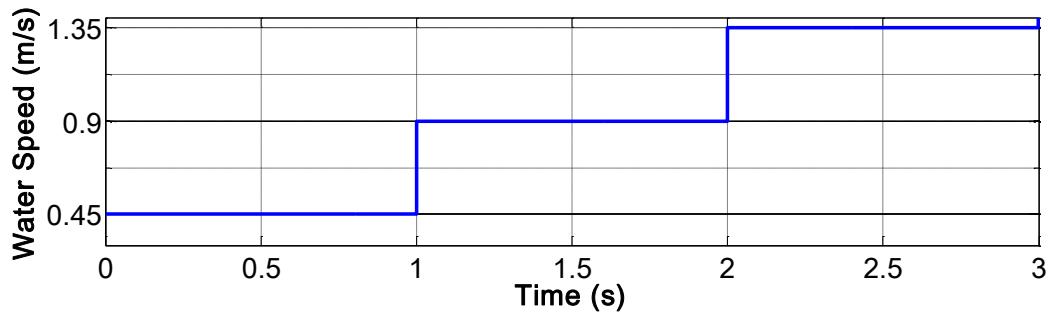


5.5 (e) Generated voltage

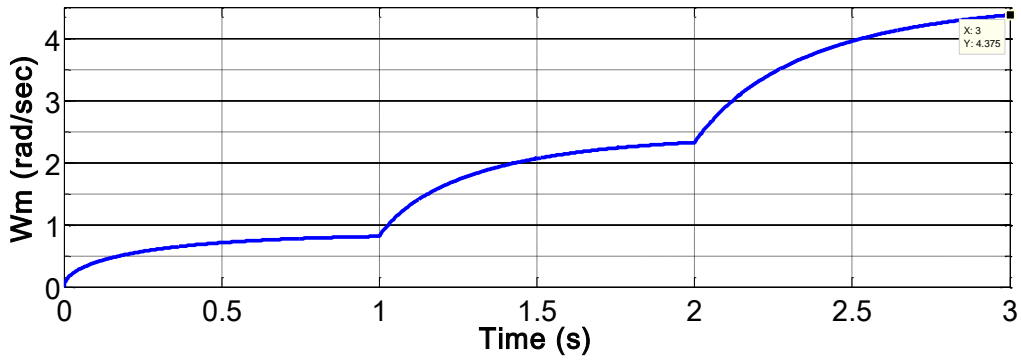


5.4.2 Case 2: PMSG with fewer pole pairs

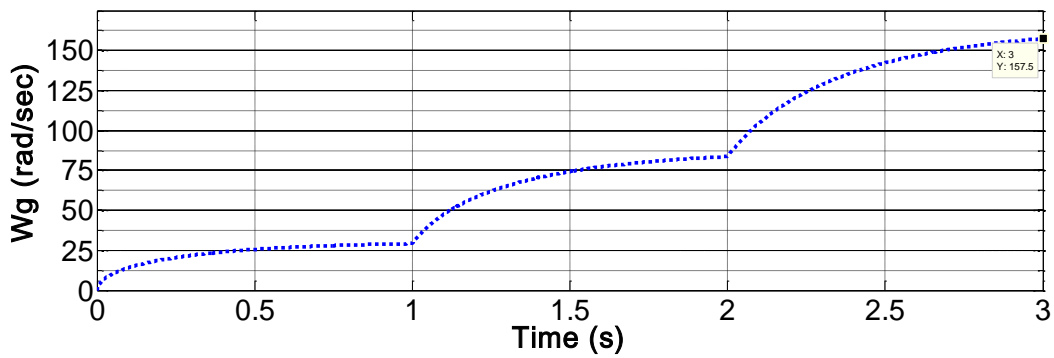
Case 2 has been simulated by making use of a surface mounted PMSG consisting of 2 pole pairs, stator resistance of 1.85Ω , stator d-axis and q-axis of 0.7mH each and permanent magnet flux of 0.915Wb . The simulation results are shown in Figures 5.6 (a) through (f) below. Based on the simulation results, it appears that this generator needs a speed of 1500rpm in order to generate the required 50Hz frequency of the induced voltage. The requirement for such high speed is due to fewer pole pairs. Hence, a gear ratio of $1:36$ has been used to allow the generator to rotate at the required speed. From Figures 5.6 (b) and (c), it can be seen that at any point in time, the angular speed of the generator is 36 times more than the angular speed of the turbine, due to the gear ratio. When the speed of the water increases to 1.35m/s (from $t=2\text{s}$ to 3s), the generator speed approached 1504rpm as shown in Figure 5.6 (d). Hence, the generated voltage was 326.8V -peak (231V_{rms}) at a frequency of 50.14 Hz .



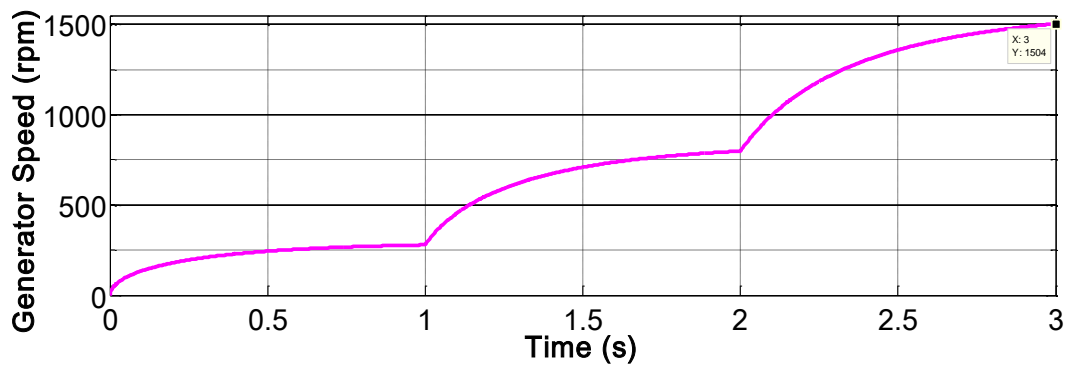
5.6 (a) Water speed



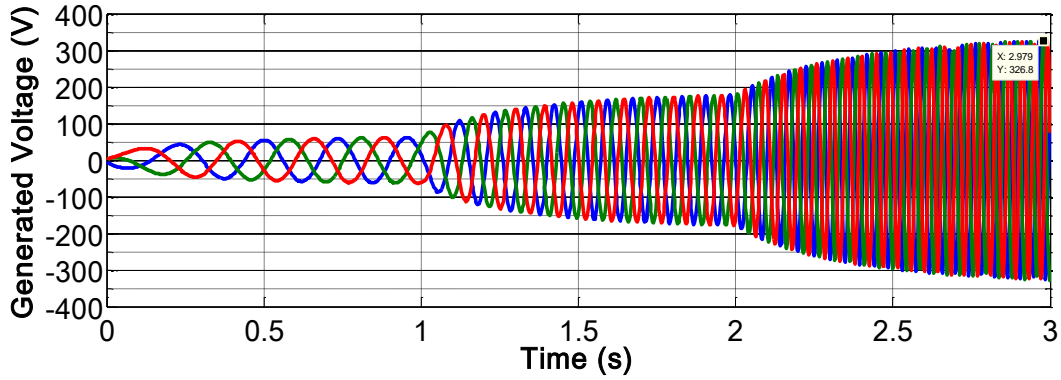
5.6 (b) Mechanical angular speed of the turbine



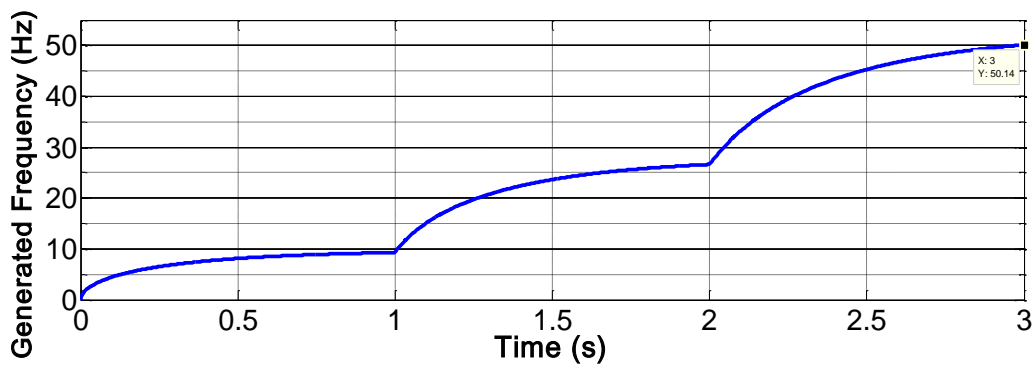
5.6 (c) Angular speed of the generator



5.6 (d) Generator speed



5.6 (e) Generated voltage



5.6 (f) Generated frequency

5.5 Conclusion

The developed model can be used by designers to study the performance of an MHR system under variable water speed. The performance can be studied using a geared or direct-driven PMSG (salient pole or non-salient pole rotor types) within the system in order to determine the trade-off/effects of choices made.

A dynamic response of a MHR system submitted to varying water flow has been investigated. It has been seen that as the water speed increases, PMSG's parameters, such as generated voltage, frequency and electromagnet torque, are also increasing. Hence, limiting the turbine output power is important to maintain the lifespan of the generator. It has also been found that in order for a small-scale wind turbine system to generate the same amount of power as small-scale hydrokinetic system, additional costs should be incurred by increasing

the turbine size, buying a generator with a large number of poles or installing a gearbox to the system. Hence, the system costs are increased. This simply proves that in isolated rural areas with access to flowing water and adequate/inadequate wind resource, hydrokinetic power is the cheapest, most reliable and efficient system to consider.

It has been observed that an increase in PMSG's poles leads to a lower required speed even though the size and the cost of the generator will increase. Alternatively, if the number of poles is reduced, the cost of the generator will decrease while the gearbox cost and weight is increasing. Hence, it is important for a designer to find a balance between the number of poles and a gearbox ratio in order to minimize the system cost, depending on the speed of the water within the selected site. When determining the balance, the maintenance costs and efficiency of each case should also be taken into account since they may impact the cost of energy production as well.

CHAPTER 6: CONCLUSION AND FUTURE STUDIES

6.1 Conclusion

This chapter provides conclusions on a techno-economic analysis of off-grid micro-hydrokinetic river system as a rural electrification option when compared to solar, wind and diesel generator systems.

Lack of electricity in isolated rural areas is a major factor impeding poverty eradication. The aim of this research was to explore an affordable, reliable and sustainable means of providing electricity to isolated rural residents. This can be achieved by making use of the untapped hydrokinetic resource potential and can play a major role in improving living standards of poor rural residents.

As a means of revealing research gaps, enabling proper selection of technologies and creating awareness based on the potential use of a flowing water resource, a global review of the current status of micro-hydrokinetic have been presented in Chapter 2. The emphasis was on various technologies, manufacturers and recent development studies. This chapter also exposed the fact that there is a huge amount of untapped flowing water in South Africa.

In Chapter 3, techno-economic analysis of off-grid micro-hydrokinetic system was performed in order to demonstrate the potential benefits to be gained at the study site when using a flowing water resource. This economic feasibility analysis was performed to compare the off-grid MHR, solar, wind and DG systems' benefits at the same study site. From the optimized base case results, an off-grid MHR system proved to be the most cost-effective, sustainable and environmentally friendly means of supplying electric power to the study site. It generates electricity more cheaply than wind, solar, and DG systems. Due to its reliability, it can compensate for the non-continuous availability of solar and wind energy sources by

generating electricity throughout the day. Its simplicity and low cost highlights a new opportunity to improve quality of life within isolated rural communities.

In Chapter 4, the mathematical model for the micro-hydrokinetic energy conversion system was presented. This model aims to study the behaviour of a micro-hydrokinetic river system using a permanent magnet synchronous generator under variable water speed. It also aims to help designers to make informed decisions during project planning stage. Using the presented model, the dynamic behaviour of an MHR system under variable water speed was simulated in Chapter 5 by making use of a MATLAB/Simulink software package. The simulation results obtained proved that even in areas with both a flowing water resource and adequate wind speed in South Africa, MHR system is the best small-scale option to consider for remote rural electrification. The developed model has also been used to:

- Analyse the relationship between the variation of input water resource and desired output voltage.
- Analyse the relationship between the number of poles and gearbox ratio.
- Demonstrate the importance of finding a balance between the number of poles and gearbox ratio in order to minimise the system cost.

6.2 Suggestions for Further Studies

The study has revealed that the following research works still need to be done:

- Numerous hydrokinetic turbines can be installed within the same river to generate electricity for the same load as revealed by HOMER optimum system architecture results. Hence, a specialised MPPT and control strategy needs to be devised and tested for such a configuration.

- More work needs to be done in integrating the MHR system with grid and/or other potential off-grid sources in order to determine an optimal hybrid configuration.
- A study based on maximum power extraction from an MHR system and also optimal system sizing when using different turbine configurations, different generators and different energy storage devices needs to be carried out. This will ensure efficient employment of this technology and can positively impact the investment cost of the system.
- An experimental prototype of an off-grid MHR system needs to be built and tested within the study site in order to validate the simulation results.

REFERENCES

- [1] Ministry of Economic Affairs, Agriculture and Innovation, (Accessed March 08, 2011) Available at:
<http://www.government.nl/documents-and-publications/reports/2011/11/01/energy-report-2011.html>
- [2] European Commission: "Climate Change", April 2009, (Accessed October 10, 2012) Available at: http://ec.europa.eu/environment/pubs/pdf/factsheets/climate_change.pdf
- [3] Nation Master: "Environmental Statistics of Carbon Dioxide Emissions by Country", (Accessed September 07, 2013) Available at:
http://www.nationmaster.com/graph/env_co2_emi-environment-co2-emissions
- [4] Eberhard A., "The future of South African Coal: Market, Investment, and Policy Challenges", *Program on Energy and Sustainability Development*, January 2011.
- [5] Department of Economic Development, Environmental Affairs and Tourism: "Renewable Energy Conference Focusing on Partnerships between the European Union and the Eastern Cape Province, South Africa", 27-30 November 2012, (Accessed December 07, 2012) Available at:
http://www.nglobal.com/uploads/media/EU_EC_Renewable_Energy_Conference_Background_Doc_01.pdf
- [6] Anyi M., Kirke B., Ali S., "Remote Community Electrification in Sarawak, Malaysia", *Renewable and Sustainable Energy Reviews*, 35(7), 1609-1613, July 2010.
- [7] Woodruff A., "An Economic Assessment of Renewable Energy Option for Rural Electrification in Pacific Island Countries", *SOPAC Technical Report 397*, February 2007, (Accessed September 07, 2012). Available at:

- <http://www.geni.org/globalenergy/library/technical-articles/generation/small-island-nations/renewable-energy-options-for-rural-electrification-in-pacific-island-countries/TR0397.pdf>
- [8] Zomers A., "The Challenge of Rural Electrification", *Energy for Sustainable Development*, 7(1), 69-76, 2003.
- [9] Winkler H, Simoes AF, LA Rovere EL, Atiq Rahman RA, Mwakasonda S: "Access and Affordability of Electricity in Developing Countries". *World Development*, 39(6), 1037-1050, 2011.
- [10] Barta B.: "Status of the small-scale hydroelectric (SSHE) development in South Africa", March 2010.
- [11] Cust J, Singh A, Neuhoﬀ K, "Rural Electrification in India: Economic and Institutional Aspects of Renewables" December 2007, (Accessed June 20, 2012) Available at: <http://www.eprg.group.cam.ac.uk/wp-content/uploads/2008/11/eprg0730.pdf>
- [12] Paish O. "Small Hydro Power: Technology and Current Status", *Renewable and Sustainable Energy Reviews*, 6(6), 537–556, December 2002.
- [13] University of Louisville: "Sustainable Power Generation Study" , 12 August 2009, (Accessed June 14, 2012) Available at: http://louisville.edu/sustainability/operations/Report%20-%20Renewable%20Energy%20Options%20for%20UofL%20-Cannon%20Design%208-12-09.pdf/at_download/file
- [14] Williams G.G., Jain P., "Renewable Energy Strategies", *Sustain: a Journal of Environmental and Sustainability issues*, the Kentucky Institute for the Environment and Sustainable Development, (23), 29-42, 2011.
- [15] Ministerial Conference on Water for Agriculture and Energy in Africa: "The

Challenges of Climate Change", 15-17 December 2008, Sirte, Libyan Arab Jamahiriya.

(Accessed June 20, 2012) Available at:

http://www.sirtewaterandenergy.org/docs/2009/Sirte_2008_BAK_3.pdf

- [16] Boccaletti C., Fabbri G., Marco J., Santini E., "An Overview on Renewable Energy Technologies for Developing Countries: the case of Guinea Bissau", *International Conference on Renewable Energy and Power Quality (ICREPQ'08)*, 12-14 March 2008, Santander, Espana.
- [17] Micro hydropower basic: "Introduction to micro hydro". (Accessed June 20, 2012) Available at:
http://josiah.berkeley.edu/2007Fall/ER200N/Readings/Micro_Hydro_2007.pdf
- [18] Bertsch D.J., "Hydrokinetic Energy: Trying to Navigate the Energy and Wave Law Framework to Develop New Renewable Energy Technology", (Accessed June 08, 2012) Available at:
<http://www.elizabethburleson.com/enbweb/HydrokineticEnergyDerekBertsch.pdf>
- [19] Mosallat F., "Specialized Power-Electronic Apparatus for Harnessing Electrical Power from Kinetic Hydropower Plants", Master's Thesis, Department of Electrical and Computer Engineering, University of Manitoba, July 2012.
- [20] van Arkel R., Owen J., Allison S., Tryfonas T., Winter A., Entwistle R., Keane E., Parr J., "Design and Preliminary Testing of a Novel Concept Low Depth Hydropower Device", *Oceans' 11*, 19-22 September 2011, Hawaii, USA.
- [21] Cada G, Ahlgrimm J, Bahleda M, Bigford T, Stavrakas SD, Hall D, Moursund R, Sale M: "Potential Impacts of Hydrokinetic and Wave Energy Conversion Technologies on Aquatic Environments". *Fisheries*, 2007, 32(4), 174–181
- [22] Canadian Hydraulics Centre: "Assessment of Canada's Hydrokinetic Power Potential",

- Phase 1 Report: Methodology and Data Review, March 2010. (Accessed June 20, 2012) Available at:
- http://canmetenergy.nrcan.gc.ca/sites/canmetenergy.nrcan.gc.ca/files/files/pubs/NRCan_CHC_Assessment_of_Canadas_Hydrokinetic_Power_Potential_FinalReport_EN.pdf
- [23] Kusakana K, Vermaak HJ,: "Feasibility study of hydrokinetic power for energy access in rural South Africa", *Fifth IASTED Asian Conference on Power and Energy Systems*, 433-438, (April 2012)
- [24] NASA Surface meteorology and Solar Energy RETScreen Data: "To access data for RETScreen". (Accessed January 20, 2013), Available at:
- <https://eosweb.larc.nasa.gov/cgi-bin/sse/retscreen.cgi?email=rets@nrcan.gc.ca>
- [25] RETScreen Software: "Online User Manual". (Accessed January 20, 2013) Available at: www.retscreen.net
- [26] Stiel A., Skyllas-Kazacos M., "Feasibility Study of Energy Storage Systems in Wind/Diesel Applications Using the HOMER Model", *Applied Science*, 2, 726-737, October 2012.
- [27] Department of Minerals and Energy: "White Paper on Renewable Energy" November 2003, (Accessed July 20, 2013) Available at:
- http://unfccc.int/files/meetings/seminar/application/pdf/sem_sup1_south_africa.pdf
- [28] Klunne, W.J., "Small Hydropower in Southern Africa - an Overview of Five Countries in the Region", *Journal of Energy in Southern Africa*, 24(3), 14-25, 2013.
- [29] Güney M.S., Kaygusuz K., "Hydrokinetic Energy Conversion Systems: a technology status review", *Renewable and Sustainable Energy Reviews*, 14(9), 2996-3004, 2010.
- [30] Gauntlett D., Asmus P., "Executive Summary: Hydrokinetic and Ocean Energy. Pike Research, Cleantech Market Intelligence", 2009, (Accessed June 06, 2012) Available

at: <https://www.pikeresearch.com/wp-content/uploads/2009/05/HYDRO-09-Executive-Summary.pdf>

- [31] Zhou H., “Maximum Power Point Tracking Control of Hydrokinetic Turbine and Low-Speed High-Thrust Permanent Magnet Generator Design”, MSc Thesis, Missouri University of Science and Technology, 2012.
- [32] Kuschke M., Strunz K., “Modeling of Tidal Energy Conversion Systems for Smart Grid Operation”, *IEEE Power and Energy Society General Meeting*, Detroit, 2011.
- [33] Maniaci D.C., Ye Li, “Investigating the Influence of the Added Mass Effect to Marine Hydrokinetic Horizontal-Axis Turbines Using a General Dynamic Wake Wind Turbine Code”, *Oceans’ 11 conference*, 19-21 September 2011, Hawaii, USA.
- [34] Grabbe M., Yuen K., Goude A., Lalander E., Leijon M., “Design of an Experimental Setup for Hydro-Kinetic Energy Conversion”, *The International Journal on Hydropower & Dams*, 16(5), 112-116, 2009.
- [35] Yuen K., Thomas K., Grabbe M., Deglaire P., Bouquerel M., Österberg D., Leijon M., “Matching a permanent magnet synchronous generator to a fixed pitch vertical axis turbine for marine current energy conversion”, *IEEE Journal of Oceanic Engineering*, 34(1), 2009.
- [36] Hydro Alternative Energy: “Hydrokinetic renewable power”. (Accessed June 05, 2012)
Available at: <http://www.haeturbines.com/hydrokinetic-renewable-power.html>
- [37] Ben Elghali S.E., Benbouzid M.E.H., Charpentier J.F., “Marine Tidal Current Electric Power Generation Technology: State of the Art and Current Status”, *Electric Machines & Drives Conference, IEEE International, IEMDC '07*, 1407-1412, 2007.
- [38] Hermann S., “Design of a Micro-Hydro Powered Battery Charging System for Rural Village Electrification”, Master’s Thesis, Postgraduate Programme Renewable Energy,

Carl von Ossietzky University, Oldenburg, 28 March 2006.

- [39] Bekker J.C., "Efficient Modelling of a Wind Turbine System for Parameter Estimation Applications", Master's Thesis, University of Stellenbosch, March 2012.
- [40] Khan M.J., Bhuyan G., Iqbal M.T., Quaicoe J.E., "Hydrokinetic energy conversion systems and assessment of horizontal and vertical axis turbines for river and tidal applications: a technology status review", *Applied Energy*, 86(10), 1823-1835, 2009.
- [41] Khan M.J., Iqbal M.T., Quaicoe J.E., "River current energy conversion systems: progress, prospects and challenges", *Renewable and Sustainable Energy Reviews*, 12(8), 2177-2193, 2008.
- [42] Hydrovolts: "In-stream Hydrokinetic Turbines", Powertech Labs, 2006, (Accessed July 06, 2012) Available at: <http://hydrovolts.com/wp-content/uploads/2011/06/In-Stream-Hydrokinetic-White-Paper2.pdf>
- [43] Tanbhir H., Nawshad U.A., Islam N., Sina I., Syfullah K., Raiyan R., "Micro hydro power: promising solution for off-grid renewable energy source", *International Journal of Scientific & Engineering Research*, 2(12), 2011.
- [44] Sornes K., "Small-scale Water Current Turbines for River Applications", *Zero Emmison Resource Organization*, January 2010.
- [45] Golecha K., Eldho T.I., Prabhu S.V., "Study on the interaction between two hydrokinetic Savonius turbines". *International Journal of Rotating Machinery*, (Article ID 581658), 2012.
- [46] Anyi M., Kirke B., "Evaluation of small axial flow hydrokinetic turbines for remote communities", *Energy for Sustainable Development*, 14(2), 110-116, 2010.
- [47] Kirke B., "Developments in ducted water current turbines" *Sustainable Energy Centre*, University of South Australia, Mawson Lakes, Australia, April 2006. (Accessed June

- 06, 2012) Available at: http://www.cyberiad.net/library/pdf/bk_tidal_paper25apr06.pdf
- [48] Birjandi A.H., Woods J., Bibeau E.L., "Investigation of macro-turbulent flow structures interaction with a vertical hydrokinetic river turbine", *Renewable Energy*, (48), 189-192, 2012.
- [49] Kirke B.K., "Tests on ducted and bare Helical and straight blade Darrieus hydrokinetic turbines", *Renewable Energy*, 36(11), 3013-3022, 2011.
- [50] Scherer L.G., de Camargo R.F., "Control of micro hydro power stations using nonlinear model of hydraulic turbine applied on microgrid systems", *Power Electronics Conference*, 812-818, 2011.
- [51] Faria J., Margato E., Resende M.J., "Self-excited induction generator for micro-hydro plants using water current turbines type", *Telecommunication Conference (INTELEC '05)*, 107-112, September 2005.
- [52] Howey D.A., "Axial flux permanent magnet generators for pico-hydropower", *EWB-UK Research Conference*, February 2009.
- [53] Dehkordi A.B., Gole A.M., Maguire T.L., "Permanent Magnet Synchronous Machine Model for Real-Time Simulation", *International Conference on Power Systems Transients (IPST'05)*, Canada 159, June 2005.
- [54] Hussein M.M., Senjyu T., Orabi M., Wahab M.A.A., Hamada M.M., "Control of a Stand-Alone Variable Speed Wind Energy", *Applied Science*, 3, 437-456, 2013.
- [55] Abbas F.A.R., Abdulsada M.A., "Simulation of Wind-Turbine Speed Control by MATLAB". *International Journal of Computer and Electrical Engineering*, 2(5), 1793-8163, October 2010.
- [56] Kante V.J., Khan Z.J., "A Review Paper on Modeling And Simulation of Permanent Magnet Synchronous Generator Based on Wind Energy Conversion System",

International Journal of Engineering Research and Applications (IJERA), 4(6), 34-43,
June 2014.

- [57] Previsic M., Polagye B., "Deployment effects of marine renewable energy technologies-tidal energy scenarios" *Report ID: RE Vision DE-002*, University of Washington (Accessed June 08, 2012) Available at:
http://www.harveyecology.com/PDF/DOE/FINAL_TIDAL_SCENARIO_REPORT_MP_6-16-10.pdf
- [58] Arango M.A., "Resource assessment and feasibility study for use of hydrokinetic turbines in the tailwaters of the Priest Rapids Project", M.Sc. thesis, University of Washington, 2011.
- [59] Lalander E., "Modelling hydrokinetic energy resources for in-stream energy converters", thesis, Department of Engineering Sciences, Uppsala University, 2010 (Accessed September 05, 2012) Available at:
http://www.el.angstrom.uu.se/Seminar/Emilia_L/Emilia%20Lalander%20Lic%20Avhandling%202010-02-01.pdf
- [60] Briand M., Ng K., "Kinetic energy recovery turbine technology: resource assessment and site development strategy", *World Energy Conference (2)1: Energy resources and technologies, today and tomorrow*, 13–17 September 2010, (Accessed June 10, 2012) Available at: <http://www.worldenergy.org/documents/congresspapers/441.pdf>
- [61] Duvoy P., Toniolo H., "HYDROKAL: a module for in-stream hydrokinetic resource assessment", *Computer & Geosciences*, 39, 171-181, 2012.
- [62] Anyi M., Kirke B., "Hydrokinetic turbine blades: design and local construction techniques for remote communities", *Energy for Sustainable Development*, 15(3), 223-230, 2011.

- [63] Golecha K., Eldho T.I., Prabhu S.V., "Influence of the deflector plate on the performance of a modified Savonius water turbine", *Applied Energy*, 88(9), 3207-3217, 2011.
- [64] Golecha K., Eldho T.I., Prabhu S.V., "Investigation on the performance of a modified Savonius water turbine with single and two deflector plates", *The 11th Asian International Conference on Fluid Machinery and the 3rd Fluid Power Technology Exhibition*, 21-23 November 2011.
- [65] Golecha K., Eldho T.I., Prabhu S.V.: "Performance study of modified Savonius water turbine with two deflector plates". *International Journal of Rotating Machinery* , (Article ID 679247) 2012.
- [66] Batten W.M.J., Weichbrodt F., Muller G.U., Hadler J., Semlow C., Hochbaum M., et al., "Design and stability of floating free stream energy converter". *Proceedings of the 34th World Congress of the International Association for Hydro-Environment Research and Engineering: 33rd Hydrology and Water Symposium and 10th Conference on Hydraulics in Water Engineering*, 2372-2379, 2011.
- [67] Batten W.M.J., Batten G.U., "Potential for using the floating body structure to increase the efficiency of a free stream energy converter", *Proceedings of the 34th World Congress of the International Association for Hydro-Environment Research and Engineering: 33rd Hydrology and Water Symposium and 10th Conference on Hydraulics in Water Engineering*, A.C.T. Engineers, Australia, 2364-2371, 2011.
- [68] Johnson J.B., Pride D.J., "River, tidal, and ocean current hydrokinetic energy technologies: status and future opportunities in Alaska", *Alaska Centre for Energy and Power*, 1 November 2010, (Accessed June 20, 2012) Available at: http://www.uaf.edu/files/acep/2010_11_1_State_of_the_Art_Hydrokinetic_Final.pdf

- [69] Caddet Renewable Energy: "Water current turbines pump drinking water", (Accessed September 17, 2012), Available at: <http://www.caddet-re.org/assets/no83.pdf>
- [70] Verdant Power: "Technology evaluation of existing and emerging technologies—water current turbines for river applications", June 2006, (Accessed September 17, 2012) Available at: http://oreg.ca/web_documents/verdant_river_turbines_report.pdf
- [71] Tidal Energy Pty Ltd: "The Davidson-hill advantage" (Accessed September 17, 2012) Available at: <http://tidalenergy.net.au/>
- [72] Seabell International Co. LTD: "Stream—hydrokinetic power generation systems" (Accessed September 18, 2012), Available at: http://www.seabell-i.com/e/img/guide_pdf.pdf
- [73] New Energy Corporation Inc.: "Encurrent hydropower turbines 5 kW and 10 kW specifications", (Accessed September 17, 2012), Available at: <http://www.newenergycorp.ca/Portals/0/documents/datasheets/ENC.005.010.DataSheet.pdf>
- [74] Eclectic Energy Ltd: "Duogen-3: combined water and wind generator", (Accessed September 18, 2012), Available at: <http://www.duogen.co.uk/page14.html>
- [75] Li Z., Boyle F., Reynolds A., "Domestic Application of Solar PV System in Ireland: The Reality of their Economic Viability", *Energy*, 36(10), 5865-5876, October 2011.
- [76] Al-Karaghoul A., Kazmerski L.L., "Optimization and Life-cycle Cost of Health Clinic PV System for a Rural Area in Southern Iraq using HOMER Software", *Solar Energy*, 84(4), 710-714, February 2010.
- [77] Campoccia A., Dusonchet L., Telaretti E., Zizzo G., "Comparison Analysis of Different Supporting Measures for the Production of Electrical Energy by Solar PV and Wind systems: Four representative European cases", *Solar Energy*, 83, 287-297,

- 2009.
- [78] Dekker J., Nthontho S., Chowdhury S., Chowdhury S.P., "Economic Analysis of PV/Diesel Hybrid Power Systems in Different Climatic Zones of South Africa", *Electrical Power and Energy Systems*, 40, 104-112, March 2012.
- [79] Blennow H., "Method for Rural Load Estimations - a case study in Tanzania", Master's Thesis, Department of Heat and Power Engineering, Lund Institute of Technology, 2004.
- [80] Adams S., "South African Consumer Attitudes Towards Domestic Solar Power Systems", Master's Thesis, Gordon Institute of Business Science, University of Pretoria, August 2011.
- [81] Nasef Abd El-Shafy, "Proposed Technique for Optimally Sizing a PV/Diesel Hybrid System", *International Conference on Renewable Energies and Power Quality*, March 2010.
- [82] Lal D.K., Dash B.B., Akella A.K., "Optimization of PV/Wind/Micro-Hydro/Diesel Hybrid Power System in HOMER for the Study Area", *International Journal on Electrical Engineering and Informatics*, 3(3), 307-325, August 2011.
- [83] Generator Sales, (Accessed April 19, 2014), Available at:
<http://www.generatorsales.com/diesel-generators.asp>
- [84] Kusakana K., Vermaak H.J., "Hydrokinetic Power Generation for Rural Electricity Supply: Case of South Africa", *Renewable Energy*, 55, 467-473, July 2013.
- [85] Rehman S., Alam M.M., Meyer J.P., Al-Hadhrami L., "Feasibility Study of a Wind-PV-Diesel Hybrid Power System for a Village", *Renewable Energy*, 38(1), 258-268, February 2012.
- [86] Fuel Price Trends and Forecast, (Accessed April 19, 2014), Available at:

<http://www.efm.co.za/News%20items/Fuel%20Price%20Trends-%20January%202014.pdf>

- [87] Agajelu B.O., Ekwueme O.G., Obuka N.S.P., Ikwu G.O.R., "Life Cycle Cost Analysis of a Diesel/Photovoltaic Hybrid Power Generating System", *Industrial Engineering Letters*, 3(1), 19-30, 2013.
- [88] Alternagy: (Accessed April 20, 2014), Available at: <http://www.alternagy.co.za/>
- [89] Hiendro A., Kurnianto R., Rajagukguk M., Simanjuntak Y.M., Junaidi, "Techno-economic Analysis of Photovoltaic/wind Hybrid System for Onshore/remote area in Indonesia", *Energy*, 59, 652-657, September 2013.
- [90] Ettah E.B., Nwabueze O.J., Njar G.N., "The Relationship Between Solar Radiation and the Efficiency of Solar Panels in Port Harcourt, Nigeria", *International Journal of Applied Science and Technology*, 1(4), 124-126, 2011.
- [91] Vermaak H.J., Kusakana K., "Design of a Photovoltaic-wind Charging Station for Small Electric Tuk-tuk in D.R.Congo", *Renewable Energy*, 67, 40-45, July 2014.
- [92] Lu M., Chang C., Lee W., Wang L., "Combining Wind Power Generation System with Energy Storage Equipments", *IEEE Transactions on Industry Applications*, 45(6), 2109-2115, November 2009.
- [93] ABS Alaskan: "Excel 7.5kW high voltage DC turbine", (Accessed March 29, 2014), Available at:
http://www.absak.com/catalog/product_info.php/cPath/32_93_107/products_id/146
- [94] Homer Energy Support: "Modeling a Hydrokinetic Turbine in HOMER", Available at:
<http://support.homerenergy.com/index.php?Knowledgebase/Article/View/136/50>
- [95] Kunaifi K., "Options for the Electrification of Rural Villages in the Province of Riau, Indonesia", Master's Dissertation, School of Engineering and Energy, Murdoch

- University, Perth Australia, 2009.
- [96] HOMER Energy Support: "10177 - Modeling a hydrokinetic turbine in HOMER", Available at:
<http://support.homerenergy.com/index.php?Knowledgebase/Article/View/136/50/10177---modeling-a-hydrokinetic-turbine-in-homer>
- [97] Koko S.P., Kusakana K., Vermaak H.J., "Micro-hydrokinetic for Remote Rural Electrification", *International Journal of Electrical, Computer, Electronics and Communications Engineering*, 8(11), 1384-1388, November 2014.
- [98] Sen R., Bhattacharyya S.C., "Off-grid Electricity Generation with Renewable Energy Technologies in India: An Application of HOMER", *Renewable Energy*, 62, 388-398, February 2014.
- [99] Jacob D., Kiene A., World Future Council: "Renewable Energy Policies for Sustainable African Development", (Accessed April 2009), Available at:
http://www.worldfuturecouncil.org/fileadmin/user_upload/PDF/World_Future_Council_Renewable_Energy_Policy_Africa_June09.pdf
- [100] Priya G.J., "Modelling and Performance Analysis of Grid Connected PMSG Based Wind Turbine", *International Journal of Advanced Research in Electrical, Electronics and Instrumentation Engineering*, 3(2), 155-165, April 2014.
- [101] Bikorimana J.M.V., "A Low-Power Floating-Turbine Generation System for Small Rural Communities", *Rwanda Journal*, 23, 56-69, 2011.
- [102] Ben Elghali S.E., Balme R., Le Saux K., Benbouzid M.E.H., Charpentier J.F., Hauville F., "A simulation model for the evaluation of the electrical power potential harnessed by a marine current turbine in the Raz de Sein", *IEEE Journal of Oceanic Engineering*, 32(4), 786-797, 2007.

- [103] Bryans AG., "Impacts of tidal stream devices on electrical power systems", Ph.D. thesis, The Queen's University of Belfast, Faculty of Engineering and Physical Science, 2006.
- [104] Rolán A., Luna A., Vázquez G., Aguilar D., "Modeling of a Variable Speed Wind Turbine with a Permanent Magnet Synchronous Generator", *IEEE International Symposium on Industrial Electronics*, 734-739, July 2009.
- [105] Skolthanasarat S., "The Modeling and Control of a Wind Farm and Grid Interconnection in a Multi-machine System", Phd Dissertation, Faculty of the Virginia Polytechnic Institute and State University, Blacksburg, 26 August 2009.
- [106] Ofualagba G., Ubeku E., "Modeling and Dynamic Characteristics of Variable Speed Wind Turbine", *Journal of Energy Technologies and Policy*, (1)(3), 10-21, 2011.
- [107] Molina M.G., Sanchez A.G., Rizzato Lede A.M., "Dynamic Modeling of Wind Farms with Variable-Speed Direct-Driven PMSG Wind Turbines", *IEEE, Transmission and Distribution Conference and Exposition*, 816-823, November 2010.
- [108] Khan J., Iqbal T., Quaiocoe J., "Power Tracking Control Challenges in Hydrokinetic Energy Conversion Systems", *IEEE, Power and Energy Society General Meeting*, 1-6, July 2011.
- [109] Dusonchet L., Telaretti, E., "Effects of electrical and mechanical parameters on the transient voltage stability of a fixed wind turbine", *Electric Power System Research*, 81, 1308-1316, March 2011.
- [110] Khan S.A., Rajkumar R.K., Aravind C.V., "Performance analysis of 20 Pole 1.5kW Three Phase Permanent Magnet Synchronous Generator for low Speed Vertical Axis Wind Turbine", *Energy and Power Engineering*, (5), 423-428, July 2013.
- [111] Zaiming F., "Mathematical Modelling of Grid Connected Fixed-Pitch Variable-Speed

- Permanent Magnet Synchronous Generator for Wind Turbines", Master's Thesis, University of Central Lancashire, June 2012.
- [112] Zhendong Zhang, M.S., "Permanent Magnet Synchronous Machine based Traction Drive Design for Hybrid Scooter Considering Control Nonlinearities and Compensations" Phd Dissertation, Graduate Program in Electrical and Computer Engineering, Ohio State University, 2013.
- [113] Sheeja V., Singh B., Uma R., "BESS Based Voltage and Frequency Controller for Stand Alone Wind Energy Conversion System Employing PMSG", *Industry Applications Society Annual Meeting, IAS 2009, IEEE*, 1-6 , October 2009.
- [114] Bolik S.M., "Modelling and Analysis of Variable Speed Wind Turbines with Induction Generator during Grid Fault", Thesis, Intitute of Energy Technology, AALBORG University, Denmark, October 2004.
- [115] Parash A., Small Scale Maximum Power Point Tracking Power Converter for Developing Country Application", Master's Thesis, Electrical and Computer Engineering, University of Canterbury, New Zealand, 2013.
- [116] Venkatraj S., Mohan G., "Modeling of Wind Farms with Variable Speed Direct Driven Permanent Magnet Synchronous Generator Wind Turbines", *International Journal of Research and Reviews in Electrical and Computer Engineering* , 1(3), 982-990, September 2011.
- [117] Kulkarni S.S., Thosar A.G., "Mathematical Modeling and Simulation of Permanent Magnet Synchronous Machine", *International Journal of Electronics and Electrical Engineering*, 1(2), 66-71, June 2013.
- [118] Barote L., Marinescu C., "PMSG Wind Turbine System for Residential Applications", *IEEE, Power Electronics, Electrical Drives, Automation and Motion (SPEEDAM)*,

772-777, June 2010.

- [119] Belloni F., Chiumeo R., Gandolfi C., Villa A. : "Simulation model of a Permanent Magnet Synchronous Generator for grid studies". *International Conference on Renewable Energies and Power Quality (ICREPO'14)*, April 2014.
- [120] Zhou Z., Sculler F., Charpentier J.F., Benbouzid M., Tang T., "Power Limitation Control for a PMSG-Based Marine Current Turbine at High Tidal Speed and Strong Sea State". *IEEE Electrical Machines and Drives Conference*, 75-80, May 2013.
- [121] Messaoud M., Abdessamed R., "Modeling and Optimization of Wind Turbine Driving Permanent Magnet Synchronous Generator", *Jordan Journal of Mechanical and Industrial Engineering*, 5(6), 489-494, December 2011.
- [122] El Saady G., Ibrahim E.A., Ziedan H., Soliman M.M., "Analysis of Wind Turbine Driven Permanent Magnet Synchronous under Different Loading Conditions", *Innovative Systems Design and Engineering*, 4(14), 97-111, 2013.
- [123] Barote L., Marinescu C., Serban I., "Energy Storage for a Stand-Alone Wind Energy Conversion System", *Rev. Roum. Sci. Techn. – Électrotechn. et Énerg*, 55(3), 235-242, 2010.
- [124] Tesfaye B., "Improved Sustainable Power Supply for Dagahabur and Kebridahar Town of Somalia region in Ethiopia", Msc Thesis, School of Science and Engineering, Reykjavik University, January 2011.
- [125] Cencelli N.A., "Aerodynamic Optimization of a Small-Scale Wind Turbine Blade for Low Wind Speed Conditions", Msc Thesis, University of Stellenbosch, December 2006.

APPENDICES

Appendix A: Hydrokinetic system report for optimal economic results

Optimum System architecture

Hydrokinetic turbine	6 x DHT Turbines
Total Rated Capacity	9 kW
Battery	72 Trojan T-105
Inverter	8 kW
Rectifier	8 kW

Net Present Costs

Component	Capital	Replacement	O&M	Fuel	Salvage	Total
	(\$)	(\$)	(\$)	(\$)	(\$)	(\$)
Darrieus Hydrokinetic Turbine (DHT)	90,000	0	23,010	0	0	113,010
Trojan T-105	13,608	11,842	3,479	0	-1,585	27,343
Converter	5,509	4,794	703	0	-642	10,364
System	109,117	16,636	27,192	0	-2,227	150,718

Annualized Costs

Component	Capital	Replacement	O&M	Fuel	Salvage	Total
	(\$/yr)	(\$/yr)	(\$/yr)	(\$/yr)	(\$/yr)	(\$/yr)
Darrieus Hydrokinetic Turbine (DHT)	7,040	0	1,800	0	0	8,840
Trojan T-105	1,065	926	272	0	-124	2,139
Converter	431	375	55	0	-50	811
System	8,536	1,301	2,127	0	-174	11,790

Appendix B: Solar system report for optimal economic results

Optimum System architecture

PV Array	42 kW
Total Rated Capacity	42 kW
Battery	204 Trojan T-105
Inverter	8 kW
Rectifier	8 kW

Net Present Costs

Component	Capital	Replacement	O&M	Fuel	Salvage	Total
	(\$)	(\$)	(\$)	(\$)	(\$)	(\$)
PV	55,482	17,300	13,423	0	-9,695	76,509
Trojan T-105	38,556	33,551	9,858	0	-4,492	77,473
Converter	5,509	4,794	703	0	-642	10,364
System	99,547	55,645	23,983	0	-14,829	164,346

Annualized Costs

Component	Capital	Replacement	O&M	Fuel	Salvage	Total
	(\$/yr)	(\$/yr)	(\$/yr)	(\$/yr)	(\$/yr)	(\$/yr)
PV	4,340	1,353	1,050	0	-758	5,985
Trojan T-105	3,016	2,625	771	0	-351	6,060
Converter	431	375	55	0	-50	811
System	7,787	4,353	1,876	0	-1,160	12,856

Appendix C: Wind system report for optimal economic results

Optimum System architecture

Wind turbine	6 x BWC Excel-R Turbines
Total Rated Capacity	45 kW
Battery	388 Trojan T-105
Inverter	8 kW
Rectifier	8 kW

Net Present Costs

Component	Capital	Replacement	O&M	Fuel	Salvage	Total
	(\$)	(\$)	(\$)	(\$)	(\$)	(\$)
BWC Excel-R	145,200	0	37,123	0	0	182,323
Trojan T-105	73,332	63,814	18,749	0	-8,543	147,351
Converter	5,509	4,794	704	0	-642	10,365
System	224,041	68,607	56,576	0	-9,185	340,039

Annualized Costs

Component	Capital	Replacement	O&M	Fuel	Salvage	Total
	(\$/yr)	(\$/yr)	(\$/yr)	(\$/yr)	(\$/yr)	(\$/yr)
BWC Excel-R	11,359	0	2,904	0	0	14,263
Trojan T-105	5,737	4,992	1,467	0	-668	11,527
Converter	431	375	55	0	-50	811
System	17,526	5,367	4,426	0	-719	26,600

Appendix D: Diesel generator system report for optimal economic results

Optimum System architecture

Generator 1	8 kW
Total Rated Capacity	8 kW
Battery	84 Trojan T-105
Inverter	8 kW
Rectifier	8 kW
Dispatch strategy	Cycle Charging

Net Present Costs

Component	Capital	Replacement	O&M	Fuel	Salvage	Total
	(\$)	(\$)	(\$)	(\$)	(\$)	(\$)
Generator 1	6,599	15,007	25,669	182,965	-1,507	228,734
Trojan T-105	15,876	32,091	4,059	0	-193	51,833
Converter	5,509	4,794	703	0	-642	10,364
Other	0	0	803	0	0	803
System	27,984	51,892	31,234	182,965	-2,342	291,734

Annualized Costs

Component	Capital	Replacement	O&M	Fuel	Salvage	Total
	(\$/yr)	(\$/yr)	(\$/yr)	(\$/yr)	(\$/yr)	(\$/yr)
Generator 1	516	1,174	2,008	14,313	-118	17,893
Trojan T-105	1,242	2,510	318	0	-15	4,055
Converter	431	375	55	0	-50	811
Other	0	0	63	0	0	63
System	2,189	4,059	2,443	14,313	-183	22,821